University of Alberta

The Long Term Performance of Large Centrifugal Sand Slurry Pumps

by

Barry Posner ©

A thesis submitted to the Faculty of Graduate Studies and Research in partial fulfillment of the requirements for the degree of Master of Science

in

Mining Engineering

Department of Civil and Environmental Engineering

Edmonton, Alberta

Fall 1998

0-612-34405-3

University of Alberta

Faculty of Graduate Studies and Research

The undersigned certify that they have read, and recommend to the Faculty of Graduate Studies and Research for acceptance, a thesis entitled *The Long Term Performance of Large Centrifugal Sand Slurry Pumps* in partial fulfillment of the requirements for the degree of Master of Science in Mining Engineering

Prof. Ian Muirhead

Dr. Ken Barron

Dr. Julian Coward

Dr. Jacob Masliyah

01 June 1998

Dr. Jozef Szymanski

Abstract

This study attempts to provide a model for the prediction of slurry pump performance with respect to cumulative throughput of sand, solids weight concentration and pump speed. Previous studies have not examined performance with respect to throughput.

Three GIW 18/20 LSA 44(45) slurry pumps were studied over the lifespan of one impeller in each pump while pumping a sand-water slurry. The pumps exhibited two different modes of behavior with respect to cumulative throughput. During an interval of 0-6000 kt of sand throughput, theorized to coincide with erosion of the impeller vanes while maintaining a constant impeller radius, the head ratio increased approximately 5% and the efficiency ratio was approximately constant. During an interval of 6000-10400 kt of sand throughput, theorized to coincide with erosive impeller diameter reduction, the head ratio decreased approximately 15% and the efficiency ratio declined approximately 7%.

Dedication

I dedicate this thesis to all the engineers and scientists that came before me and made this work possible. To those giants upon whose shoulders I am so privileged to stand.

Acknowledgements

There are so many people upon whom I have imposed and relied over the past two years. I must, firstly, thank my supervisors, Ian Muirhead and Julian Coward, for their patience, encouragement and free benefit of their vast knowledge and experience. For knowing when to push (or badger) me, and knowing when to lay back.

To all the Syncrude staff who so ably assisted me. Owen Nieman, especially for the original idea, Kevin Idland, Peter Read, Graham Peters and Steve Dembecki, as well as the countless others upon whom I occasionally relied. And to Eric Newell and Jim Carter, for fostering such an enlightened and proactive corporate attitude on education and research, and for the funding for this study.

To my friends for seeing me through this, especially during the periods of doubt. Corinne, Sabrina, Saloni, Christal, Shelly, Roger, Peter, Kim, Shreela, Scott, Miodrag. I couldn't have done it without your varying degrees of support, encouragement and accompaniment.

And I certainly don't want to forget John Zorn, The Big Rock Brewery, The MacAllan Distillery, The Second Cup on Campus or TSN for providing the diversions that made the work possible...

Table of Contents

List of Tables

List of Figures

Nomenclature

a	Unscaled Correlation Constant Term	
$\angle A$	Impeller Inlet Vane Angle	
b	Unscaled Correlation Coefficient	
$\angle B$	Impeller Outlet Vane Angle	
C_D	Drag Coefficient	
C_V	Concentration by Volume	
C_W	Concentration by Weight	
d	Particle Diameter	m
d_{50}	Diameter of 50th Percentile Particle	m
d_W	Mean Weighted Particle Diameter	m
D_{in}	Impeller Intake Diameter	m
F	PI Input Flow	L/s
FHP	Fluid Horsepower	HP
Fr	Froude Number	
g	Acceleration of Gravity	m/s^2
H	Head	ft, m
H_R	Head Ratio	
I_1	Amperage, Pump 1	A
I_2	Amperage, Pump 2	A
I_3	Amperage, Pump 3	A
k	Empirical Constants	
K_H	Head Performance Factor	
K_η	Efficiency Performance Factor	
N	Pump Speed	rpm
N_S	Specific Speed	
p	Pressure	kPa
p_1	Pump 1 Suction Pressure	kPa
p_2	Pump 2 Suction Pressure	kPa
p_3	Pump 3 Suction Pressure	kPa
p_4	Pump 3 Discharge Pressure	kPa
P	Power	kW
P_E	Motor Power	kW
P_I	VFD Power	kW
Q	Flow Rate	m^3/s, USGPM
s	Sample Standard Deviation	
S	Specific Gravity	
SHP	Shaft Horsepower	HP
u	Impeller Tangential Velocity	m/s
v	Velocity	m/s
z	Elevation	m, ft
$\Re p$	Particle Reynolds Number	

α	Scaled Correlation Constant Term	
β	Scaled Correlation Coefficient	
ϕ	Flow Index	
η_E	Motor Efficiency	
η_D	Drive Efficiency	
η_R	Efficiency Ratio	
η_{VFD}	VFD Efficiency	
κ	Empirical Constant	
μ	Viscosity	cP
ρ	Density	kg/m^3
ψ	Pressure Index	

Subscripts

in	At Pump or Impeller Inlet
f	Fluid
fr	Friction
L	Liquid
Loc	Local
m	Slurry, Mixture
obs	Observed
out	At Pump or Impeller Outlet
R	Resultant
s	Solid
sf	Secondary Flow
w	Water

1.0 Introduction

1.1 Project Description

Centrifugal pumps are frequently used in slurry transportation applications. While a rigorous, well-established procedure for the design of centrifugal pumps in single phase, Newtonian fluid service exists, the process for design of a slurry pump is less well defined. The presence of solids in a two-phase, solid-liquid slurry causes a reduction in the performance of pumps. This reduction in performance is known as the solids effect. The effect of solids on the performance of a slurry pump has been found to be related to the same parameters as single-phase flow, namely fluid density and viscosity. However, slurries often exhibit complicated rheological properties, and in addition to density and viscosity, characteristics such as particle density, weight concentration of solids and particle size distribution have been found to be variables effecting the solids effect. It has also been found that performance is very specific to pump design, so that a universal procedure for the determination of the reductions in head and efficiency has yet to be established.

The performance of slurry pumps is not a static phenomenon. As abrasive solids are transported though the pump, the pump internal components are eroded. This leads to changes in the geometry and diameter of the impeller, and the geometry of the pump casing. The performance thus changes with time.

1.2 Project Objectives

There is an absence of universal, application-independent methods of calculating the effects of solids on pump performance in advance. It is desired to study several pumps in an industrial application to obtain the actual operating values for head and efficiency reduction, and compare these values with those specified by the manufacturer. The performance over a long span of time will be examined, and a model of the solids effect with respect to time shall be developed and described.

The application in question is the pumping of tailings sand slurries at Syncrude Canada Limited (SCL). SCL is the world's largest producer of crude oil from bitumen, extracted from oilsands deposited near Fort McMurray, Alberta. SCL's Mildred Lake complex is an integrated mining, extraction and upgrading facility, and has been in operation since 1979. On an average operating day approximately 120,000 tonnes of tailings sand is generated. This sand is transported to two large holding facilities by an extensive network of pipelines and centrifugal pumps as a water borne slurry.

2.0 Theory

2.1 Centrifugal Pump Performance

2.1.1 Definitions

A centrifugal pump is a device designed to impart energy to a fluid. This energy is necessary to enable the fluid to move through pipelines, overcoming the forces of gravity and friction. The fluid, of density ρ moves through the pump at a flow rate, or discharge denoted by Q. It is common practice in fluid dynamics to express potential, kinetic and pressure energy in terms of the height of a column of fluid, otherwise known as the head.

If the inlet, or suction side of a centrifugal pump is denoted by subscript "in" and the outlet, or discharge side is denoted by subscript "out", then the total dynamic head (TDH) added to a fluid by a centrifugal pump is defined thus:

$$\Delta H = TDH = \frac{V_{out}^2 - V_{in}^2}{2g} + \frac{p_{out} - p_{in}}{\rho g} + \left(z_{out} - z_{in}\right) \qquad \text{...(2.1)}$$

When described solely in terms of pressure added by the pump, the head is defined as follows:

$$\Delta H = \frac{\Delta p}{\rho g}, \quad or\ \Delta p = \Delta H \rho g \qquad ...(2.2)$$

The hydraulic power output (or fluid horsepower, FHP) of a centrifugal pump is defined thus:

$$\begin{aligned} FHP &= Q\Delta p \\ &= Q\rho g \Delta H \end{aligned} \qquad ...(2.3)$$

Input (Shaft) Power:

$$SHP = P_E \cdot \eta_E \cdot \eta_D \qquad ...(2.4)$$

The efficiency is the ratio of the output over input power, or fluid horsepower over shaft power, thus:

$$\eta = \frac{FHP}{SHP} \qquad ...(2.5)$$

2.1.2 Theoretical and Actual Head.

Head is added to a fluid by a centrifugal pump by accelerating the fluid in a centrifugal manner, hence increasing its velocity. This kinetic energy is added in the impeller, and is converted to pressure energy in the volute, or casing, of the pump. In order to find the head added, it is necessary to describe the velocity of a fluid element at the inlet and exit of the impeller. Velocity triangles, as displayed in Figures 2.1 and 2.2 are used to describe the components of velocity at the impeller inlet and outlet. The tangential and meridional velocities, denoted by u and v on the diagram, are plotted, and the vector resultant of the two components of velocity, v_R, is found. This describes the velocity of a fluid particle relative to a stationary reference point at a specific time. The head added by the impeller is described in the velocity triangle analysis purely as velocity head. The head added is described thus:

$$\Delta H = \frac{v_{R,out}^2 - v_{R,in}^2}{2g} \qquad ...(2.6)$$

A complete analysis can be found in Wilson, et al. (1). The result of this analysis shows that the theoretical head developed by a pump is a linear equation of form $H=k_1-k_2Q$, where k_1 and k_2 are constants derived from the geometry and speed of the pump. The actual head developed is much closer to a second-degree curve, as illustrated in Figure 2.3. There are two main components to the deviation from theoretical flow. The first is known as the "shock" loss. When referring to Equation (2.6), it can be seen that head will be maximized if the $v^2_{R,in}$ term is minimized. This term describes the resultant inlet velocity, which is minimized if there is only a meridional, and no tangential component to the flow. In other words, if rotation of the flow at the entry of the impeller is minimized then the head added by the pump will be maximized.

v_{in} = Inlet Meridional Velocity

u_{in} = Inlet Tangential Velocity

$v_{R,in}$ = Resultant Inlet Velocity

$\angle A$ = Vane Inlet Angle

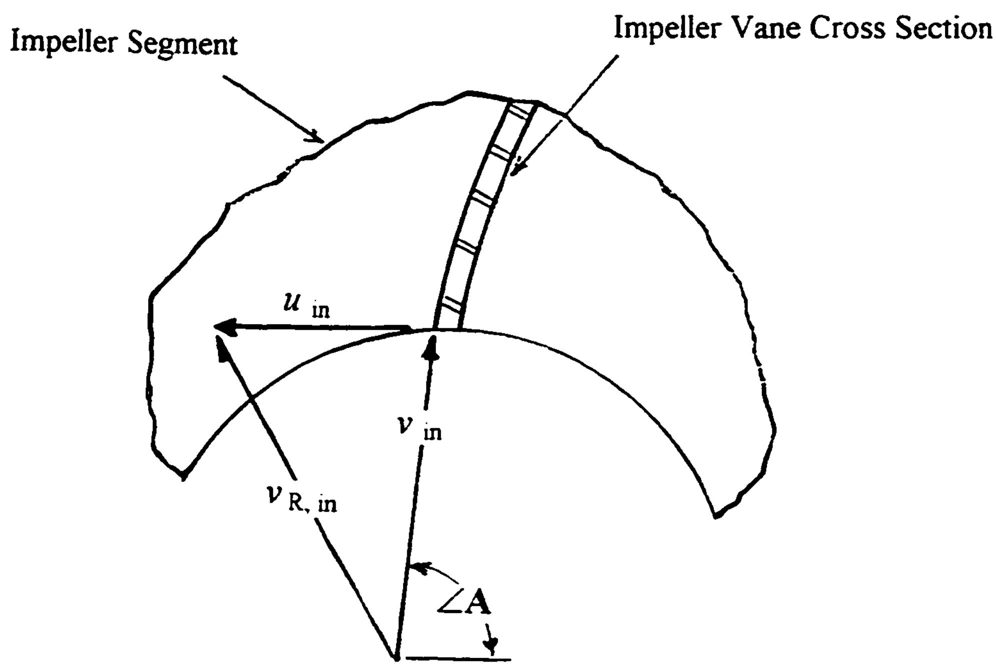

Figure 2.1: Impeller Inlet Velocity Triangle

v_{out} = Outlet Meridional Velocity

u_{out} = Outlet Tangential Velocity

$v_{R,out}$ = Resultant Outlet Velocity

$\angle B$ = Vane Outlet Angle

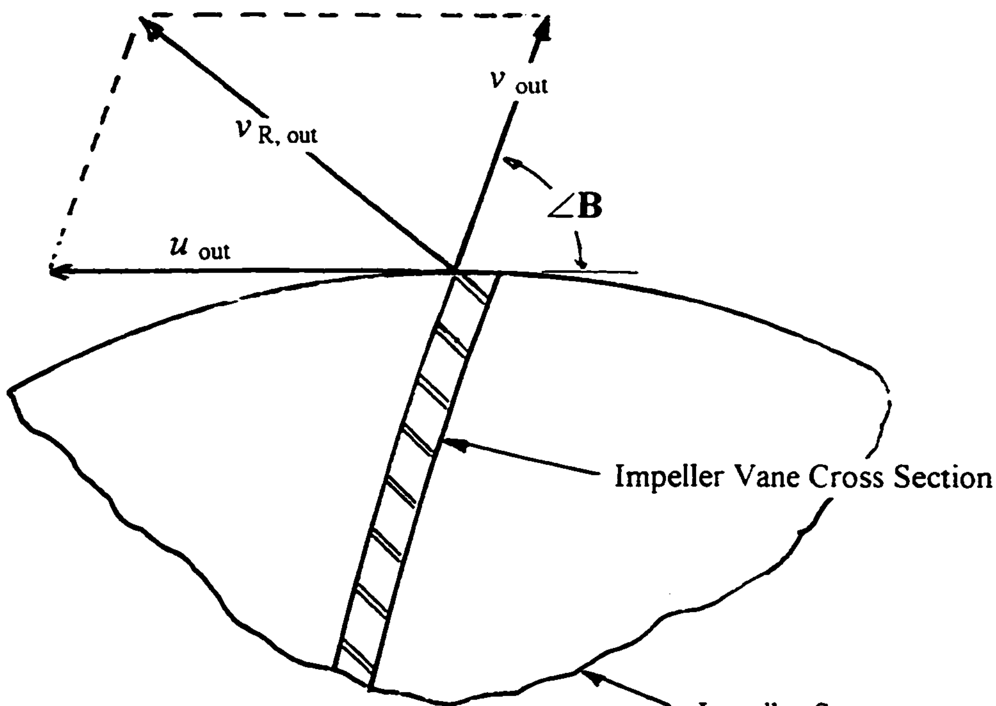

Figure 2.2: Impeller Outlet Velocity Triangle

The loss caused by pre-rotation of the fluid is called a "shock" loss. It is commonly observed that the pre-rotation is only zero for any specific pump over a certain range of discharges. Above and below this discharge range the shock loss is observed. The other source of deviation from the ideal pump curve is illustrated of Figure 2.3 as "Friction" loss. This term encompasses several components of loss, such as wall friction, secondary flow losses and recirculation from the discharge to suction. An additional loss comes from slip. Power losses come from all of these factors, as well as friction in the driveline. When examining the velocity triangle for the impeller exit the meridional velocity is assumed to be travelling in the same direction as the impeller vane, denoted as $\angle$B in Figure 2.2. In reality, upon exiting the impeller, the angle of the meridional velocity component is reduced to a value below the observed $\angle$B of the impeller vane. The difference between the ideal and actual angles is referred to as the "slip angle". This leads to a reduction in the resultant velocity, and thus a reduction in the head added by the impeller.

The speed of a centrifugal pump, N, is usually described in terms of revolutions per minute (rpm), or occasionally s^{-1}. A frequently used term to describe the pump design is the specific speed. It is defined thus:

$$N_S = \frac{N\sqrt{Q}}{H^{3/4}} \qquad \text{...(2.7)}$$

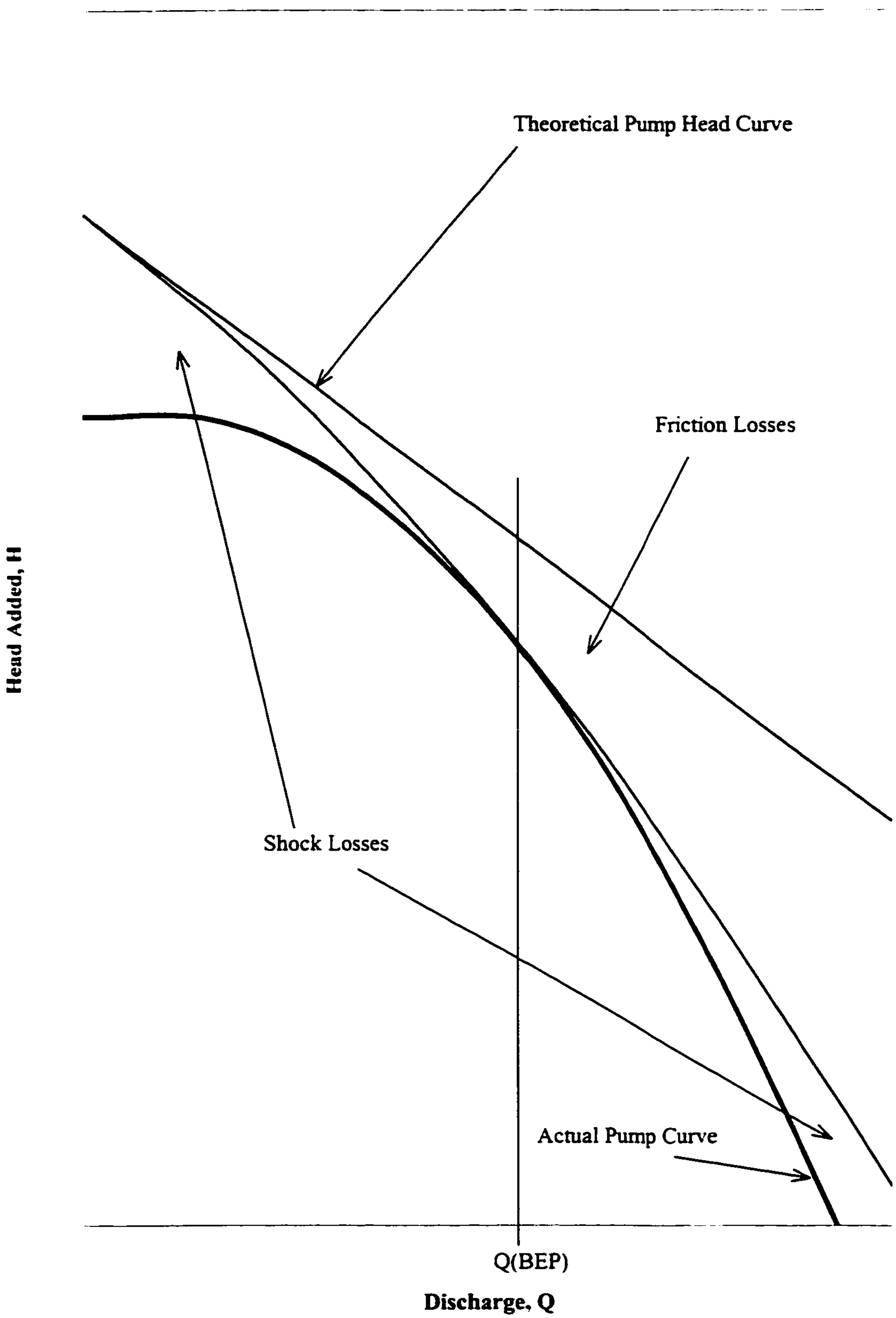

Figure 2.3: Actual and Theoretical Pump Curves

The values used in Equation (2.7) are all taken from the best efficiency point of the pump head curve. This parameter is used to describe the performance of a family of pumps of similar geometry, but different size and speed. Obviously, this parameter does not have units of speed (rpm), and is thus the use of the word "speed" in its name is misleading. In the Imperial measurement system the units used are rpm for speed, USGPM for flow and feet for head, thus yielding units of $USG^{1/2}/(min^{1\frac{1}{2}}ft^{3/4})$ for specific speed. Due to the ungainliness of these units, specific speed is simply quoted as being in Imperial or SI units, with the actual units omitted. It is possible to obtain a true dimensionless number by dividing Equation (2.7) by the acceleration of gravity raised to the power of 0.75, but this method is not widely used in the pump manufacturing industry. Several studies of slurry pump performance list specific speed as a variable.

2.1.3 The "Solids Effect"

It has been observed that when pumping a mixture of solids and liquids, known as a slurry, for the same discharge and pump speed a pump (a) generates less head, and (b) consumes more power (at the same head) than when pumping clear water. This can be attributed to several factors. Firstly, a centrifugal pump is an area of high acceleration. When the water-solids mixture is accelerated rapidly the solid particles, due to their greater density, accelerate slower than the fluid due to momentum effects. This leads to solid-liquid friction losses, and is thought to be the principal contributor to head and efficiency depression in a slurry pump. Collisions of the solid particles with other particles and with pump walls add additional friction and energy losses, many models of which have been derived for pipeline slurry flow. In addition, the energy required to keep the solid particles in suspension caused a loss in head to occur. Slurry flow in pipelines, examining both solid-solid effects and suspension effects, is explored in depth in Shook and Roco (2).

2.1.4 Pump Performance Calculations

The performance of slurry pumps is usually described by the ratios of the head and efficiencies observed during operation pumping slurries versus those observed during clear water operation. These factors are referred to as the head ratio and efficiency ratio, and are defined thus:

Head Ratio:

$$H_R = \frac{\Delta H_m}{\Delta H_w} \qquad ...(2.8)$$

Efficiency Ratio:

$$\eta_R = \frac{\eta_m}{\eta_w} = \frac{\left[\frac{FHP_m}{SHP_m}\right]}{\left[\frac{FHP_w}{SHP_w}\right]} = \left(\frac{FHP_m}{FHP_w}\right)\left(\frac{SHP_w}{SHP_m}\right) \qquad \text{...(2.9)}$$

Substituting Equation (2.3) into Equation (2.9) we get

$$\eta_R = \left(\frac{Qg\rho_m \Delta H_m}{Qg\rho_w \Delta H_w}\right)\left(\frac{SHP_w}{SHP_m}\right) = H_R\left(\frac{\rho_m}{\rho_w}\right)\left(\frac{SHP_w}{SHP_m}\right) \qquad \text{...(2.10)}$$

The authors of several studies have described slurry pump operation with the use of performance factors defined thus (expressed as fractions, not percentages):

Head Performance Factor:

$$K_H = 1 - H_R \qquad \text{...(2.11)}$$

Efficiency Performance Factor:

$$K_\eta = 1 - \eta_R \qquad \text{...(2.12)}$$

2.2 Literature Review

2.2.1 General Comments

There is a very small body of literature concerning the performance of slurry pumps. The earliest frequently cited reference is Stepanoff (3), which dates to 1965. Slurry flow was identified as a focus area by the British Hydromechanics Research Association (BHRA), and a series of conferences entitled "Hydrotransport" were held during the 1970's and early 1980's. The proceedings of these conferences are the source of most of the published work on the solids effect on centrifugal pumps. Much of the work performed in recent years has come from the two largest manufacturers of slurry pumping equipment, GIW of Grovetown, GA, USA and Warman International of Artarmon, NSW, Australia. Both companies have extensive in-house research, as well as sponsoring and collaborating in work at several Universities

In recent years much this work has tended to focus in detail on components of slurry pump performance, such as slip factors and concentration and velocity distributions. The major focus of study is in the area of wear. Unfortunately, none of the papers examined described performance versus wear rate, or performance versus time.

Almost without exception the literature cited attempts to describe centrifugal slurry pump performance as a function of three variables: solids concentration, particle size, and particle density. None of the studies cited time on stream or cumulative throughput as a variable, and mention of the effects of speed or specific speed was made only in rare instances.

.

2.2.2 Stepanoff (1965)

This monograph (3) is recognized as the first comprehensive study of solid-liquid two-phase centrifugal pump performance. Stepanoff made two fundamental statements that have since been the focus of further examination. Firstly, he stated that the head ratio and efficiency ratio are the same. Secondly, he stated that the power required to pump a slurry is directly proportional to the slurry density. Stepanoff did not attempt to develop correlations for head and efficiency ratio versus particle size or particle density. He did, however, show the results of several studies performed on materials such as clay, phosphate, fly ash, sand, gypsum, gravel and coal.

2.2.3 Wiedenroth (1970)

This paper (4) describes the first recorded attempts at describing slurry pump performance as a function of dimensionless pump and slurry parameters, as opposed to empirical, manufacturer developed determinations for specific pumps, which was all that was extant prior to 1970.

Wiedenroth used two pumps in this study, a KSB Type 150-30, operated at speeds of 1000 and 1250 rpm, and an O&K pump operated at 500, 750 and 875 rpm. The sizes of the pumps were not indicated in the publication. Solids concentrations of 0 to 30% by weight were examined, using five different sand mixtures and one gravel mixture.

Wiedenroth defined two dimensionless numbers specific to pump performance. These are the "pressure index", defined thus:

$$\psi = \frac{p_f}{\rho_m Q\left(u^2/2\right)} \qquad \text{...(2.13)}$$

and a "flow index", defined thus:

$$\phi = \frac{4Q}{\pi D_{in}^2 u} \qquad \text{...(2.14)}$$

Using these factors, Wiedenroth plotted a non-dimensional pump curve, with the pressure index plotted along the ordinate, or y-axis, and the flow index plotted along the abscissa, or x-axis. The non-dimensional pump curves vary for different concentrations. Wiedenroth looked at pressure index versus concentration of solids by weight, and discovered that the head index decreased linearly with increased solids concentration. The author attempted to define the relationship between the loss in head index versus concentration, and came up with the following relationship:

$$\psi = 48 \times 10^{-4} C_W \Re_p N_S^{-2.46} \qquad ...(2.15)$$

The particle Reynolds number, $\Re_p$, was used as it allows for the incorporation of more information about the particle than simply particle diameter. The particle Reynolds number is defined thus:

$$\Re_p = \frac{d_{particle} v_{settling} \rho_w}{\mu_w} \qquad ...(2.16)$$

Wiedenroth also addresses the question of efficiency loss. While not listing any formulae, he described finding a reduction in efficiency linearly proportional to the weight concentration, and linearly proportional to the particle Reynolds number.

2.2.4 Hunt and Faddick (1971)

This paper (5) details some numerical findings for head and efficiency changes in centrifugal pump operation. The experiments were quite different from most others detailed here, in that they utilized plastic chips of dimension 12 x 8 x 2 mm, and of specific gravity 1.02. As such, the results are not particularly applicable to the present study. The most interesting fact discovered while reading this paper was the finding that head and efficiency actually increased for certain impeller geometry/speed combinations.

2.2.5 Vocadlo, Koo and Prang (1974)

This paper (6) presents a detailed theoretical examination of head and efficiency ratios, and describes the correlation of this examination with test results. The authors describe the head ratio with the following equation:

$$K_H = C_V\left(\frac{\rho_S}{\rho_L}-1\right)\left(k_1+\frac{k_2}{\phi\psi}\sqrt{\frac{d}{D}\left(\frac{\rho_S}{\rho_L}-1\right)}\right) \qquad ...(2.17)$$

Where $\psi = \frac{Hg}{u^2}$, described as a "head coefficient", and $\phi = \frac{v}{u}$, described as a "capacity coefficient". These two values are the same as the "pressure index" and "flow index" as described by Wiedenroth. k_1 and k_2 in Equation (2.16) are constants that are derived from different pump geometries. The authors derive a relation between head and efficiency ratios, as follows:

$$\eta_R = H_R S_m\left(\frac{P_W}{P_m}\right) \qquad ...(2.18)$$

According to this equation, if the head output varies linearly with power consumption at the same flow rate, then the efficiency ratio is simply a linear function of slurry specific gravity. The experiments were performed on Worthington 3M-111 and 3R-111 centrifugal pumps (metal and rubber lined, respectively), of impeller diameter

280 mm, and operated at both 1780 rpm and 1180 rpm. Sands of four different particle sizes, 0.19 mm, 0.47 mm, 0.58 mm and 2.0 mm were used in this experiment. The authors found that the experimental results correlated closely with the previously derived theoretical equation. In addition, the authors found that a linear relationship between slurry density and power consumption did exist.

This study was unique amongst all of the existing literature in that it mentioned time as a variable in pump performance. The authors observed that for the metal pumps the performance improved for a period of approximately one hour, due to the "smoothing" or polishing effect of the slurry on the surface of the impeller. After this initial hour performance was steady or decreased. The rubber-lined pump displayed no discernible change in operation versus time, as there was no change in the surface texture during the duration of the test.

2.2.6 Burgess and Reizes (1976)

The authors of this study (7) state the need for a method to predict slurry pump performance without having to perform individual tests on every new pump design. Burgess and Reizes make considerable use of dimensional analysis and conclude that the functions for head and efficiency ratios can be described solely as functions of solids weight concentration, particle size distribution and slurry density.

The authors found that head ratio was independent of flow rate and specific speed. The authors settle upon the following relationship:

$$H_R = (1 - C_W)^n \qquad \text{...(2.19)}$$

where: $$n = f(S_{solids}, d_{50}) \qquad \text{...(2.20)}$$

Burgess and Reizes included a plot in this paper describing n as a function of solids density and average particle size.

This study was performed on a Warman pump with a 150 mm suction and 100 mm discharge line, and an impeller diameter of 371 mm. Four materials were tested: beach sand, river sand, Ilmenite (a titanium ore), and an unspecified heavy mineral. The concentrations were varied from 0 to 60%. The pumps were operated at a number of speeds varying from 780 to 1270 rpm. The authors found that the pump affinity laws held true over this range of speeds.

The solids characteristics, the experimentally observed values of "n", and a calculated head ratio at a concentration of 30% by weight are given in Table 2.1, below:

Table 2.1: Material Properties and Experimental Results, Burgess and Reizes

Solid	Solid SG	d_{50}(mm)	n	H_R at C_w=30%
Beach Sand	2.67	0.295	0.333	0.888
River Sand	2.64	1.29	0.589	0.811
Ilmenite	4.63	0.17	0.450	0.852
Coarse Heavy Mineral	4.35	0.29	0.561	0.818

The authors of this study were unable to draw many conclusions concerning efficiency ratios due to malfunctioning instruments. However, when the authors were able to observe efficiency ratios, they were found to be slightly higher than head ratios.

2.2.7 Cave (1976)

Cave studied the performance of slurry pumps of impeller size 2 inch to 12 inch (50 mm to 300 mm), examining the head and efficiency ratios versus three variables: solids concentration, solids specific gravity and solids particle size distribution. He reported the performance as "performance factors", K_H=(1-H_R).

For solids concentration, Cave found that the performance to be practically linear with solids concentration, for concentrations of up to 60% by weight. For solids specific gravity, Cave found no apparent relationship for K_H versus S at a fixed concentration. Examining particle size, the following empirical relationship was derived:

$$K_H = 0.0385(S-1)\ln\left(\frac{d_{50}}{22.7}\right) \qquad ...(2.21)$$

When combining the effects of specific gravity, particle size and weight concentration, the following relationship was derived:

$$K_H = (1-H_R) = 0.000385(S-1)\left(1+\frac{4}{S}\right)C_W \ln\left(\frac{d_{50}}{22.7}\right) \qquad ...(2.22)$$

Cave reported that experimentally determined values for K_H closely agreed with the values determined from this equation. The solids used for this study were as follows: beach sand, river sand, Ilmenite and an unspecified heavy mineral. Curiously, this was the same group of materials studied by Burgess and Reizes. Both Burgess and Cave were employed by Warman International at the time of these studies. The pumps were operated at speeds of 1500 and 1780 rpm.

2.2.8 Sellgren (1979)

The principal difference between this study (9) and most of the previous ones is that Sellgren used industrial slurries with broad particle size distributions, as opposed to the lab type, narrow particle size distribution solids used other studies. Sellgren builds upon the ideas espoused by Burgess and Reizes, but also considers the effect of particle shape, settling velocity and distribution factor, as well as mean particle size.

This study utilized a rubber lined 152 x 152 mm Morgardshammar pump with a 430 mm diameter impeller. The tests were run at two pump speeds, 760 rpm and 1140 rpm. Sellgren used a variety of slurries taken from industrial facilities in Sweden. These included iron ores, lead ores, perlite and crushed granite.

Sellgren derived a relationship for head performance factor as follows:

$$K_H = 0.32 C_w^{0.7} (S_{solid} - 1) C_D^{-0.25} \qquad ...(2.23)$$

Where C_D is the mean weighted particle drag coefficient. Sellgren found the efficiency performance factor to be much more complicated than the head performance factor. He concludes by stating the following relationship: $K_H \leq K_\eta \leq C_w$.

2.2.9 Mez (1984)

Mez (10) begins by examining the formulae developed by Wiedenroth, Vocadlo et al, Cave, Burgess & Reizes and Sellgren. He concludes that the results of these different studies vary greatly when applied outside of the narrow ranges indicated by the authors, leading Mez to conclude that the behavior of the solids in the pump, and not just the solid properties themselves, is a variable in determining pump performance.

Mez performed experiments using two ROPU pumps, one of size 350 x 300 mm (inlet x discharge), impeller diameter 825 mm, and one of size 200 x 150 mm, impeller diameter 650 mm. Raw, run of mine coal was used as the test solid, and the pumps were run at speeds of 740 and 870 rpm.

Mez does not develop his own performance correlations, but compares his test results with the aforementioned correlations developed by other experimenters. He concluded that the correlations of Cave and Vocadlo were best suited for the coarse solids pumped, and that each equation was better at predicting performance at different concentrations. Below concentrations of 30% by weight the correlation developed by Cave is better, but as concentration increases towards 60% the correlation of Vocadlo provides better results.

Mez concludes with the following points:

- Head reduction is linear with increasing solids concentration, even with a broad particle size distribution.
- For coarse solids, the head reduction is proportional to $[(\rho_s/\rho_f)-1]$.
- When approximating a broad particle size distribution with a single d_{50} value, large deviations between experimental and predicted values of pump performance are frequently observed.

- A mean particle drag coefficient and particle Reynolds number methodology may yield more consistent results, as such a methodology takes more particle properties into consideration.
- When pumping a slurry of broad particle size distribution, the different grain sizes effect performance in different ways, and these effects cannot be separated.

2.2.10 Roco, Marsh, Addie and Maffett (1986)

This paper (11) details a wide-ranging study designed to aid engineers in the prediction of dredging pump performance. Unlike most of the other studies examined here, this one focused on pumps with large flow rates, in the order or 300 to 10,000 m^3/h. The pumps in question are from the same manufacturer as those under examination in the present study.

The end result of this paper is a computer program that will generate head-flow curves for a slurry pump based on a number of inputs pertaining to pump geometry and slurry composition.

The authors of this paper examined many of the other studies of the solids effect, such as Wiedenroth (1970), Vocadlo, et al. (1974), Cave (1976), Burgess and Reizes (1976) and Sellgren (1979). They stated that the results of these studies, when applied to designs of large dredging pumps, were largely unsatisfactory. The reasons given were: firstly, the differential effects of solids on the different types of head loss, such as friction, secondary flow, leakage to suction, and minor losses, are not discussed. Roco *et al.* feel that as pump size increases greatly, the losses associated with these various mechanisms vary at different rates. Secondly, the dimensionless numbers cited in the previous studies were designed for convenience of analysis, and not from physical principles. Roco *et al.* feel that for a correct theoretical analysis to be partaken, many of the traditional dimensionless numbers used in fluid mechanics, such as the Froude, Reynolds and Richardson Numbers, must be considered. Lastly, all of the other studies were performed at or near the best efficiency points on a limited number of pumps, all considerably smaller than those normally used for industrial dredging and slurry pumping applications.

This study also goes further than any of the previous analyses by addressing pump casing geometry. All of the other studies had only considered such things as specific speed and impeller diameter as variables.

Instead of defining a single equation for head loss due to the solids effect, the authors segregated losses into three components: losses from secondary flow, local losses and friction. The derived relationships for these head loss factors are as follows:

Secondary Flow:

$$H_{R.sf} = C_W(S-1)\kappa'\Re^{x1}N_S^{y1} \quad ...(2.24)$$

Local Losses:

$$H_{R.Loc} = C_W(S-1)\kappa'_{Loc}Fr^{x2}N_S^{y2} \quad ...(2.25)$$

Frictional Losses:

$$H_{R.fr} = C_W(S-1)\kappa'_{fr}\frac{gDW_0}{V^3} \quad ...(2.26)$$

where k_i, x_i and y_i are all empirically derived constants.

Roco *et al.* also mention the loss from pump wear, but do not attempt to derive any expressions for wear loss.

2.2.11 Gahlot, Seshadri and Malhotra (1992)

Gahlot *et al.* (12) examined the effects of density, particle size distribution and solid concentration on the performance of centrifugal slurry pumps. They studied two different pumps, one with an impeller diameter of 280 mm and speed of 1400 rpm, and one with an impeller diameter of 270 mm and speed of 1400 rpm and 1450 rpm. The solids utilized were zinc tailings and coal. The authors of this study reported that the head and efficiency ratios correlated in a negative, linear fashion with concentration, up to concentrations of about 50% solids by weight. Above this value the efficiency and head ratios decreased exponentially. After examining the effects of particle size, Gahlot *et al* derived the following relationship:

$$K_H = (1 - H_R) = 0.00056(S-1)^{0.72}\left(1+\frac{3}{S}\right)C_W \ln(50d_W) \qquad ...(2.27)$$

The authors assumed that the efficiency reduction factor would be similar to the head reduction factor up to a particle concentration by weight of 20-25%. Above this point, based on previous studies, they stated that efficiency ratios would be about 2-9% higher than head ratios

2.2.12 Summary

Upon study of the existing literature it can be seen that three ideas have been established that will have importance to this study. These are as follows:

- as weight concentration increases, head and efficiency ratios decrease;
- the efficiency ratio usually has a slightly higher value than the head ratio, and
- that pump speed is not a discernible variable in pump performance.

These three ideas will be examined for the pumps used in this study. Unlike many of the other studies, this study will not take solids density or particle size distribution into consideration, so it will not be possible to test the validity of many of the developed correlations for the pumps in question. However, this has been done by others, particularly Roco *et al.* (11), and it has been shown that the main correlations are not suitable for the design of large-scale slurry pumps.

3.0 Equipment

3.1 Pumps

This study examines a battery of three close-coupled centrifugal pumps. The pumps are manufactured by Georgia Iron Works (GIW), of Grovetown, GA. Their model number is designated 18/20 LSA 44(45) .The pump and drive motor design parameters are listed in Tables 3.1 and 3.2, below.

Table 3.1: Pump Design Parameters

Parameter	Value
Impeller Diameter	45" / 1143 mm
Suction Line Diameter	17.25" / 438 mm
Impeller Inlet Diameter	18" / 457 mm
Discharge Line Diameter	20" / 508 mm
Number of Vanes	5
Design Discharge	16400 USGPM / 1035 L/s
Design TDH	162 ft / 49.3 m
Design Slurry Specific Gravity	1.03 to 1.57
Design Pump Speed	499 rpm
Specific Speed	1407 (Imperial)/ 27.3 (SI)

Table 3.2: Motor Design Parameters:

Parameter	Value
Output Power	1650 HP / 1231 kW
Current Requirements	4160 V / 3 phase / 60 Hz
Rated Speed	1800 rpm
Frame Size	T6810
Enclosure Type	Totally Enclosed, Ambient Air Cooled

The motors are speed controlled by a variable frequency drive (VFD) control system, which allows continuously variable speed control of the pumps, from 20% to 110% of the rated motor speed. This translates to a motor speed range of 360 to 1980 rpm, or a pump speed range of 100 to 552 rpm. In addition to allowing speed control, the VFD reduces the severity of the transient startup shockwave by starting at a motor speed of 90 rpm, or pump speed of 25 rpm, at which there is essentially no flow. The motor speed then increases to 360 rpm at a rate of 45 rpm/s (pump: increase to 100 rpm at 12.5 rpm/s). After reaching 100 pump rpm the VFD will accelerate the system to the operator selected control speed, at the same acceleration of 12.5 rpm/s. Any time a control setpoint is changed, the VFD will accelerate or decelerate at the same rate.

The variable frequency drive (VFD) system works in the following manner:

1) 3-phase utility power, at a frequency of 60 Hz, is converted from AC to DC using a silicon-controlled rectifier, commonly known as a thyristor.
2) The DC current is converted to a variable frequency AC current by use of a current inverter.

The VFD has an advertised efficiency of 97%.

The drive train between the motor and pump consists of a high speed solid coupling, a speed reducing gear coupling, with a reduction ratio of 3.588:1, and a low speed solid coupling. The pumps are constructed of a hard iron alloy, known as Gasite 28G, with additional weld-applied hard coating in the suction and discharge spools. A set of pump operating curves is displayed in Figure 3.1. These pumps have backward inclined vanes and have had the pump-out, or expeller vanes on the back of the impeller filled in order to reduce turbulence and friction between the rear casing and impeller. The pump outlet orientations are as follows: Pump #1 : top horizontal; Pump #2: bottom horizontal; Pump #3: top horizontal. A schematic diagram of the pumps and instrumentation is shown in Figure 3.2, and the pump assembly arrangement in Figure 3.3.

The pumps are fed from a feed hopper that is open to the atmosphere. Suction pressure of the first pump is controlled by the slurry level in this feed hopper. The pump discharge feeds into a 24" diameter pipeline of approximate length 5 km, which feeds into another open pump feed hopper at the next pump battery.

3.2 Instrumentation

3.2.1 Flowmeters

The flow is measured by a venturi flowmeter. The dimensions of the venturi are detailed in Figure 3.4. The design flow rate is 8,000 to 18,000 USGPM, or 504 to 1135 L/s. The inlet and throats are tied to a 3" diameter pancake type pressure differential meter via 2" diameter impulse lines. A 4-20 mA transmitter delivers a signal to the plant's Honeywell TDC control system.

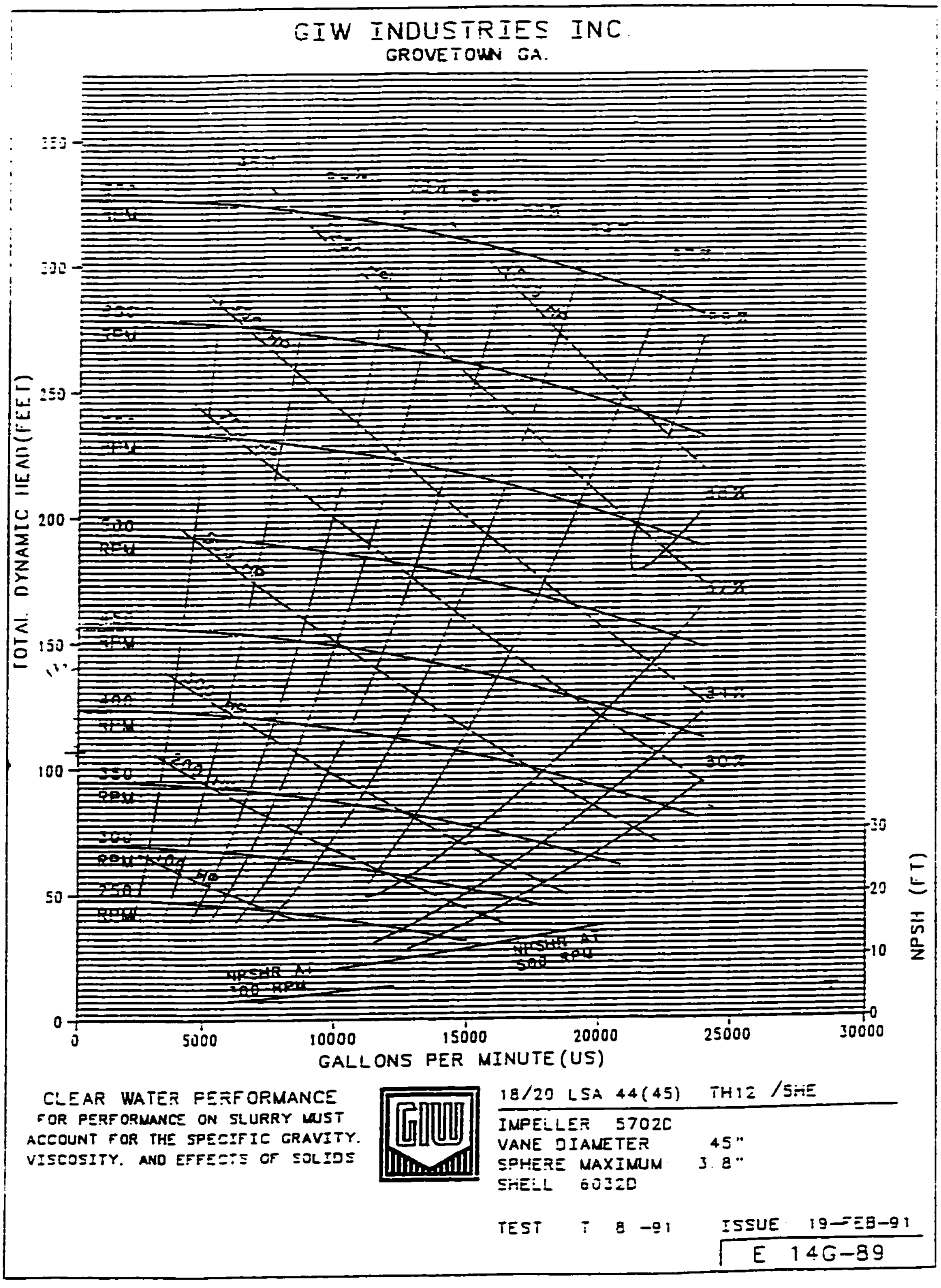

Figure 3.1: Manufacturer's Pump Curves

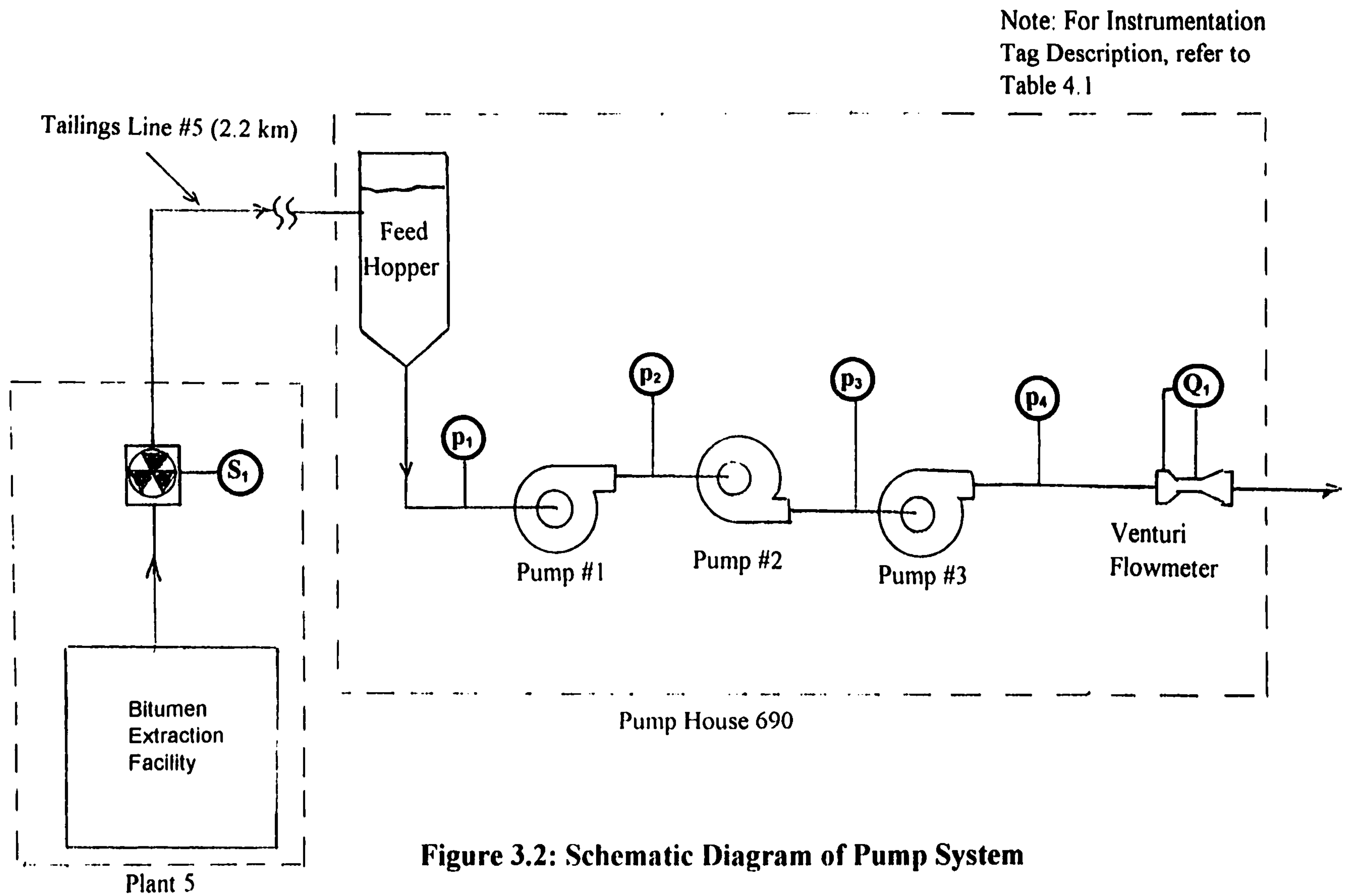

Figure 3.2: Schematic Diagram of Pump System

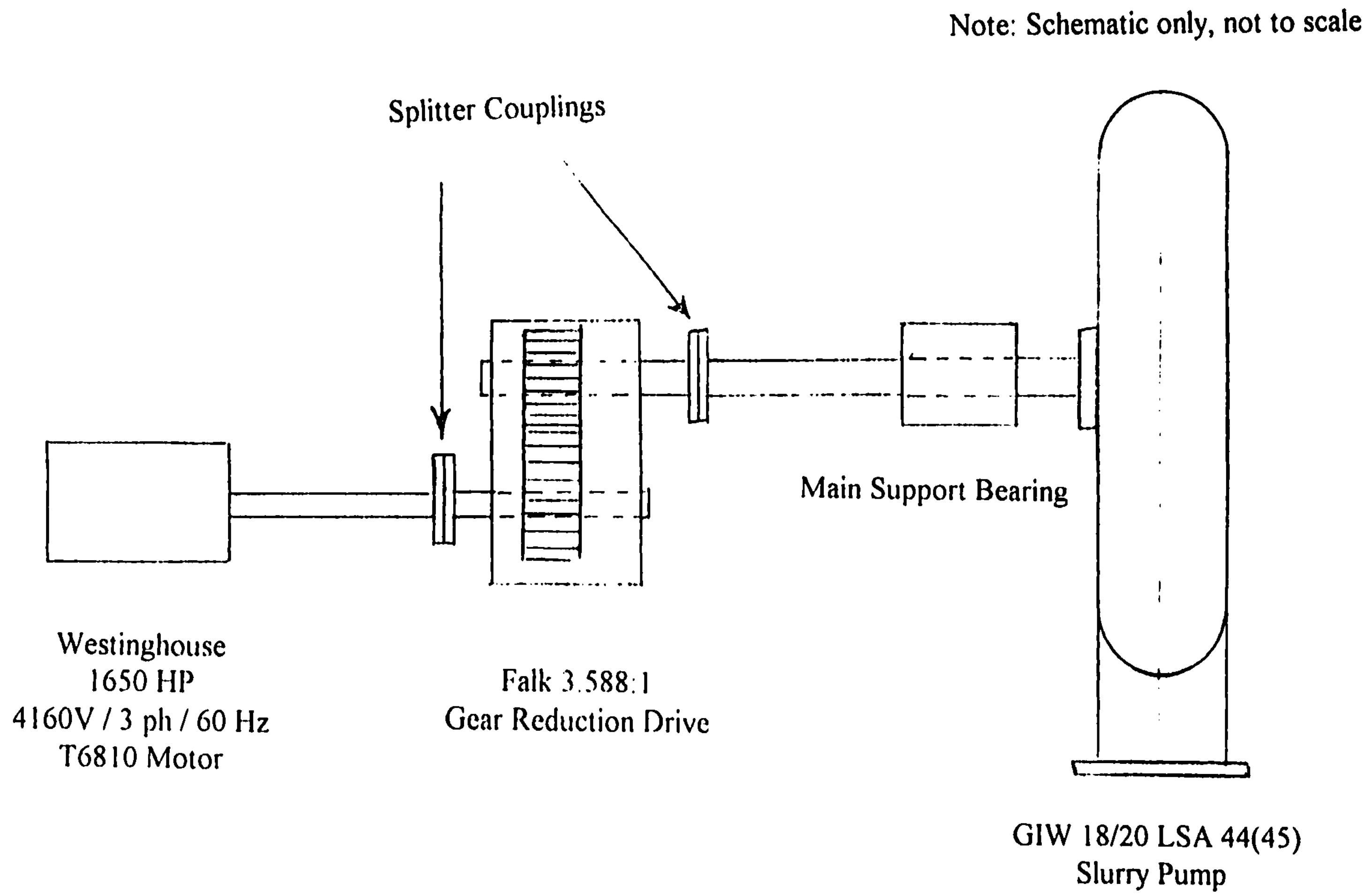

Figure 3.3: Pump Assembly Arrangement

NO.	DESCRIPTION	QTY.	MATERIAL
1	24" 300 LBS. SLIP-ON RF FLANGE	2	ASTM A105
2	24" PIPE SCH. XS	2	ASTM A106B
3	INLET CONE	1	ASTM A516 GR70
4	VENTURI THROAT SECTION	1	ASTM A106B
5	EXIT CONE	1	ASTM A516 GR70
6	3" FNPT THREADED ANVILET 3M	2	ASTM A105
7	CHROMIUM CARBIDE COATING 0.25" THICK - 2 PASSES	1	CHROMIUM CARBIDE

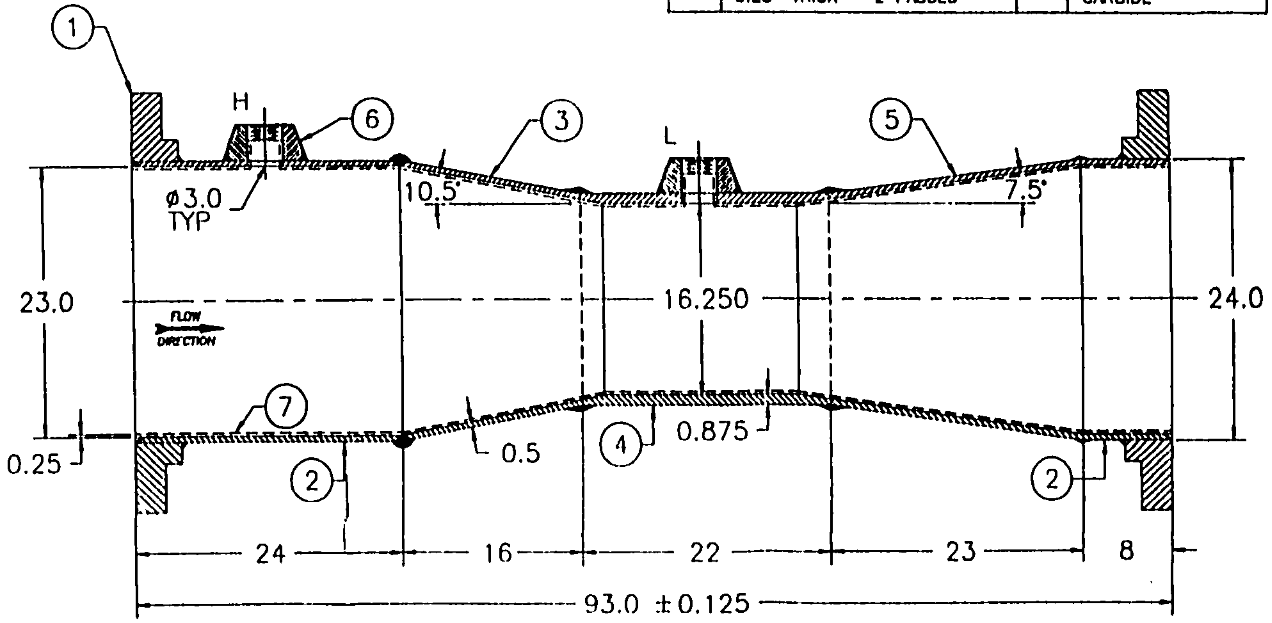

Figure 3.4: Venturi Flowmeter Details

3.2.2 Pressure Instruments

There are four pressure-measuring devices (PI's) on the pump battery. They are located on the suction of Pump #1, on the interstage spools between Pumps #1 and #2, and between Pumps #2 and #3, and on the discharge of Pump #3. All pressure instruments are located on nominal 20" pipeline, so that no correction for different velocity pressures is required. The instruments utilize 3" diameter pancake type stainless steel diaphragms, connected to the pipelines by 2" impulse legs. The suction PI has a maximum rated pressure of 200 kPa, and a transmitter range of 0-689.5 kPa. The other three PI's have maximum rated pressures of 2700 kPa, with transmitter output ranges of 0-6895 kPa. The transmitters send 4-20 mA signals to the TDC control system.

3.2.3 Density Instruments

The fluid density is measured by a nuclear density meter, labelled S_1, in the base plant, approximately 2 km upstream from the pumphouse containing the pump battery in question. The meter is located in a stretch of vertical pipe, thus avoiding errors due to flow stratification.

3.2.4 Other Instrumentation

The electrical power is measured in the DC section of the VFD, as it is much simpler to measure the power of a DC current than that of an AC current. There are no power or 3-phase considerations when measuring DC power, only voltage and amperage need be measured. The advertised efficiency of a VFD unit is 97%. If one assumes that power losses are approximately equal in the thyristor and inverter sections, as has been confirmed by Syncrude electrical engineering personnel, then the line power fed to the motor can be assumed to be 98.5% of the measured VFD DC power.

The three phase AC current flow is measured after the VFD, after the output from the VFD has been split into three individual lines feeding each of the motors. The motor speed is also an output of the VFD control system.

3.2.5 Syncrude PI System

Syncrude Canada Limited uses the Plant Information (PI) Data Acquisition and Analysis system, marketed by Oil Systems Inc. of San Leandro, CA. This is a secondary data acquisition system, in that it receives output data from the plant's primary data acquisition and control system, the Honeywell TDC Distributed Control System (DCS). The PI system is designated as a low priority application, in terms of mainframe time-sharing. As such it does not archive all TDC DCS data, which is sampled at a rate of 1 Hz or better. The PI system can be programmed to receive data from the DCS at sampling intervals as small as six seconds, but the normal sampling interval is one minute. The largest single drawback of this sampling interval is that data acquisition of different data tags is not synchronous, i.e., while the sampling rate may be the same, the sampling time is not. For any two data tags the sampling time will be out of phase by as much as 30 seconds. This makes analysis using single minute data highly unreliable, and necessitates the use of averaging techniques.

A multitude of data analysis and trending tools are available in PI, but the practice in this study was to simply use it as a data archive, and use a query program to import the data in a text format into Microsoft Excel spreadsheets.

4.0 Procedure

4.1 Advance Work

Before the commencement of this study it was necessary to identify a system that would be amenable to analysis. At their Mildred Lake plant site, Syncrude Canada Limited has 53 large scale slurry pumps handling tailings sand. In addition, there was an experimental oilsand slurry pumping facility which featured five more pumps. Since the commencement of this study a permanent oilsand slurry pumping system has come on line, in September 1997, currently using four slurry pumps, with an additional four scheduled to come on line in the near future. Four different manufacturers are represented in this sample. Of the tailings pumps 22 are constant speed and 31 variable speed.

Oilsand slurry pumping will play a much larger part in SCL operations over the next few years than it has in the recent past, although tailings sand slurry pumping will maintain importance. As such, it would have been preferable to study the performance of oilsand slurry handling pumps. However, it was decided that tailings sand pumps would be studied, for the following reasons: (1) the experimental oilsand slurry system, known as the Extraction Auxiliary Production System (EAPS) did not have sufficient instrumentation, (2) a mass balance on EAPS was never able to be satisfactorily closed; and (3) much of the instrumentation that had been installed during the initial test of this system had been removed. It was felt that any data collected from EAPS would engender so large a margin of error as to invalidate any conclusions that may have been drawn from such a study. In addition, the permanent oilsand slurry-pumping network, known as the North Mine Hydrotransport System, did not come on line in time to be contained within the scope of this study.

Of the seven pipelines handling tailings sand at SCL, only one was equipped with any method of flow measurement, thus rapidly narrowing the choice of pumps to be analyzed. The battery of three close-coupled pumps located on Southwest Sand Storage System pipeline #3, located in Pump House 690, was chosen for analysis, as this was the battery that had the venturi meter located in close proximity to it, approximately 20 metres downstream of the third pump.

All necessary instrumentation for the analysis of these pumps was in place except for interstage pressure instruments. A work order for the design and installation of pressure transmitters on the interstages between Pumps #1 and #2 and between Pumps #2 and #3 was initiated in June of 1996, and the installation, calibration and commissioning of the two new pressure transmitters was completed on May 30, 1997.

4.2 Data Collection Mechanisms

4.2.1 Collection of Data from PI System

Beginning in January 1997, data pertaining to the performance of this pump battery was downloaded from PI and archived in Microsoft Excel. The variables downloaded, their PI identifier tag names, the units associated with each tag, and the abbreviated tag names by which the variable will henceforth be referred to in this study are listed in Table 4.1, below. These variables were archived on a once per minute sampling rate by the PI system. These data were downloaded monthly into Excel spreadsheets entitled "97_01.XLS", "97_02.XLS", and so on, until March 1998.

Table 4.1: Summary of PI Variable Information

Variable	PI Tag Name	Units	Abbrev. Tag Name
Pump #1 Suction Pressure	23pi1725	kPa	p_1
First Interstage Pressure	233p2500	kPa	p_2
Second Interstage Pressure	233p2501	kPa	p_3
Pump #3 Discharge Pressure	23pi1726	kPa	p_4
Slurry Specific Gravity	5di351	SG	S_1
Flow	23fi1729	L/s	Q_1
Motor Speed	23si1748	rpm	N_1
Pump #1 Amperage	23ii1742	Amps	I_1
Pump #2 Amperage	23ii1743	Amps	I_2
Pump #3 Amperage	23ii1744	Amps	I_3
VFD Power Output	23ji1747	kW	P_1

4.2.2 Computer Models of Pump Curves

It was necessary to translate the pump curves as illustrated in Figure 3.1. The first attempt at modelling these curves involved fitting a second degree polynomial function to a central pump curve, in this case the curve observed at 450 rpm, and using the pump affinity laws to model the curves at different speeds. Such a correlation was found for this curve:

$$\text{Head (ft)} = -7.81 \times 10^{-8} \times (\text{USGPM})^2 - 2.03 \times 10^{-5} \times \text{USGPM} + 156.3 \qquad \text{...(4.1)}$$

However, when this curve was extended to fit the curves observed at other speeds using the pump affinity laws (assuming constant density and impeller diameter), thus:

$$H_2 = H_1\left(\frac{N_2}{N_1}\right)^2 \qquad \text{...(4.2)}$$

$$Q_2 = Q_1\left(\frac{N_2}{N_1}\right) \qquad \text{...(4.3)}$$

the observed resultant curves did not appear to match properly with the actual manufacturer's pump curves. As one moved further away from the root curve of 450 rpm the discrepancies increased. It was later learned that the manufacturer uses a third-degree function to fit test data to system curves, and this is the likely source of the discrepancy. For this reason, it was decided to model both the head and power curves in tabular form. These are illustrated in Tables 4.2 and 4.3. In Table 4.2, the head table, one reads the observed speed, in rpm, along the x-axis and observed flow, in USGPM, along the y-axis. The appropriate head reading, in feet, can be found at the intersection of these two values. The speed was tabulated in increments of 5 rpm, and the flow in increments of 500 USGPM. In Table 4.3, the power table, one reads the observed flow, in USGPM, along the x-axis, and the observed head (from Table 4.2), in feet, along the y-axis. The appropriate input shaft power reading, in HP, is found at the intersection of these two values. The flow was tabulated in increments of 500 USGPM, and the head was tabulated in increments of 5 feet of head.

4.2.3 Definition of Steady State Operation

This study was performed using on-line operating data, and as such the pump operations were not controlled by the author. The actual operating point of the pumps fluctuated a great deal, largely due to the fact that these pumps were controlled by the level in the feed hopper. The tuning of the level controller in the feed hopper was very aggressive, and operated in such a way that the pump speed was continuously varied to maintain the level to a very small tolerance. This resulted in pump operation that frequently resembled a square-wave function. In addition, the specific gravity of the feed was also a variable, although usually operator controlled to maintain a value close to 1.50. As previously stated, due to the non-synchronous nature of the collected per-

Table 4.2: Head Curve Table

Speed, rpm →

Flow, USGPM ↓

Flow, USGPM	350	355	360	365	370	375	380	385	390	395	400	405	410	415	420	425	430	435	440	445
2500	94	97	100	102	105	108	111	114	117	120	123	126	129	132	136	139	142	146	149	152
3000	94	97	99	102	105	108	111	114	117	120	123	126	129	132	135	139	142	145	149	152
3500	94	96	99	102	105	108	110	113	116	119	122	126	129	132	135	138	142	145	148	152
4000	93	96	99	102	104	107	110	113	116	119	122	125	128	132	135	138	141	145	148	152
4500	93	96	98	101	104	107	110	113	116	119	122	125	128	131	134	138	141	144	148	151
5000	93	95	98	101	104	107	109	112	115	118	121	125	128	131	134	137	141	144	147	151
5500	92	95	98	100	103	106	109	112	115	118	121	124	127	130	134	137	140	144	147	150
6000	92	94	97	100	103	106	109	112	115	118	121	124	127	130	133	136	140	143	146	150
6500	91	94	97	100	102	105	108	111	114	117	120	123	126	130	133	136	139	143	146	149
7000	91	93	96	99	102	105	108	111	113	117	120	123	126	129	132	135	139	142	145	149
7500	90	93	96	98	101	104	107	110	113	116	119	122	125	128	132	135	138	142	145	148
8000	90	92	95	98	101	103	106	109	112	115	118	121	125	128	131	134	138	141	144	148
8500	89	92	94	97	100	103	106	109	112	115	118	121	124	127	130	134	137	140	144	147
9000	88	91	94	96	99	102	105	108	111	114	117	120	123	126	130	133	136	140	143	146
9500	88	90	93	96	99	101	104	107	110	113	116	119	123	126	129	132	135	139	142	146
10000	87	89	92	95	98	101	104	107	109	112	116	119	122	125	128	131	135	138	141	145
10500	86	89	91	94	97	100	103	106	109	112	115	118	121	124	127	131	134	137	141	144
11000	85	88	91	93	96	99	102	105	108	111	114	117	120	123	127	130	133	136	140	143
11500	84	87	90	92	95	98	101	104	107	110	113	116	119	122	126	129	132	136	139	142
12000	83	86	89	92	94	97	100	103	106	109	112	115	118	121	125	128	131	135	138	141
12500	82	85	88	91	93	96	99	102	105	108	111	114	117	121	124	127	130	134	137	140
13000	81	84	87	90	92	95	98	101	104	107	110	113	116	120	123	126	129	133	136	139
13500	80	83	86	89	91	94	97	100	103	106	109	112	115	118	122	125	128	132	135	138
14000	79	82	85	87	90	93	96	99	102	105	108	111	114	117	121	124	127	130	134	137
14500	78	81	84	86	89	92	95	98	101	104	107	110	113	116	120	123	126	129	133	136
15000	77	80	82	85	88	91	94	97	100	103	106	109	112	115	118	122	125	128	132	135
15500	76	78	81	84	87	90	93	96	98	101	105	108	111	114	117	120	124	127	130	134
16000	75	77	80	83	86	88	91	94	97	100	103	106	110	113	116	119	122	126	129	133
16500	73	76	79	81	84	87	90	93	96	99	102	105	108	111	115	118	121	124	128	131
17000	72	75	77	80	83	86	89	92	95	98	101	104	107	110	113	117	120	123	127	130
17500	71	73	76	79	82	85	87	90	93	96	99	102	106	109	112	115	119	122	125	129
18000	69	72	75	77	80	83	86	89	92	95	98	101	104	107	111	114	117	120	124	127
18500	68	70	73	76	79	82	85	88	90	94	97	100	103	106	109	112	116	119	122	126
19000	66	69	72	75	77	80	83	86	89	92	95	98	101	104	108	111	114	118	121	124
19500	65	67	70	73	76	79	82	85	88	91	94	97	100	103	106	109	113	116	119	123
20000	63	66	69	71	74	77	80	83	86	89	92	95	98	101	105	108	111	114	118	121
20500	62	64	67	70	73	76	78	81	84	87	90	94	97	100	103	106	110	113	116	120
21000	60	63	65	68	71	74	77	80	83	86	89	92	95	98	101	105	108	111	115	118
21500	58	61	64	67	69	72	75	78	81	84	87	90	93	97	100	103	106	110	113	116
22000	57	59	62	65	68	71	73	76	79	82	85	89	92	95	98	101	105	108	111	115
22500	55	58	60	63	66	69	72	75	78	81	84	87	90	93	96	100	103	106	109	113

Flow, USGPM	450	455	460	465	470	475	480	485	490	495	500	505	510	515	520	525	530	535	540	545	550
2500	156	159	163	166	170	174	177	181	185	189	192	196	200	204	208	212	216	220	224	229	233
3000	156	159	163	166	170	173	177	181	185	188	192	196	200	204	208	212	216	220	224	228	233
3500	155	159	162	166	169	173	177	181	184	188	192	196	200	204	208	212	216	220	224	228	232
4000	155	158	162	166	169	173	176	180	184	188	192	195	199	203	207	211	215	220	224	228	232
4500	155	158	162	165	169	172	176	180	184	187	191	195	199	203	207	211	215	219	223	228	232
5000	154	158	161	165	168	172	176	179	183	187	191	195	199	203	207	211	215	219	223	227	231
5500	154	157	161	164	168	172	175	179	183	187	190	194	198	202	206	210	214	219	223	227	231
6000	153	157	160	164	168	171	175	179	182	186	190	194	198	202	206	210	214	218	222	226	231
6500	153	156	160	163	167	171	174	178	182	186	190	193	197	201	205	209	213	218	222	226	230
7000	152	156	159	163	167	170	174	178	181	185	189	193	197	201	205	209	213	217	221	225	230
7500	152	155	159	162	166	170	173	177	181	185	188	192	196	200	204	208	212	216	221	225	229
8000	151	155	158	162	165	169	173	176	180	184	188	192	196	200	204	208	212	216	220	224	228
8500	150	154	157	161	165	168	172	176	180	183	187	191	195	199	203	207	211	215	219	224	228
9000	150	153	157	160	164	168	171	175	179	183	186	190	194	198	202	206	210	214	219	223	227
9500	149	153	156	160	163	167	171	174	178	182	186	190	194	198	202	206	210	214	218	222	226
10000	148	152	155	159	162	166	170	174	177	181	185	189	193	197	201	205	209	213	217	221	226
10500	147	151	154	158	162	165	169	173	176	180	184	188	192	196	200	204	208	212	216	221	225
11000	147	150	154	157	161	164	168	172	176	179	183	187	191	195	199	203	207	211	215	220	224
11500	146	149	153	156	160	164	167	171	175	179	182	186	190	194	198	202	206	210	215	219	223
12000	145	148	152	155	159	163	166	170	174	178	181	185	189	193	197	201	205	209	214	218	222
12500	144	147	151	154	158	162	165	169	173	177	180	184	188	192	196	200	204	208	213	217	221
13000	143	146	150	153	157	161	164	168	172	176	179	183	187	191	195	199	203	207	212	216	220
13500	142	145	149	152	156	160	163	167	171	175	178	182	186	190	194	198	202	206	211	215	219
14000	141	144	148	151	155	159	162	166	170	173	177	181	185	189	193	197	201	205	209	214	218
14500	140	143	147	150	154	157	161	165	169	172	176	180	184	188	192	196	200	204	208	212	217
15000	138	142	145	149	153	156	160	164	167	171	175	179	183	187	191	195	199	203	207	211	215
15500	137	141	144	148	151	155	159	162	166	170	174	178	182	186	189	194	198	202	206	210	214
16000	136	139	143	147	150	154	157	161	165	169	173	176	180	184	188	192	196	200	205	209	213
16500	135	138	142	145	149	152	156	160	164	167	171	175	179	183	187	191	195	199	203	207	212
17000	133	137	140	144	148	151	155	159	162	166	170	174	178	182	186	190	194	198	202	206	210
17500	132	135	139	143	146	150	153	157	161	165	169	172	176	180	184	188	192	196	200	205	209
18000	131	134	138	141	145	148	152	156	159	163	167	171	175	179	183	187	191	195	199	203	207
18500	129	133	136	140	143	147	151	154	158	162	166	169	173	177	181	185	189	193	198	202	206
19000	128	131	135	138	142	145	149	153	157	160	164	168	172	176	180	184	188	192	196	200	204
19500	126	130	133	137	140	144	148	151	155	159	163	166	170	174	178	182	186	190	194	199	203
20000	125	128	132	135	139	142	146	150	153	157	161	165	169	173	177	181	185	189	193	197	201
20500	123	127	130	134	137	141	144	148	152	156	159	163	167	171	175	179	183	187	191	195	200
21000	121	125	128	132	136	139	143	146	150	154	158	162	165	169	173	177	181	185	190	194	198
21500	120	123	127	130	134	137	141	145	149	152	156	160	164	168	172	176	180	184	188	192	196
22000	118	122	125	129	132	136	139	143	147	151	154	158	162	166	170	174	178	182	186	190	194
22500	116	120	123	127	130	134	138	141	145	149	153	156	160	164	168	172	176	180	184	188	192

Table 4.3: Power Curve Table

Flow, USGPM →

Head, Feet ↓

	2500	3000	3500	4000	4500	5000	5500	6000	6500	7000	7500	8000	8500	9000	9500	10000	10500	11000	11500	12000	12500	13000	13500	14000	14500	15000
60	n/a	n/a	n/a	n/a	n/a	n/a	n/a	n/a	n/a	n/a	n/a	n/a	n/a	n/a	n/a	n/a	n/a	n/a	n/a	n/a	n/a	n/a	n/a	n/a	n/a	n/a
65	n/a	n/a	n/a	n/a	n/a	n/a	n/a	n/a	n/a	n/a	n/a	n/a	n/a	n/a	n/a	n/a	n/a	n/a	n/a	n/a	n/a	n/a	n/a	n/a	n/a	n/a
70	n/a	n/a	n/a	n/a	n/a	n/a	n/a	n/a	n/a	n/a	n/a	n/a	n/a	n/a	n/a	n/a	n/a	n/a	n/a	n/a	n/a	n/a	n/a	n/a	n/a	n/a
75	n/a	n/a	n/a	n/a	n/a	n/a	n/a	n/a	n/a	n/a	n/a	n/a	n/a	n/a	n/a	n/a	n/a	n/a	n/a	n/a	n/a	n/a	291	301	310	319
80	n/a	n/a	n/a	n/a	n/a	n/a	n/a	n/a	n/a	n/a	n/a	n/a	n/a	n/a	233	241	251	260	269	278	289	299	309	319	330	340
85	n/a	n/a	n/a	160	167	174	181	189	197	204	212	221	230	239	248	256	266	276	286	296	306	317	327	338	350	362
90	n/a	159	166	173	181	188	195	203	211	219	227	236	245	254	263	273	283	293	303	313	324	335	347	358	371	383
95	165	172	180	187	194	202	209	217	226	234	243	251	260	270	280	289	300	310	321	332	343	355	367	379	392	405
100	178	185	193	200	208	216	224	232	240	249	258	267	276	286	296	306	317	328	339	351	363	375	387	400	414	427
105	191	199	206	214	222	230	238	247	255	264	274	283	293	303	313	324	335	347	358	370	382	395	408	421	436	450
110	204	212	219	227	236	244	253	261	271	280	290	300	309	320	331	342	353	366	377	390	403	416	429	443	458	473
115	217	225	233	241	250	258	267	277	286	296	306	316	326	337	349	360	372	385	397	410	423	437	451	465	480	496
120	230	238	247	255	264	273	282	292	302	312	323	333	344	355	367	379	391	405	417	430	444	458	473	488	503	519
125	243	252	260	269	278	288	298	308	318	328	339	351	361	373	385	398	411	424	437	451	465	480	495	510	526	543
130	257	265	274	284	293	303	313	323	334	345	356	368	380	392	404	417	430	445	458	472	487	502	517	533	549	566
135	270	279	289	298	308	318	329	340	351	362	374	386	398	410	423	437	450	465	479	494	509	524	540	557	573	590
140	284	293	303	313	323	334	345	356	367	379	391	404	416	429	443	457	471	486	500	515	531	547	563	580	597	614
145	298	308	318	328	339	350	361	373	384	397	409	422	435	449	462	477	491	507	521	537	553	569	586	603	620	638
150	312	322	333	343	354	366	377	389	402	414	427	440	454	468	482	497	512	528	543	559	575	592	609	627	644	662
155	327	337	348	359	370	382	394	407	419	432	445	459	473	488	502	517	533	549	564	581	598	615	633	651	668	687
160	341	352	363	375	387	399	411	424	437	450	464	478	493	508	523	538	554	570	586	603	620	638	656	674	692	711
165	356	368	379	391	403	416	429	442	455	469	483	497	512	528	543	559	575	592	608	625	643	661	679	698	716	735
170	372	383	395	408	420	433	446	460	473	487	502	517	532	548	564	580	596	613	630	648	666	684	703	722	741	760
175	387	399	412	424	437	450	464	478	492	506	521	536	552	568	584	601	618	635	652	670	689	707	726	745	765	784
180	403	416	428	441	454	468	482	496	510	525	540	556	572	588	605	622	639	657	675	693	712	731	750	769	789	809
185	419	432	445	458	472	486	500	515	529	545	560	576	592	609	626	643	661	679	697	716	735	754	773	793	813	833
190	436	449	462	476	490	504	518	533	548	564	580	596	613	630	647	665	683	701	719	738	758	777	797	817	837	857
195	452	466	479	494	508	522	537	552	568	584	600	617	633	651	668	686	705	723	742	761	781	800	820	840	861	881
200	469	483	497	511	526	541	556	571	587	603	620	637	654	672	690	708	727	745	765	784	804	824	844	864	885	905
205	486	500	515	529	544	559	575	591	607	623	640	658	675	693	711	730	749	768	787	807	827	847	867	887	909	929
210	503	518	532	547	562	578	594	610	626	643	661	679	696	714	733	752	771	790	810	830	850	870	891	911	932	953
215	521	535	550	565	581	597	613	629	646	664	681	699	717	736	755	774	793	813	833	853	873	893	914	935	955	976
220	538	553	568	584	599	616	632	649	666	684	702	720	739	758	777	796	816	836	856	877	897	917	938	958	978	1000
225	555	571	586	602	618	634	651	669	686	704	723	741	760	779	799	819	839	859	880	900	920	940	961	982	1001	1023
230	573	588	604	620	636	653	671	688	707	725	743	762	782	802	821	841	862	882	903	924	944	964	n/a	n/a	n/a	n/a
235	590	606	622	638	655	672	690	708	727	746	764	783	804	824	844	864	885	906	n/a	n/a	n/a	n/a	n/a	n/a	n/a	n/a
240	607	623	640	656	673	691	709	728	747	766	n/a	n/a	n/a	n/a	n/a	n/a	n/a	n/a	n/a	n/a	n/a	n/a	n/a	n/a	n/a	n/a

Table 4.3 Cont.

Flow, USGPM →

Head, Feet ↓

	15500	16000	16500	17000	17500	18000	18500	19000	19500	20000	20500	21000	21500	22000	22500
60	n/a	n/a	n/a	n/a	n/a	n/a	336	348	361	375	390	403	420	436	453
65	n/a	n/a	n/a	n/a	333	346	359	371	384	399	414	428	444	460	477
70	n/a	n/a	332	344	356	369	382	396	409	424	439	454	470	487	503
75	331	342	354	367	380	393	407	421	435	450	465	481	497	514	531
80	352	364	377	390	404	417	431	446	461	477	492	508	525	542	560
85	374	387	400	414	428	442	457	472	488	504	520	537	554	572	589
90	396	410	423	438	452	467	482	498	515	531	548	565	583	601	620
95	419	433	447	462	477	492	508	525	542	559	576	594	613	631	650
100	442	456	471	486	502	518	535	551	569	587	605	623	642	661	680
105	465	480	495	511	527	544	561	578	596	615	633	652	671	691	711
110	488	504	520	536	552	570	587	605	624	642	661	681	701	720	741
115	511	528	544	561	578	596	614	632	651	670	690	710	730	750	770
120	535	552	569	586	603	622	640	659	678	698	718	738	758	779	800
125	559	576	593	611	629	648	667	686	705	725	745	766	786	807	828
130	583	601	618	637	655	674	693	712	732	752	773	793	814	835	857
135	607	625	643	662	681	700	719	739	759	779	800	821	842	863	885
140	632	650	668	687	706	726	746	766	786	806	827	848	869	891	913
145	656	675	694	713	732	752	772	792	812	833	854	875	896	918	941
150	681	700	719	738	758	778	798	818	839	859	881	902	924	946	969
155	706	725	744	764	783	804	824	844	865	886	907	929	951	974	997
160	730	749	769	789	809	829	850	871	891	913	934	956	978	1002	1026
165	755	774	794	814	835	855	876	897	917	939	961	983	1006	1031	1056
170	780	799	819	840	860	881	901	923	944	966	988	1011	1035	1061	1087
175	804	824	844	865	886	906	927	949	970	993	1016	1040	1065	1092	1119
180	829	849	869	890	911	932	953	975	997	1021	1044	1069	1096	1124	1154
185	853	874	894	915	936	957	979	1002	1025	1049	1074	1101	1129	1159	1191
190	878	898	919	940	962	983	1006	1029	1053	1078	1104	1133	1164	1196	1231
195	902	923	944	965	987	1009	1032	1056	1081	1107	1136	1168	1201	1235	n/a
200	926	947	968	990	1012	1035	1059	1083	1111	1138	1170	1205	1241	n/a	n/a
205	950	971	993	1015	1037	1061	1086	1111	1141	1170	1205	1244	n/a	n/a	n/a
210	974	995	1017	1040	1062	1088	1114	1140	1173	n/a	n/a	n/a	n/a	n/a	n/a
215	997	1019	1041	1064	1087	1115	1143	n/a	n/a	n/a	n/a	n/a	n/a	n/a	n/a
220	1021	1042	1065	1089	n/a	n/a	n/a	n/a	n/a	n/a	n/a	n/a	n/a	n/a	n/a
225	n/a	n/a	n/a	n/a	n/a	n/a	n/a	n/a	n/a	n/a	n/a	n/a	n/a	n/a	n/a
230	n/a	n/a	n/a	n/a	n/a	n/a	n/a	n/a	n/a	n/a	n/a	n/a	n/a	n/a	n/a
235	n/a	n/a	n/a	n/a	n/a	n/a	n/a	n/a	n/a	n/a	n/a	n/a	n/a	n/a	n/a
240	n/a	n/a	n/a	n/a	n/a	n/a	n/a	n/a	n/a	n/a	n/a	n/a	n/a	n/a	n/a

minute data it was necessary to define an averaging routine. It was decided to average the input data over one-hour periods.

In addition to dampening the effects of the non-synchronous data, the averaging helped ameliorate another difficulty with the data collection. This arose from the fact that the density meter was located in the base extraction plant, some 2.29 km upstream of Pump House 690, where the pump battery in question was located. There was also a feed hopper with an approximate capacity of 200 m^3. The combined effect was that the density of the fluid passing through the pump system would have been measured by the density meter at some point in time considerably earlier than the time of entry into the pumps. A calculation of the residence time between the density meter and the pump entry was performed. The level control setpoint of the feed hopper was normally ≈85% of the level indicator range. At this value, the volume between the density meter and pump inlet was found to be 818 m^3. The residence time is defined as the system volume divided by the flow rate. Using Litres per second as the units for flow, the equation for residence time, in minutes, reduces to:

$$t_{res} = \frac{13633}{Q} \qquad \text{...(4.4)}$$

A plot of this function is shown in Figure 4.1. As can be seen, for most typical flow rates (1000-1200 L/s), the residence time ranges from 11 to 13 minutes. For this reason, it was assumed that a standard time delay of 12 minutes be used for data

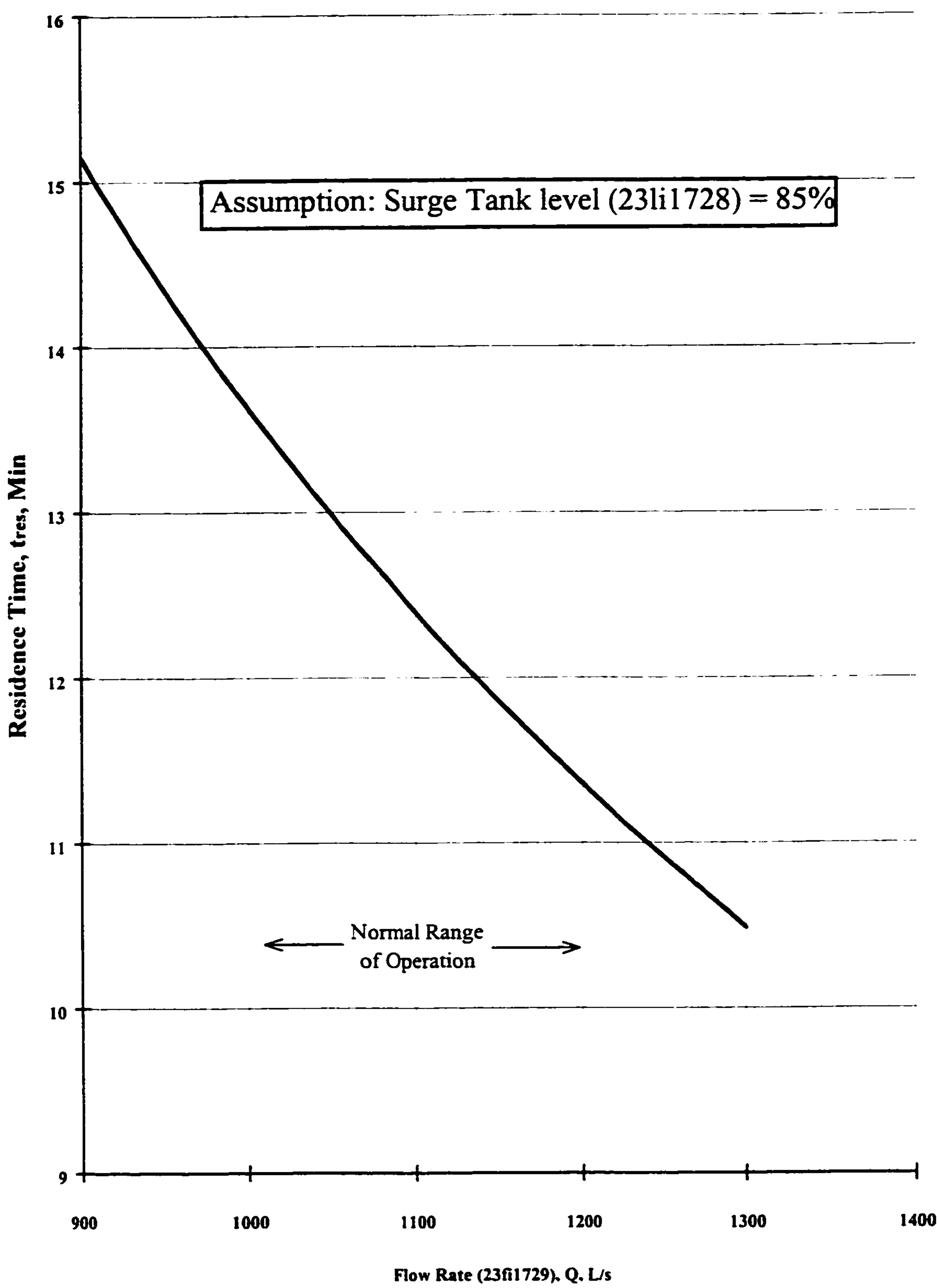

Figure 4.1: Residence Time vs. Flow, Line 3, Plant 5 - Pumphouse 690

analysis. This means that for any set of pressure, flow and electrical measurements taken at time $t=t_0$, the accompanying density measurement should not be that registered at $t=t_0$, but that registered at $t=t_0$-12 minutes.

In addition to the time delay between density measurement and flow measurement, one has to consider mixing effects. While it is not unreasonable to make the assumption of no axial mixing in the pipeline, such an assumption may not be valid for the feed hopper. While the author did not attempt to model the mixing behaviour of the feed hopper, it is clear that its behaviour would range between the ideal mixing assumed in a constantly stirred tank and the zero axial mixing model of a plug flow reactor. The process of averaging data over a one hour time period is assumed to filter out any distortions due mixing of slurry in the feed hopper.

For every one-minute data observation, an average was obtained by taking the mean of all the one-minute observations for a sixty-minute period beginning at the time of the one-minute observations. Thus, in any one-hour period sixty one-hour averages were obtained.

It was then necessary to filter these data to remove any data that may have been recorded during transient operation. A parameter was required to separate steady-state operational data from transient data. A method referred to here as the "Measure of Transience" (MoT) method was utilized. The process for using this methodology is as follows:

1) For any data point "x", the mean of 60 consecutive one-minute observations is obtained. This referred to as $\bar{x}$.

2) For the same data point "x", the standard deviation of the same 60 consecutive one-minute observations is obtained. This is referred to as $s(x)$.

3) The Measure of Transience (MoT) is obtained for data point "x". This is defined as:

$$MoT = \frac{s(x)}{\bar{x}} \qquad ...(4.5)$$

The value of the MoT is the criteria for deciding whether a one-hour period of operation is to be considered as a steady-state or transient period of operation. In this study, the MoT's of both pump speed and slurry density were examined as selection criteria.

4.2.4 Extraction of Steady State Data

In this study the data was manipulated at this stage in seven-day (10,080-minute) blocks. For each one-minute observation, the one-hour averages for all of the input parameters as described in Table 4.1 were calculated. The standard deviations of the one-hour blocks were calculated for pump speed and slurry density. The MoT's, as described above, were calculated for each hourly average observation of pump speed and slurry density. Plots of pump speed MoT and slurry density MoT for a typical day of operation are shown in Figures 4.2 and 4.3.

A cutoff value for inclusion or rejection of a data point was then defined. If both the speed and density MoT's fell below the cutoff point then the data point was assumed to be describing steady state operation for the enclosed one-hour period of operation. If either MoT fell above the specified cutoff value then the data point was assumed to be describing transient operation, and the data point was rejected. The method of selecting the cutoff value is described in Section 5.1.5.

The data points that were assumed to be describing steady state operation were then segregated and sorted according to time. As any one-hour average observation encompasses sixty separate one-minute observations, it was necessary to cull the accepted data point such that data were not duplicated. For example, when one examines Figure 4.2, it will be observed that several data points immediately after 9:00 fall below the 2% speed MoT. However, we cannot use all of these observations, as data would be duplicated. The hourly average data point for 9:00 encompasses all the one-minute observations for 9:00 to 9:59. If one was to use the 9:00 data point in an analysis, one would have to then reject all hourly average data point observations for 9:01 to 9:59, as these average observations use data that has already been included in the hourly average observation for 9:00. Thus, it was necessary to observe all data points that fell within the cutoff criteria and to make sure that any observations that

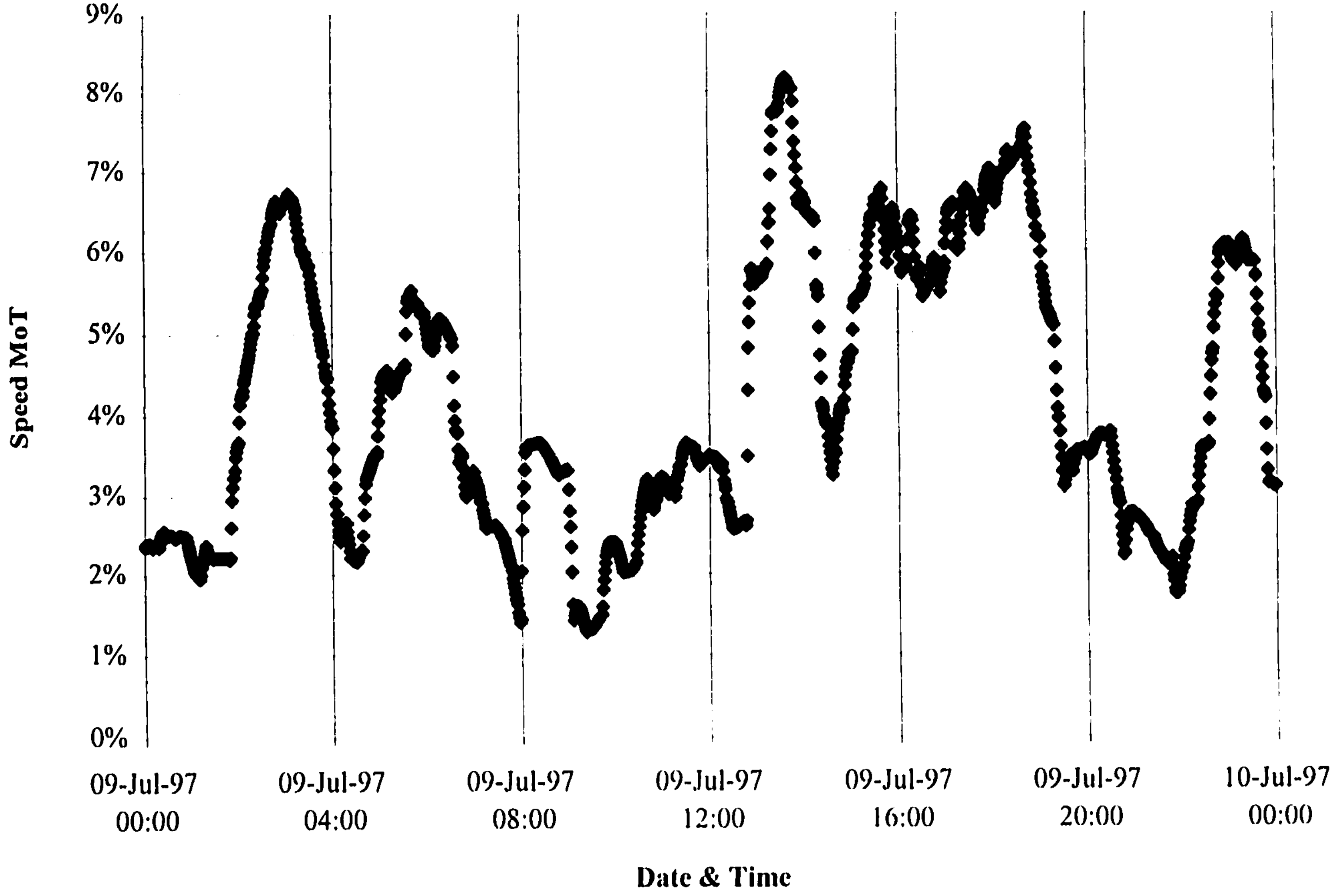

Figure 4.2: Speed MoT vs. Time, Typical Period of Operation

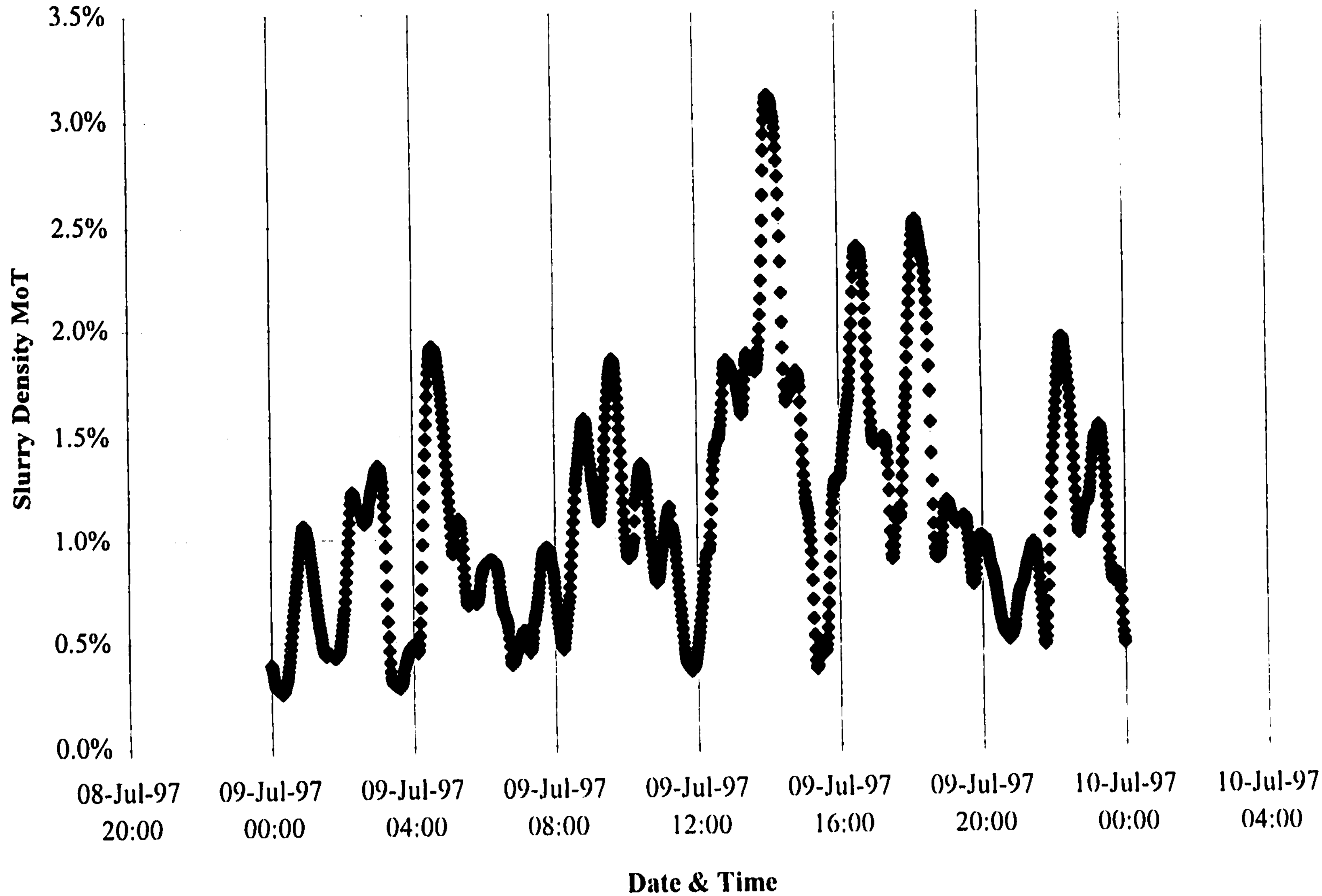

Figure 4.3: Slurry Density MoT vs. Time, Typical Period of Operation

were advanced for inclusion in any further analysis did not encroach upon the one-hour envelope inherent in all the other data points. In brief, it was necessary to ensure that all forwarded observations fell at least one hour apart.

4.2.5 Data Handling in Microsoft Excel

After all data had been filtered according to the procedures described in sections 4.2.3 and 4.2.4, a population of one-hour average periods of steady state operation had been assembled. These data points were then analyzed to yield values for pump performance factors, namely head and efficiency ratios. Although all of the PI data was collected in *SI* units, the pump curves were tabulated in Imperial units. For this reason it was decided to convert all PI input data from *SI* to Imperial units. The head, in feet, was calculated using the input data from Table 4.1 in Equation (2.1):

$$\Delta H = TDH = \frac{v_{out}^2 - v_{in}^2}{2g} + \frac{p_{out} - p_{in}}{\rho g} + (z_{out} - z_{in}) \qquad ...(2.1)$$

As all pressure indicators were located on pipe spools of equal diameter, the velocity head terms in Equation (2.1) cancel each other out. The head calculations, using the tag names as assigned in Table 4.1, are as follows:

Observed Head Added, Pump #1 (feet of fluid):

$$\Delta H_{1.obs} = \left[\frac{(p_2 - p_1)}{gS_1} + (z_2 - z_1) \right] \times 3.2808 ft / m \qquad ...(4.6)$$

Observed Head Added, Pump #2 (feet of fluid):

$$\Delta H_{2.obs} = \left[\frac{(p_3 - p_2)}{gS_1} + (z_3 - z_2) \right] \times 3.2808 ft / m \qquad ...(4.7)$$

Observed Head Added, Pump #3 (feet of fluid):

$$\Delta H_{3.obs} = \left[\frac{(p_4 - p_3)}{gS_1} + (z_4 - z_3) \right] \times 3.2808 ft / m \qquad ...(4.8)$$

The flow value is converted from L/s to USGPM thus:

$$Q = Q_1 \times \left(0.26417 USGal/_L \right) \times \left(60 s/_{\min} \right) \qquad ...(4.9)$$

The observed shaft power per pump is required. As the power indicator measures the total power fed from the VFD to the three pumps, it is necessary to apportion the power from the VFD according to the ratio of amperages going to each pump. The VFD efficiency of 98.5% is to be included in this calculation Equations (4.10) to

(4.12) describe the shaft horsepower of each pump. For example, the share of power going to Pump #1 is calculated by dividing the amperage of the current to Pump #1 divided by the total amperage to the three pumps. The VFD power is multiplied by this fraction, and by the VFD, motor, and gear drive efficiencies to obtain the estimation of the shaft power into Pump #1. These calculations are detailed in Appendix A.

Observed Shaft Power, Pump #1 (HP):

$$SHP_{1.obs} = \frac{I_1}{(I_1 + I_2 + I_3)} P_1 \eta_{VFD} \eta_E \eta_D \times \left(\frac{1.34HP}{kW} \right) \qquad ...(4.10)$$

Observed Shaft Power, Pump #2 (HP):

$$SHP_{2.obs} = \frac{I_2}{(I_1 + I_2 + I_3)} P_1 \eta_{VFD} \eta_E \eta_D \times \left(\frac{1.34HP}{kW} \right) \qquad ...(4.11)$$

Observed Shaft Power, Pump #3 (HP):

$$SHP_{3.obs} = \frac{I_3}{(I_1 + I_2 + I_3)} P_1 \eta_{VFD} \eta_E \eta_D \times \left(\frac{1.34HP}{kW} \right) \qquad ...(4.12)$$

At this point the formulae for head and efficiency ratios should be recalled:

Head Ratio:

$$H_R = \frac{\Delta H_m}{\Delta H_w} \qquad \text{...(2.8)}$$

Efficiency Ratio:

$$\eta_R = H_R\left(\frac{\rho_m}{\rho_w}\right)\left(\frac{SHP_w}{SHP_m}\right) \qquad \text{...(2.10)}$$

The predicted head is extracted from Table 4.2, using Microsoft Excel table lookup functions, with observed speed and flow as inputs. The exact value of predicted head is obtained by two-dimensional linear interpolation. Similarly, the predicted shaft power is extracted from Table 4.3, using the value of observed head from Table 4.2 and the flow as inputs. The exact value of predicted shaft power is also obtained via two-dimensional linear interpolation. These values, along with the observed heads and shaft powers are entered into Equations (2.8) and (2.9) to yield values for head and efficiency ratio. These calculations are detailed in Appendix A.

5.0 Results

5.1 Data Analysis

5.1.1 Period of Analysis

The lifespan of three impellers, one in each of the three pumps, from installation to removal from the pumps, was examined. The impellers were installed during a shutdown in April 1997, and began pumping slurry on May 8, 1997. Pump #1 had a new impeller and casing installed at this time, and in essence was a completely new pump. Pump #2 had a new impeller installed, but the casing was described by SCL maintenance personnel as having "lots of wear in the throat area." Pump #3 had a used impeller that had been patched and repaired. It is not know if the repairs had been made to the impeller shrouds or the vanes. The casing was not changed, but described as being "OK". Refer to Figure 3.2 for the orientation of the three pumps.

The impeller in Pump #1 was replaced on August 18, 1997. The impellers in Pumps #2 and #3 were replaced on October 20-22, 1997.

5.1.2 Estimation of Interstage Pressures

It was desired to analyze operating data from the installation of new impellers in the pumps. These impellers were installed during a shutdown in April of 1997, and came on line on May 8, 1997. The interstage pressure meters, denoted as p_2 and p_3 in Figure 3.2, did not come on-line until June 6, 1997. In order to use the data collected between May 8 and June 6, it was necessary to estimate the interstage pressures during that period. This was done by dividing the fraction of the head developed by each pump by the fraction of amperage each pump was consuming. That is, the proportion of the total head added by each pump was assumed to be a function of its current draw.

For the period of operation from June 6 to June 30, 1997 for each observation a value of % head/% amperage, termed a "pump factor" was calculated for each pump These factors were plotted versus cumulative sand throughput, and a linear best fit curve was calculated by the method of least squares for each of the three pumps. These curves were extrapolated back to zero cumulative flow. These calculations are detailed in Appendix B. The pump factors and best-fit curves are shown in Figure 5.1. For each of the observations between May 8 and June 6 the observed cumulative throughput was multiplied by the function of the respective best fit curve, and estimates of the interstage pressures were obtained.

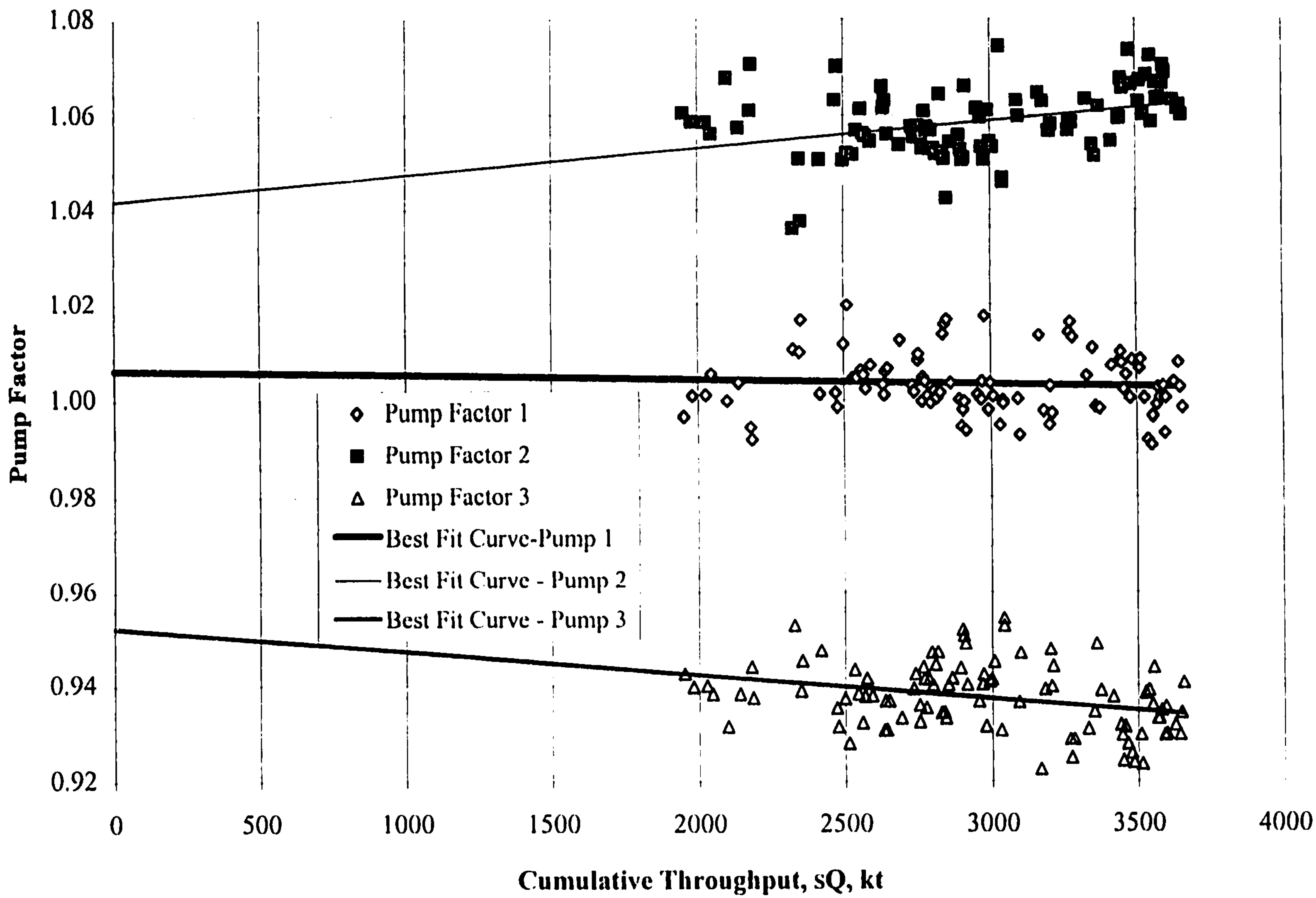

Figure 5.1: Actual and Best Fit Pump Factors vs. Cumulative Throughput

The functions of the best-fit curves are as follows:

Pump #1: Pump Factor = $[-0.99 \times 10^{-6} \times (\text{Cum Sand Flow})] + 1.006$ ...(5.1)

Pump #2 Pump Factor = $[5.60 \times 10^{-6} \times (\text{Cum Sand Flow})] + 1.042$ ...(5.2)

Pump #3 Pump Factor = $[-4.97 \times 10^{-6} \times (\text{Cum Sand Flow})] + 0.952$ ...(5.3)

Cumulative Sand Flow is measured in kilotonnes.

5.1.3 Correction of Power Readings before May 30, 1997

Power reading taken before May 30, 1997 seemed to be abnormally low. An analysis of these power readings, extracting the power factor, showed a power factor of above one for most of these readings. It was decided that these power readings should be corrected by estimating a correct power factor. Power factors for all power readings after May 30, 1997 were calculated as a function of motor output. A second degree least-squares best-fit curve was fitted to the power factors. After rearranging, and solving the resulting quadratic equation, the actual power at observations before May 30, 1997 was calculated from Equation 5.4, below:

$$P = \frac{\left(\frac{1}{NI} - 1.65x10^{-6}\right) - \sqrt{\left(1.65x10^{-6} - \frac{1}{NI}\right)^2 - 8.466x10^{-12}}}{-5.10x10^{-10}} \qquad ...(5.4)$$

(Note: N= pump speed, I = pump current draw).

5.1.4 Motor Efficiencies

The motor efficiency is a function of motor load, which is defined as input line power divided by rated power. The rated power of these motors is 1650 HP. Figure 5.2 shows the manufacturer's plot of efficiency and motor power factor. The curve of efficiency versus load factor (LF) was fitted to a third degree least-squares best fit curve with the following equation (both load factor and efficiency are cited as fractions, and not percentages):

$$\eta_E = 0.089LF^3 - 0.266LF^2 + 0.245LF + 0.891 \qquad ...(5.5)$$

As per manufacturer's specifications, the efficiency of the reducing gear drive was assumed to be 98.5%.

5.1.5 Volume of Steady State Data

The period of study for these pumps was May 8, 1997 to October 21, 1997. This was the period between change of impellers in Pumps #2 and #3. The impeller in Pump #1

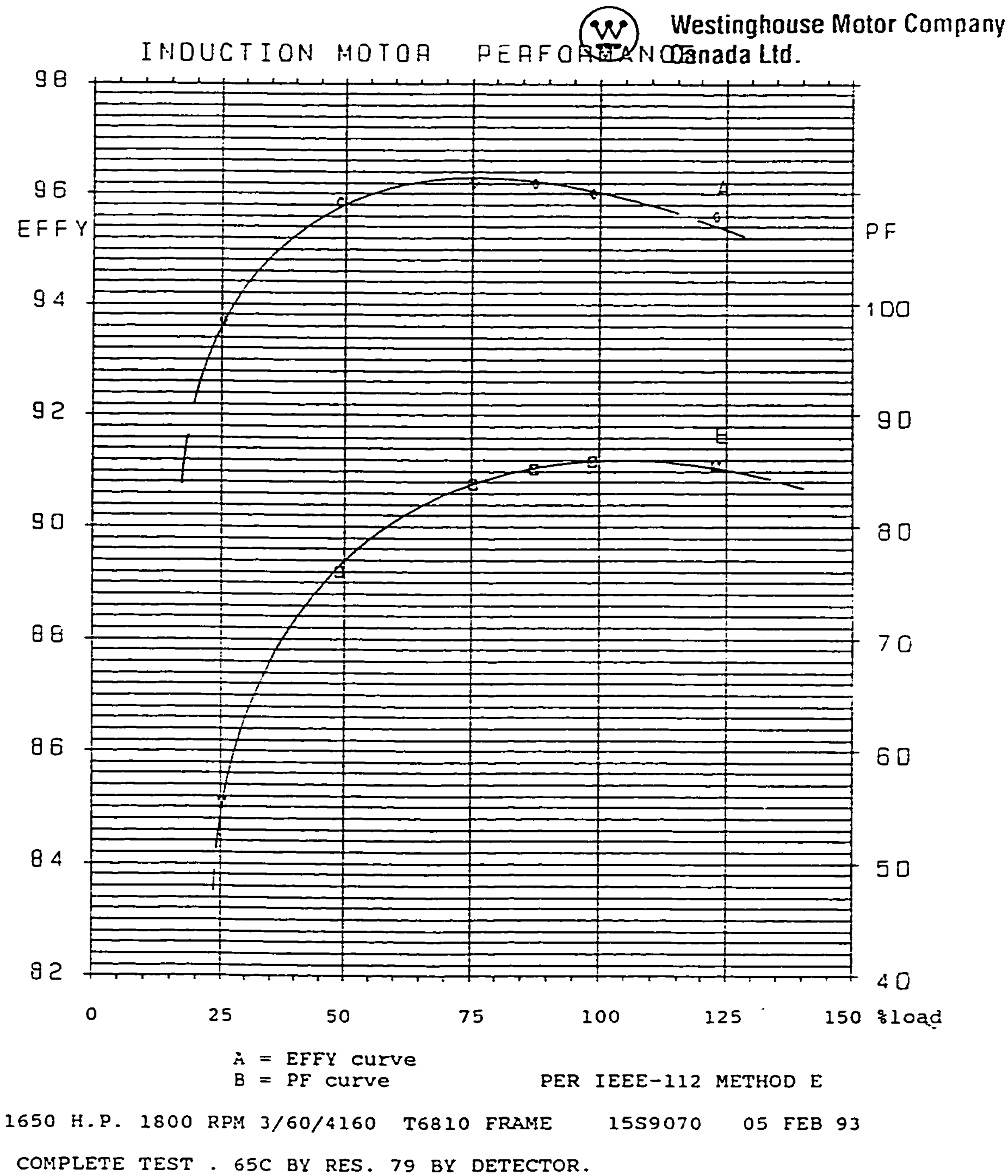

Figure 5.2: Motor Efficiency and Power Factor

was installed at the same time as those in Pumps #2 and #3, but it was changed out on August 18, 1997.

The period of study encompasses 3973 hours of elapsed time. Of this time, 653 hours were spent in downtime, 81 hours were spent operating on water, and a further 30 hours were spent ramping the slurry density from water to operating density, or vice versa. This left a total of 3209 hours of time with the pumps in operation pumping sand slurry. Utilizing the "Measure of Transience" methodology previously described, data describing steady state operation was extracted. The number of per minute observations meeting various pump speed and specific gravity MoT's is shown in Table 5.1. The entries in Table 5.1 are the number of occurrences when both the pump speed and slurry specific gravity MoT's are below the specified amount in the headers of the columns. For example, in the column headed by "1%", for each week of the study the number of observations for which both the pump speed and SG MoT's are below 1% is listed. Remember that the MoT is defined as the standard deviation of the observations of a variable over a continuous 60-minute interval divided by the mean value of the same variable over the same continuous 60-minute interval. If the MoT is described as being 1%, then the standard deviation has a value that is 0.01 times, or 1% of, the mean for that period of operation.

Table 5.1: Occurrences Within Specified MoT's

	Cutoff MoT					
Week of Study	**1%**	**1.5%**	**2%**	**3%**	**4%**	**5%**
1	149	413	717	1371	2465	3949
2	289	915	1422	2874	5078	7226
3	95	419	821	2323	4402	7037
4	210	474	701	1257	2084	3709
5	92	381	784	1843	2952	4862
6	348	713	1306	2830	4005	5194
7	3271	4774	5580	6479	7221	7949
8	503	1028	2212	5185	6895	8186
9	762	1458	2375	4475	6082	7409
10	124	530	1044	2788	4846	6205
11	1201	1738	2474	3679	4798	5485
12	199	594	1220	3065	4902	6284
13	199	880	1834	3977	5498	6539
14	243	600	964	2349	3983	5285
15	2699	3228	3739	4752	5288	5826
16	108	358	834	1937	3475	4796
17	1466	2741	3770	5725	7492	8318
18	3354	5402	6481	7685	8196	8430
19	218	410	485	532	578	589
20	2110	2739	3360	3805	4081	4241
21	1533	2607	3489	4582	5612	7002
22	663	1451	2383	4444	6086	6945
23	1042	1735	2673	5007	6766	8637
24	1779	3065	3882	5633	6845	7721
Total	22,657	38,653	54,550	88,597	119,630	147,824

The physical meaning of the MoT is described as follows, and illustrated in Figure 5.3. If the pump speed and specific gravities are assumed to be distributed in a Normal, or Gaussian fashion, then the MoT describes how close to the mean the data are clustered. If the MoT is assumed to be 1%, and the mean of a variable is 1.0, then a single standard deviation has a value of 0.01. In a Gaussian distribution 68% of the data are contained within ±1 standard deviation of the mean, or in this case an interval

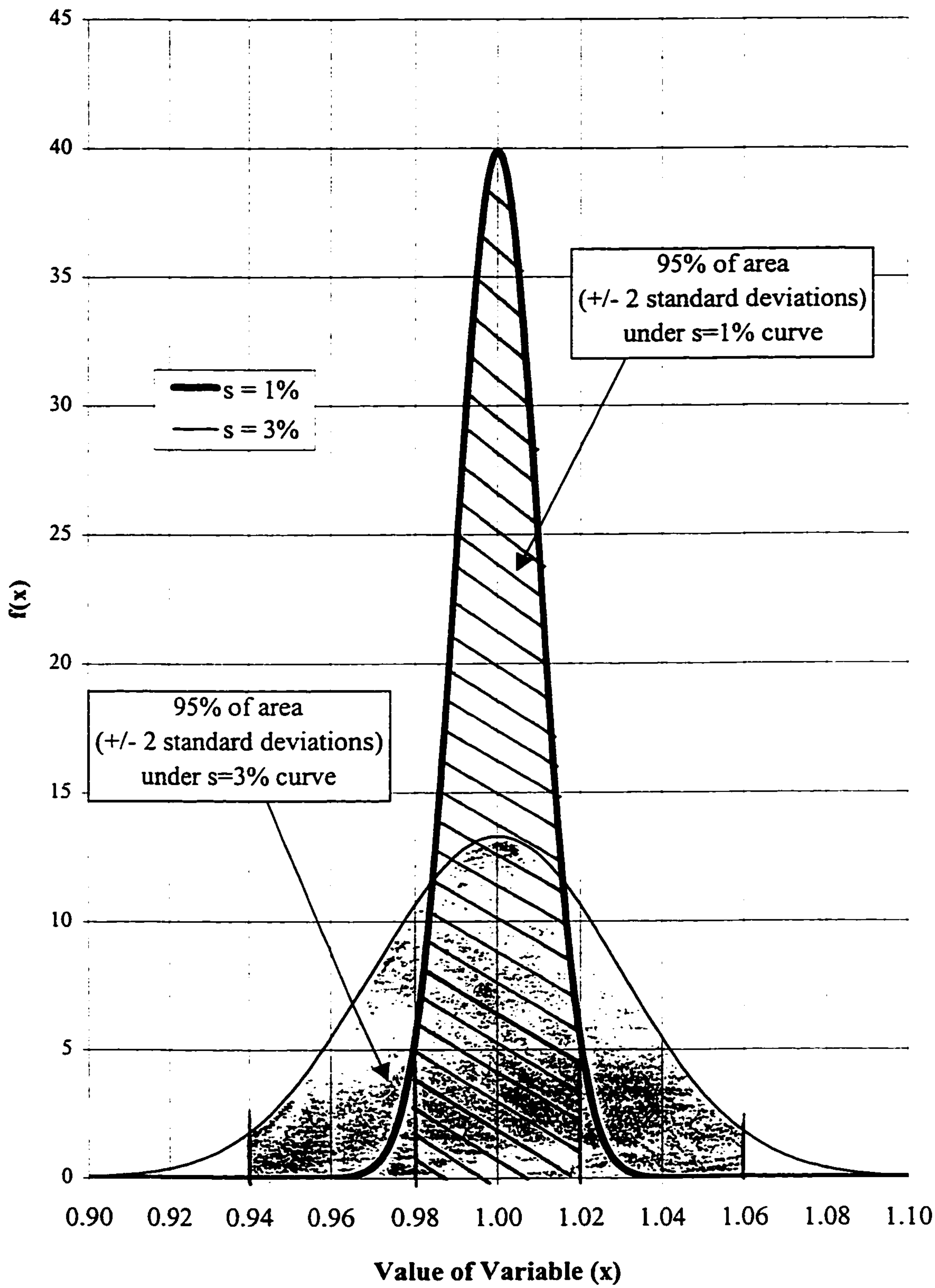

Figure 5.3: Gaussian Distributions

of 0.99 to 1.01. Similarly, 95% of the data are contained within ±2 standard deviations, or an interval of 0.98 to 1.02. Two Gaussian distributions, each with a mean value of 1.0, and standard deviations (and thus MoT's) of 0.01 and 0.03 are plotted in Figure 5.3. The areas representing 95% of the areas under the curves, and thus 95% of the observations, are shaded on the diagram. As can be seen, at a MoT of 0.01 the data are much closer to the mean than at a MoT of 0.03. It will be shown that the pump speed and specific gravity did observe a near Gaussian distribution.

Many of the observations found in Table 5.1 describe observations that are contiguous with each other. It is necessary to make sure that any data points extracted be at least 60 minutes apart from any other observation, so that no single minute observations are contained in more than one hourly average observation. The data for a 2% cutoff MoT were examined, and there were found to be 614 separate one-hour average observations. This is approximately one data point for every 88 observations. Why was a cutoff value of 2% assumed? When one uses a criteria as defined above, an arbitrary decision must be made as to what defines steady state and what defines transient. The value of 2% was chosen by the author as that representing a compromise between obtaining enough data to perform further analysis, and having data that are as close as possible to "steady" operation. Using a MoT of 3% would have yielded approximately 60% more data, but much more of it would have been obtained from increasingly unsteady periods of observation, and the inherent errors would be 1.5 times those of a 2% cutoff MoT.

Of the 3209 hours of operation, using the 2% cutoff, 614 hours were identified as falling within this definition of "steady state", and 2595 hours were identified as "transient". The distribution of operational status is described in Table 5.2.

Table 5.2: Distribution of Hours Studied.

Condition	Hours	% of Total Time	% of Uptime
Downtime	653	16.4	n/a
Water	81	2.0	n/a
Ramping	30	0.8	n/a
Steady State	614	15.5	19.1
Transient	2595	65.3	80.9
Total	3973	100	100

5.1.6 Pump Performance Data

Figures 5.4 to 5.12 contain plots of the head and efficiency ratios for Pumps 1,2 and 3 versus cumulative throughput, weight concentration of solids, and pump speed. It was decided to use weight concentration of solids as a variable instead of slurry specific gravity as weight concentration was commonly used in all of the literature surveyed, and head and efficiency ratios were generally observed to have linear relationships with weight concentration.

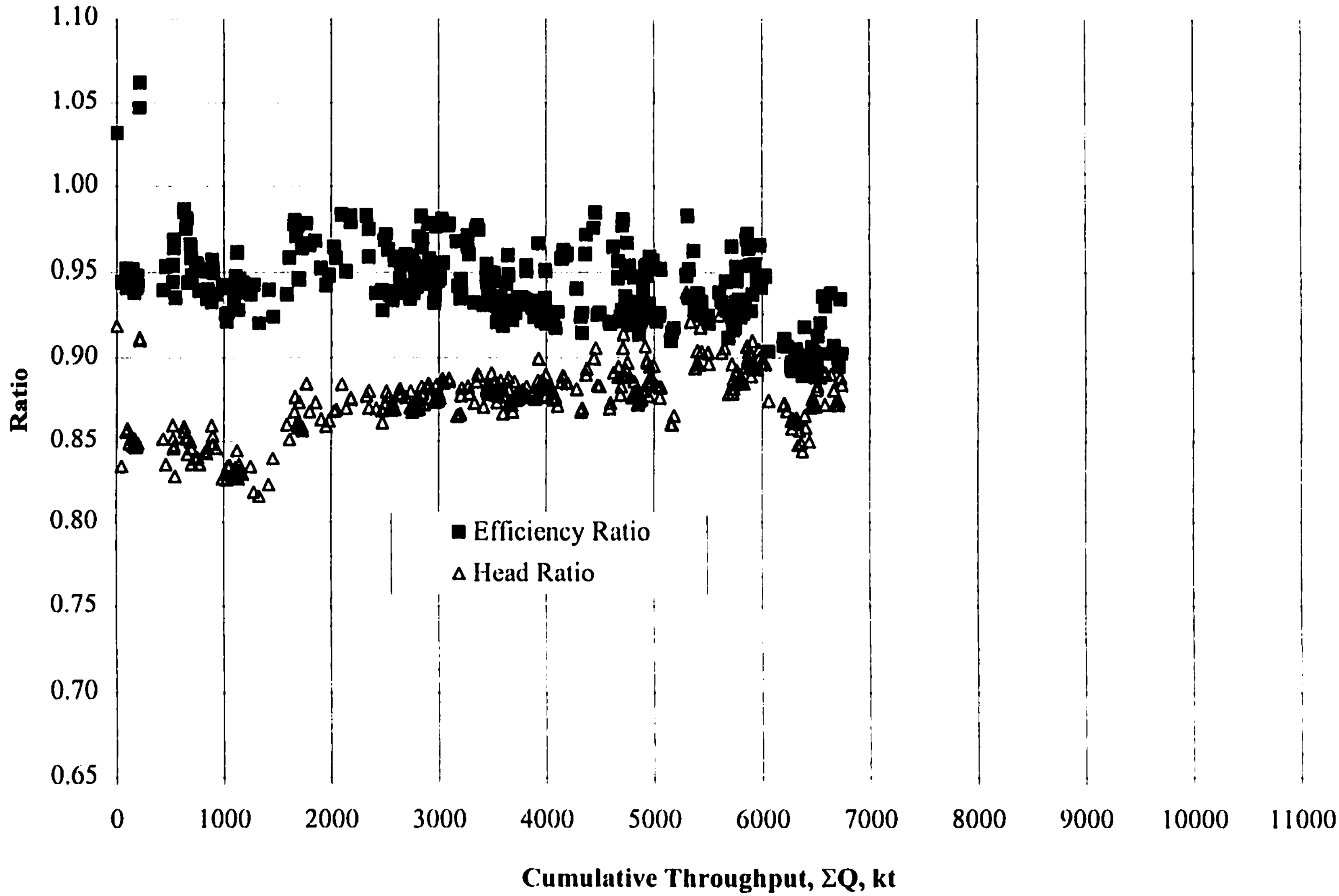

Figure 5.4: Slurry Performance vs. Cumulative Throughput, Pump #1

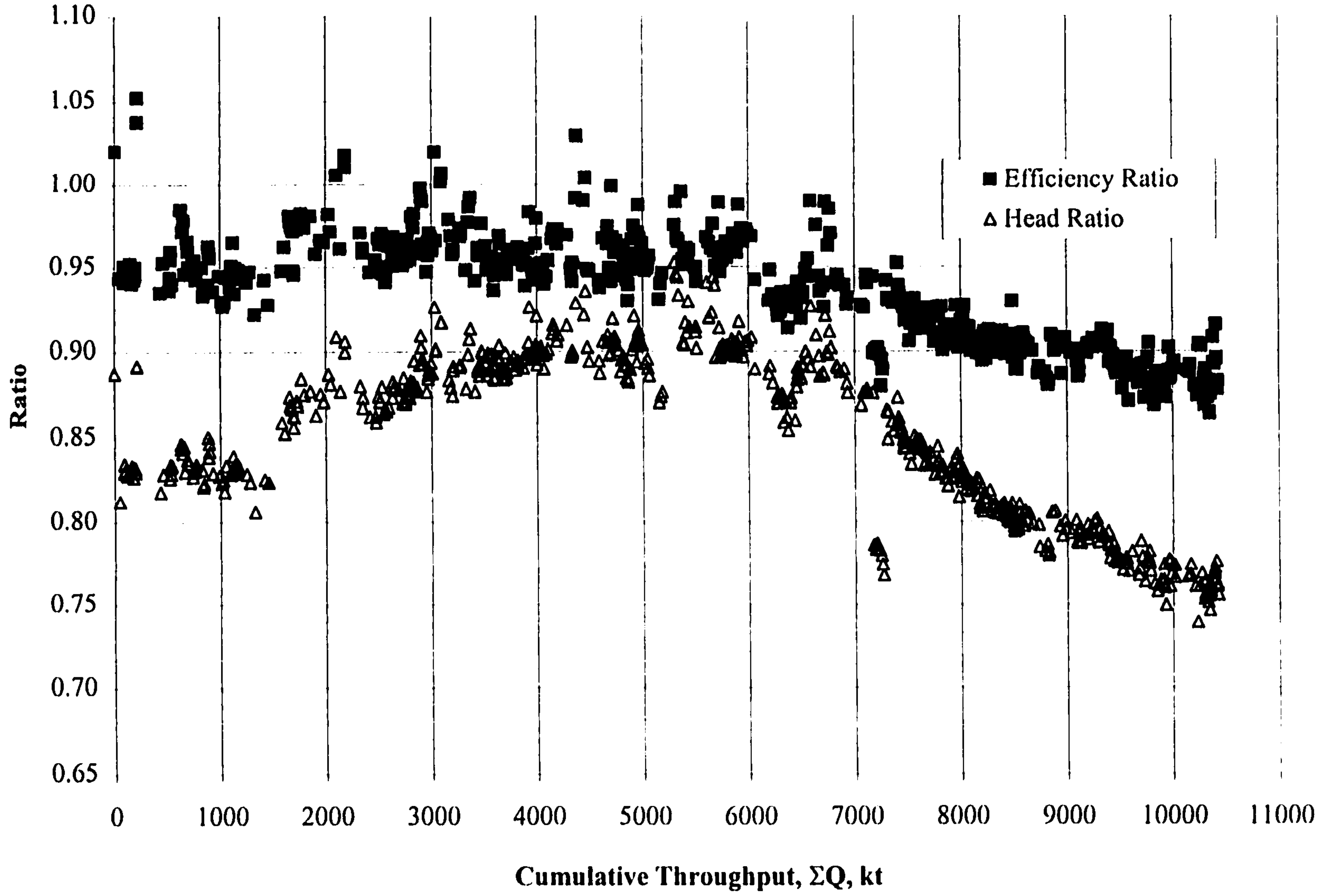

Figure 5.5: Slurry Performance vs. Cumulative Throughput, Pump #2

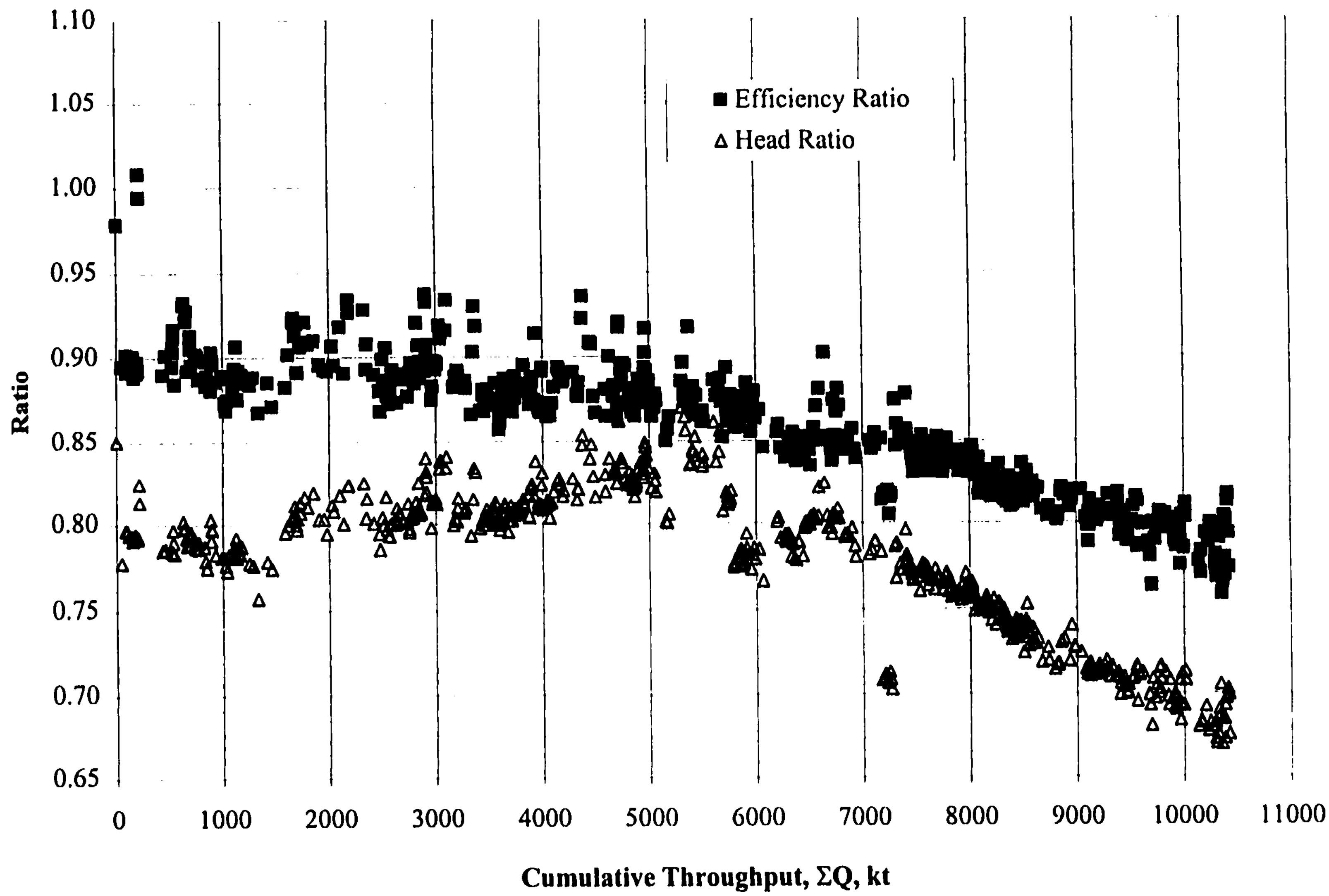

Figure 5.6: Slurry Performance vs. Cumulative Throughput, Pump #3

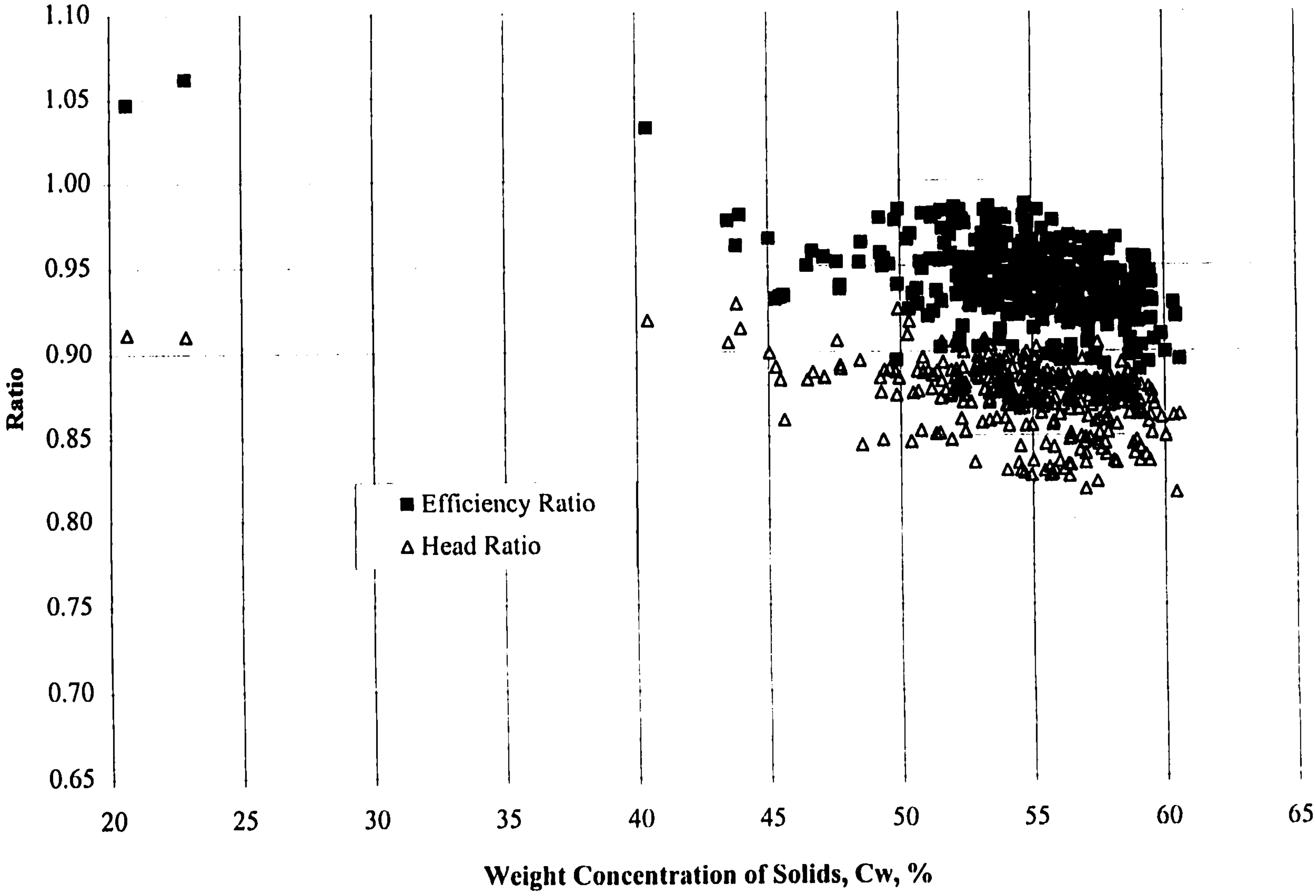

Figure 5.7: Slurry Performance vs. Weight Concentration of Solids, Pump #1

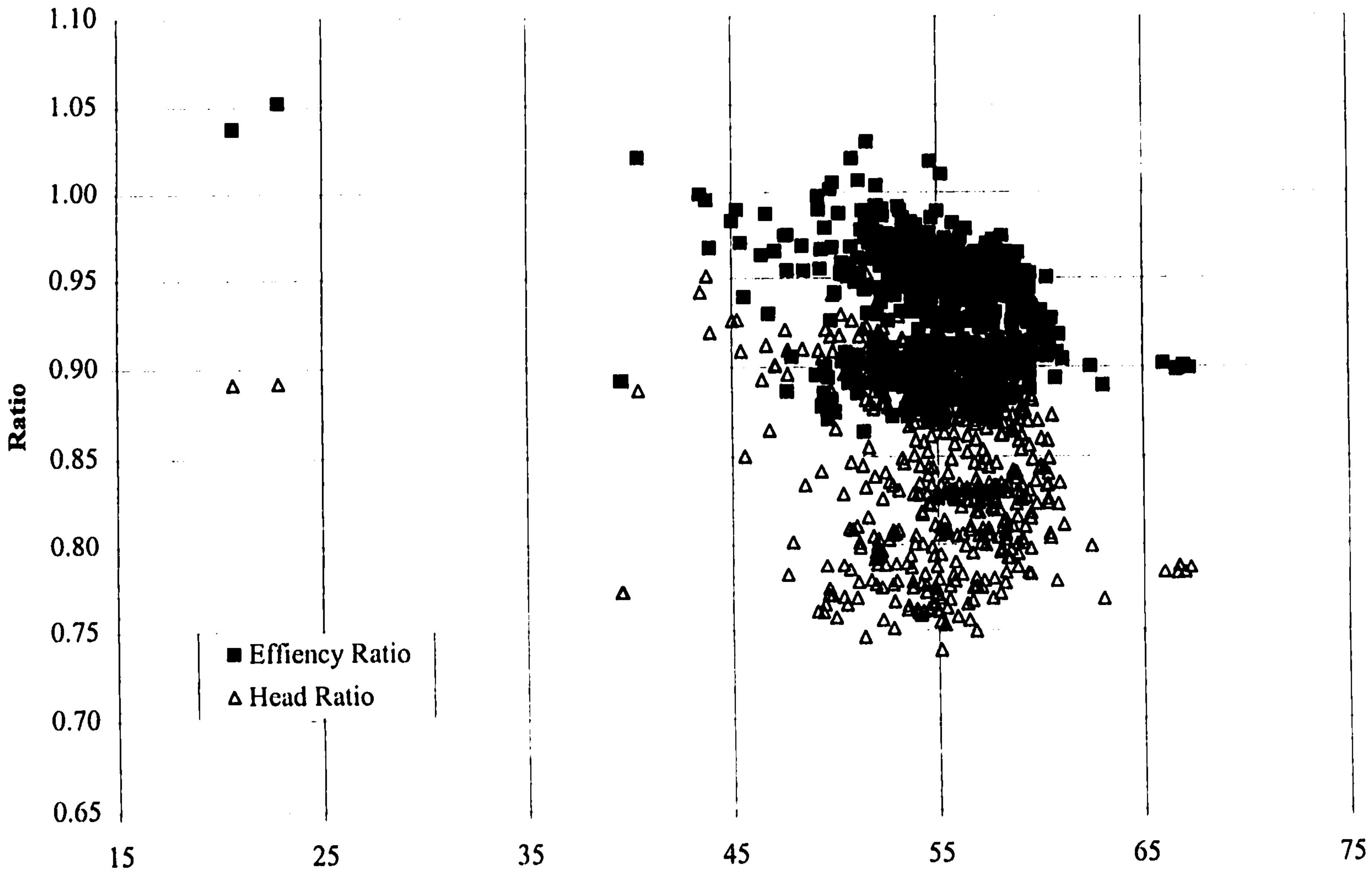

Figure 5.8: Slurry Performance vs. Weight Concentration of Solids, Pump #2

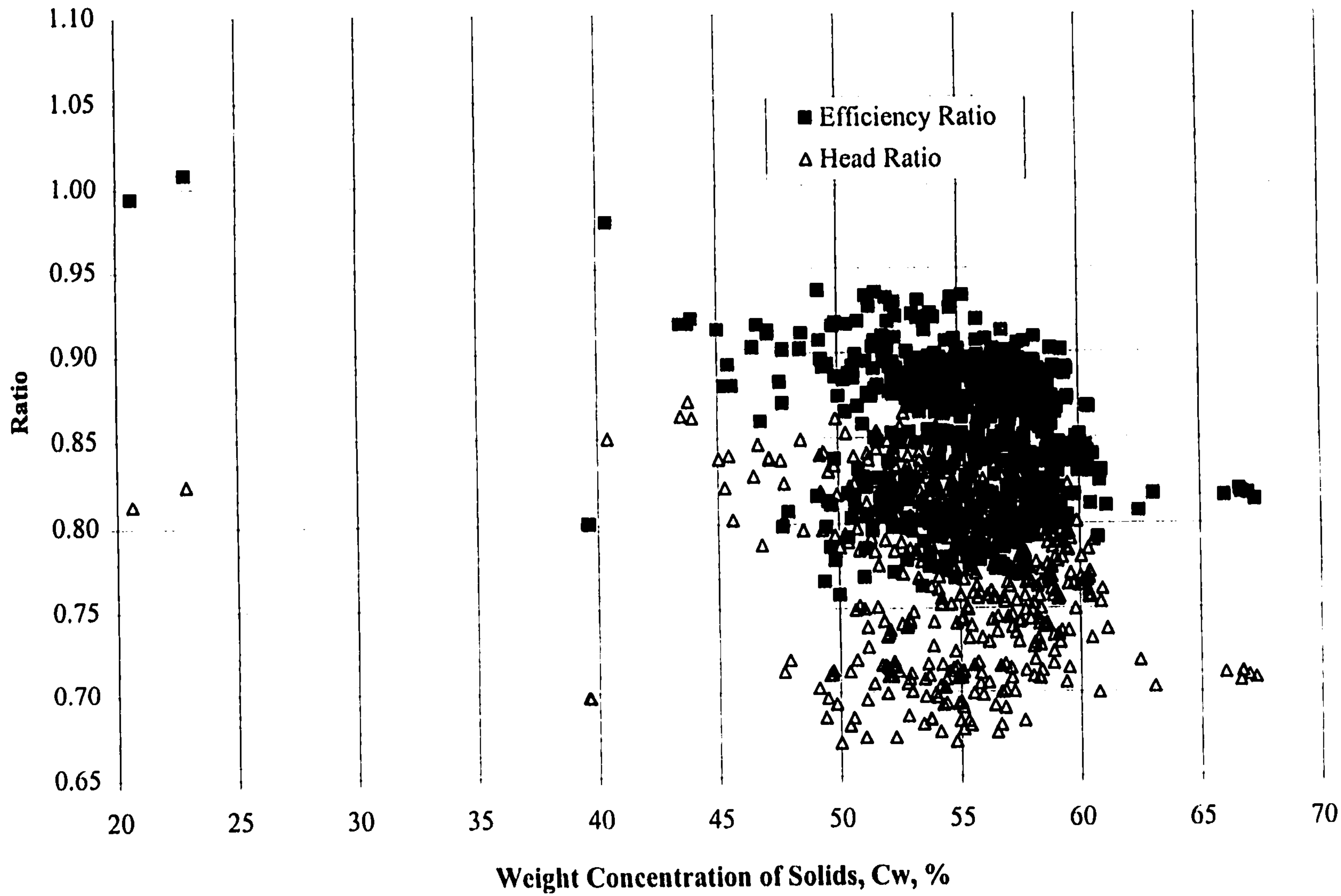

Figure 5.9: Slurry Performance vs. Weight Concentration of Solids, Pump #3

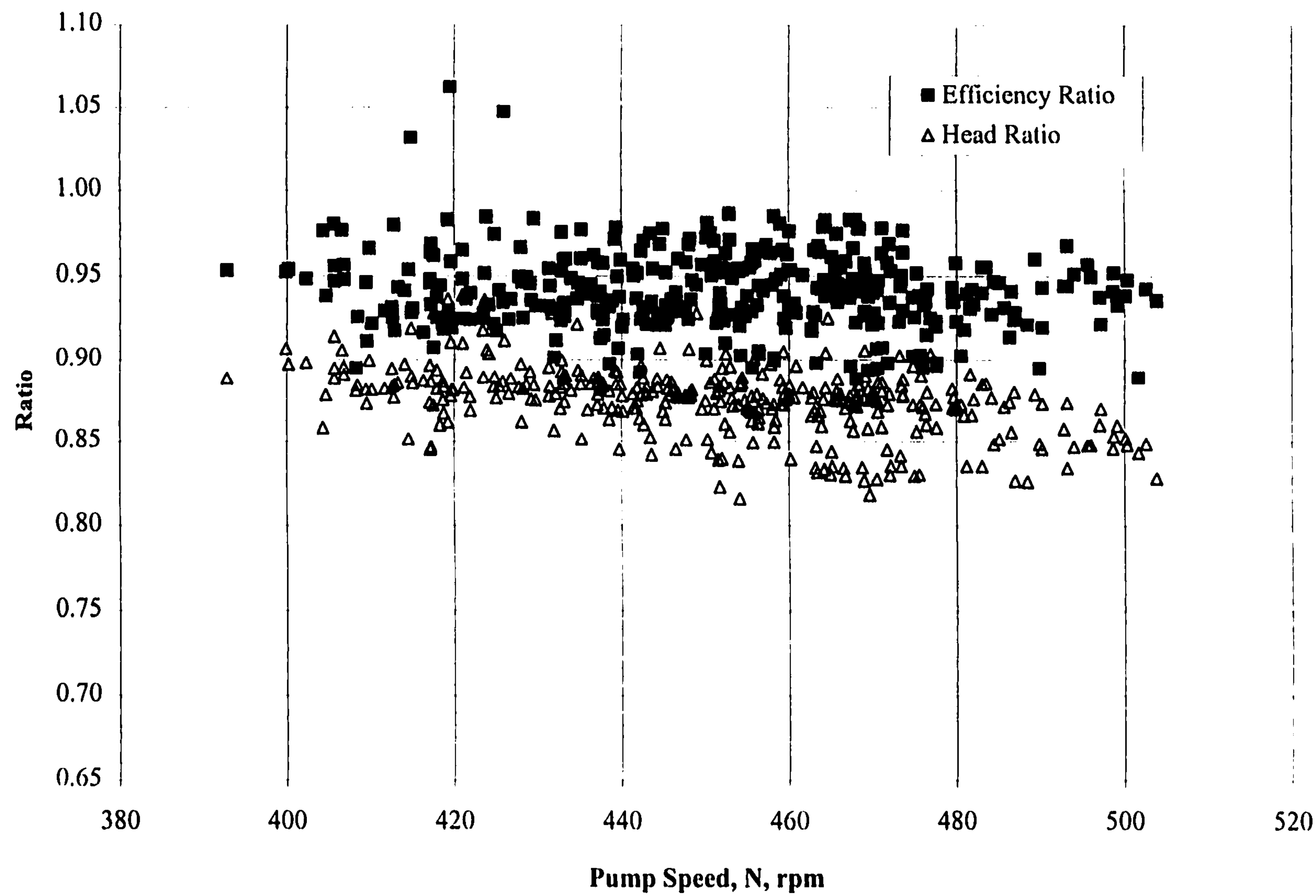

Figure 5.10: Slurry Performance vs. Pump Speed, Pump #1

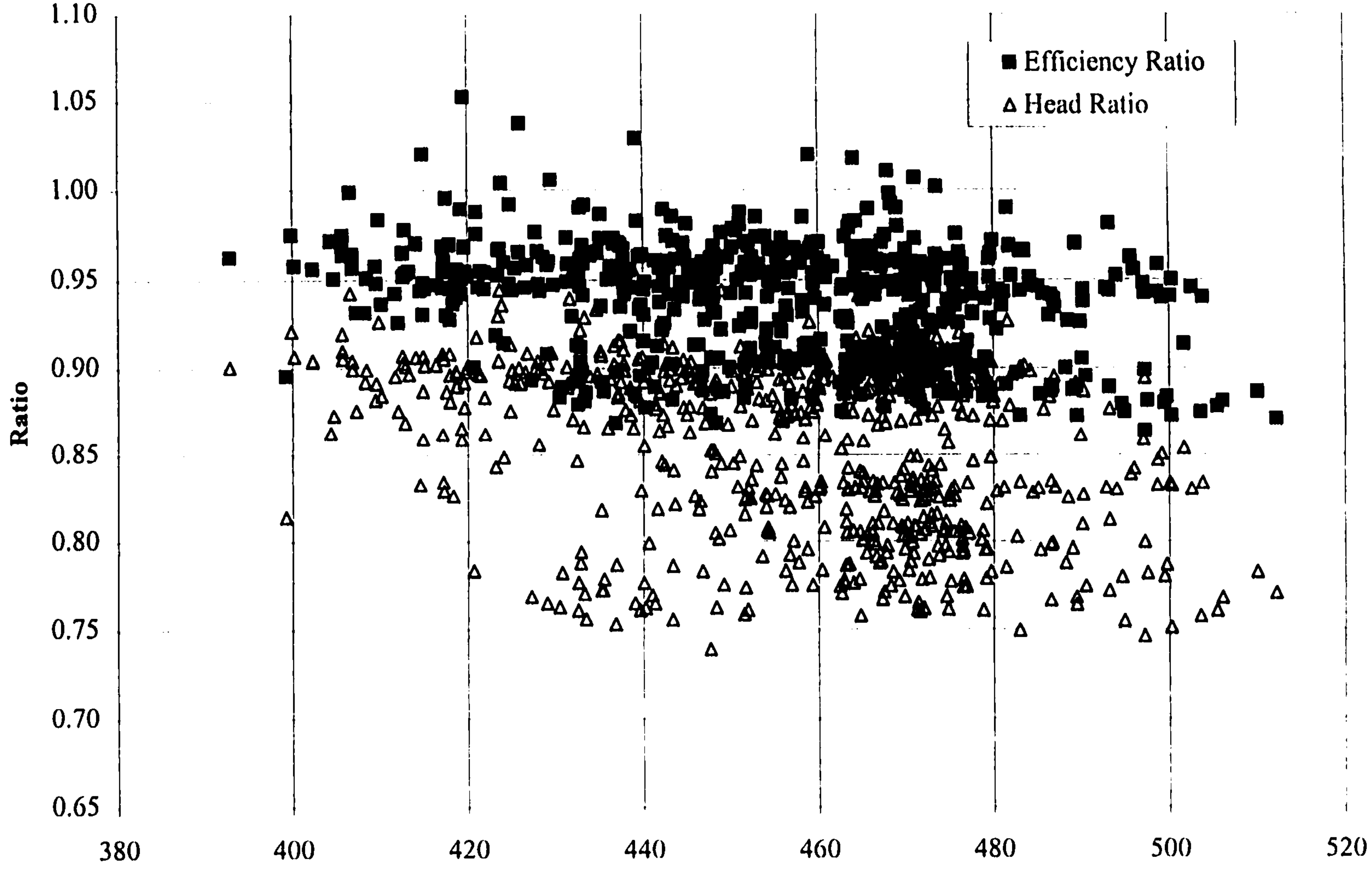

Figure 5.11: Slurry Performance vs. Pump Speed, Pump #2

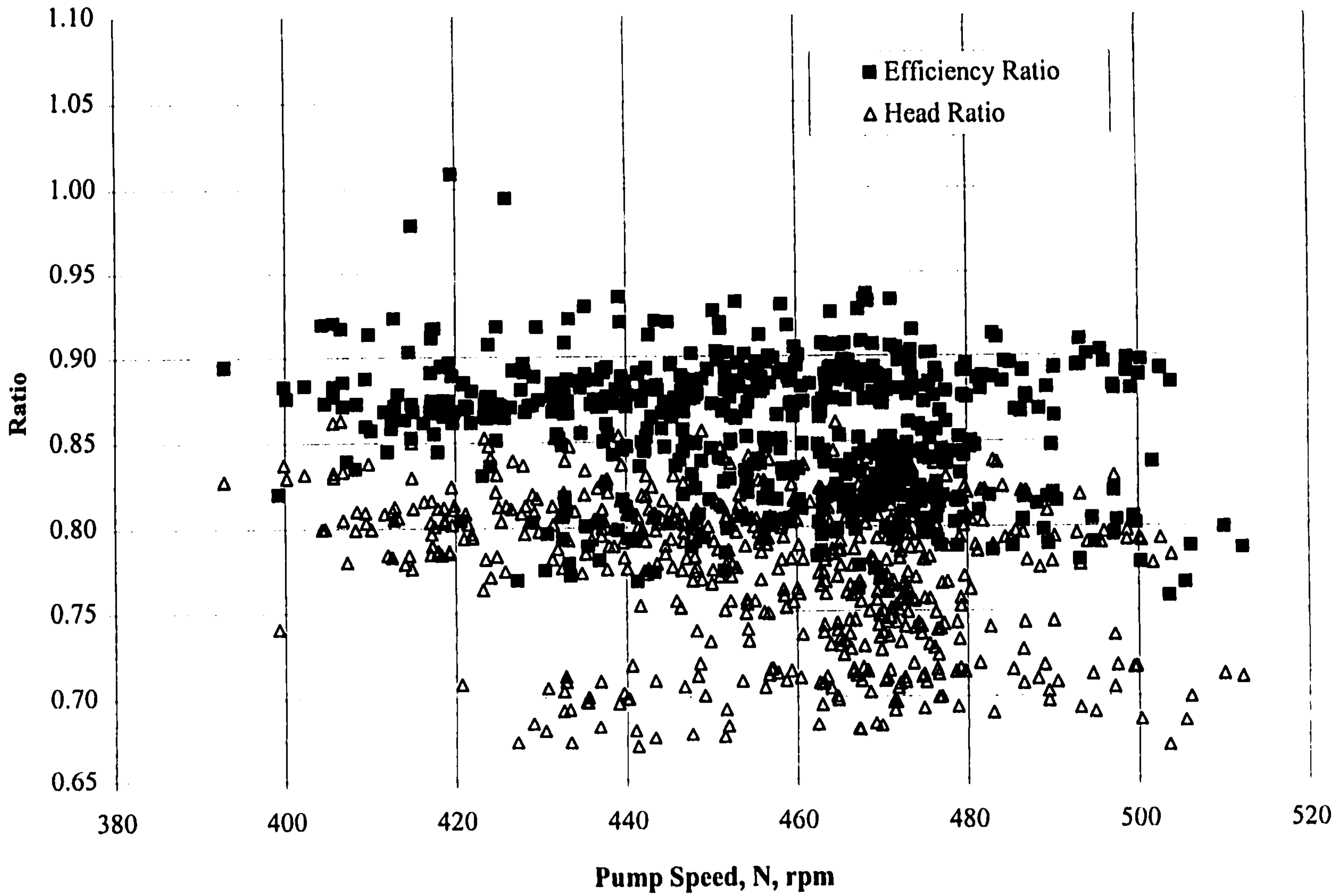

Figure 5.12: Slurry Performance vs. Pump Speed, Pump #3

Specific gravity is converted to weight concentration using the following formula:

$$C_W = \frac{S_s S_m - S_s S_w}{S_s S_m - S_m S_w} \qquad \text{...(5.6)}$$

Assuming a solid SG of 2.65 and a water SG of 1, this reduces to the following:

$$C_W = 1.606\left(1 - \frac{1}{S_m}\right) \qquad \text{...(5.7)}$$

5.2 Development of Correlations

5.2.1 Description

In order to evaluate the effect of all input variables on the pump performance, it was desired to develop multivariate correlations of the form:

$$y = \alpha + \beta_1 x_1 + \beta_2 x_2 + \beta_3 x_3 + \beta_{11} x_1^2 + \beta_{22} x_2^2 + \beta_{33} x_3^2 \qquad \text{...(5.6)}$$

Where y is the dependent variable, in this case head or efficiency ratio. The x's denote independent input variables, in this case cumulative throughput, weight concentration of sand and pump speed.

5.2.2 Transformation Functions

It was necessary to standardize all input variables to a range of [-1,1] for the purpose of developing the correlations. This is necessary in order to test the significance of each constant coefficient (beta value, β_i) in the correlations.

The actual ranges for the input variables over the period of study are shown in Table 5.3.

Table 5.3: Ranges of Input Variables

Variable	Minimum Observation	Maximum Observation
Cumulative Throughput	0 kt	10424 kt
Weight Concentration	20.6%	67.3%
Pump Speed	392 rpm	512 rpm

Frequency polygons for the approximate distributions of the three variables are displayed in Figures 5.13 to 5.15. As can be seen, pump speed and weight concentration are distributed in approximately Gaussian distributions.

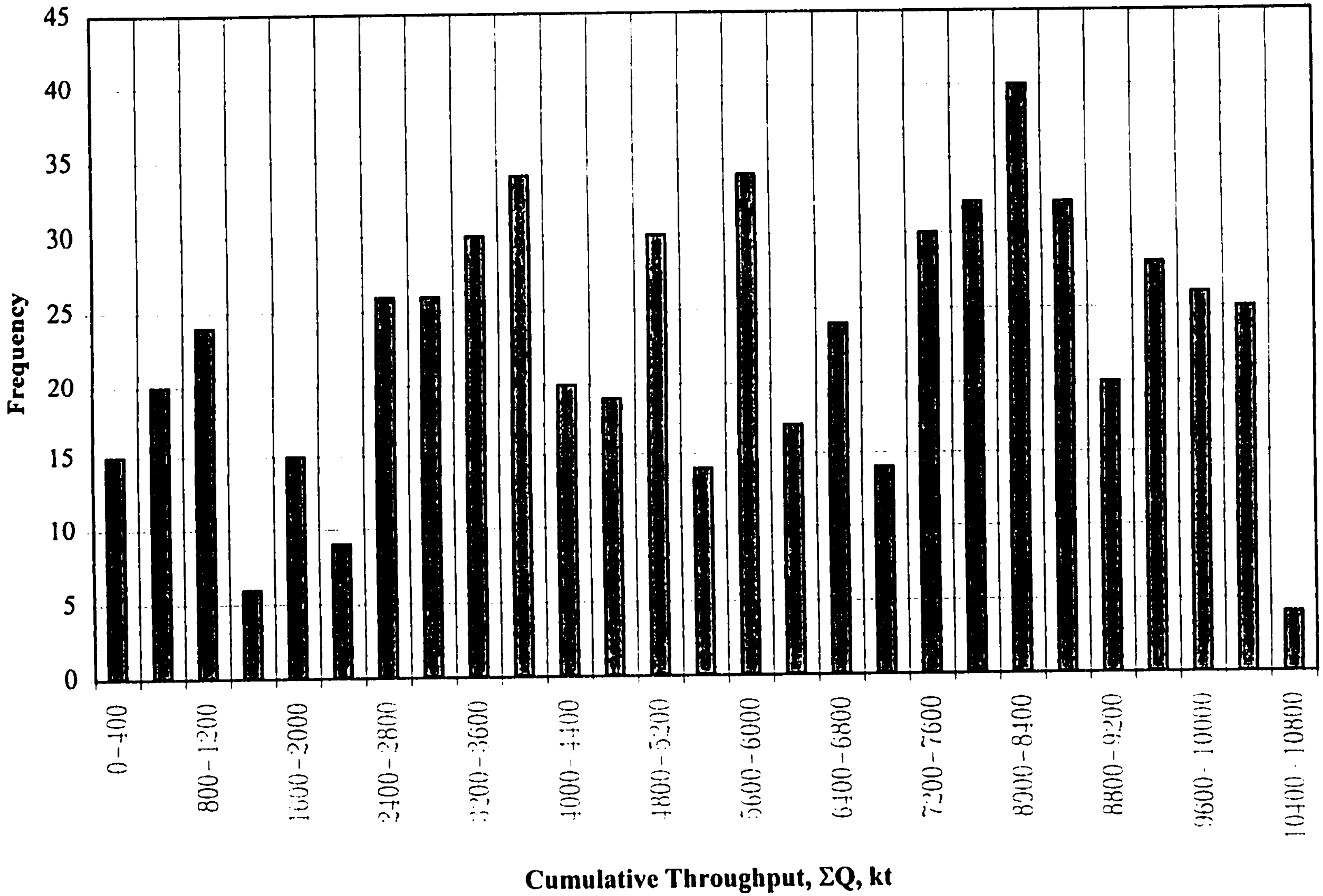

Figure 5.13: Frequency Distribution of Cumulative Throughput Observations

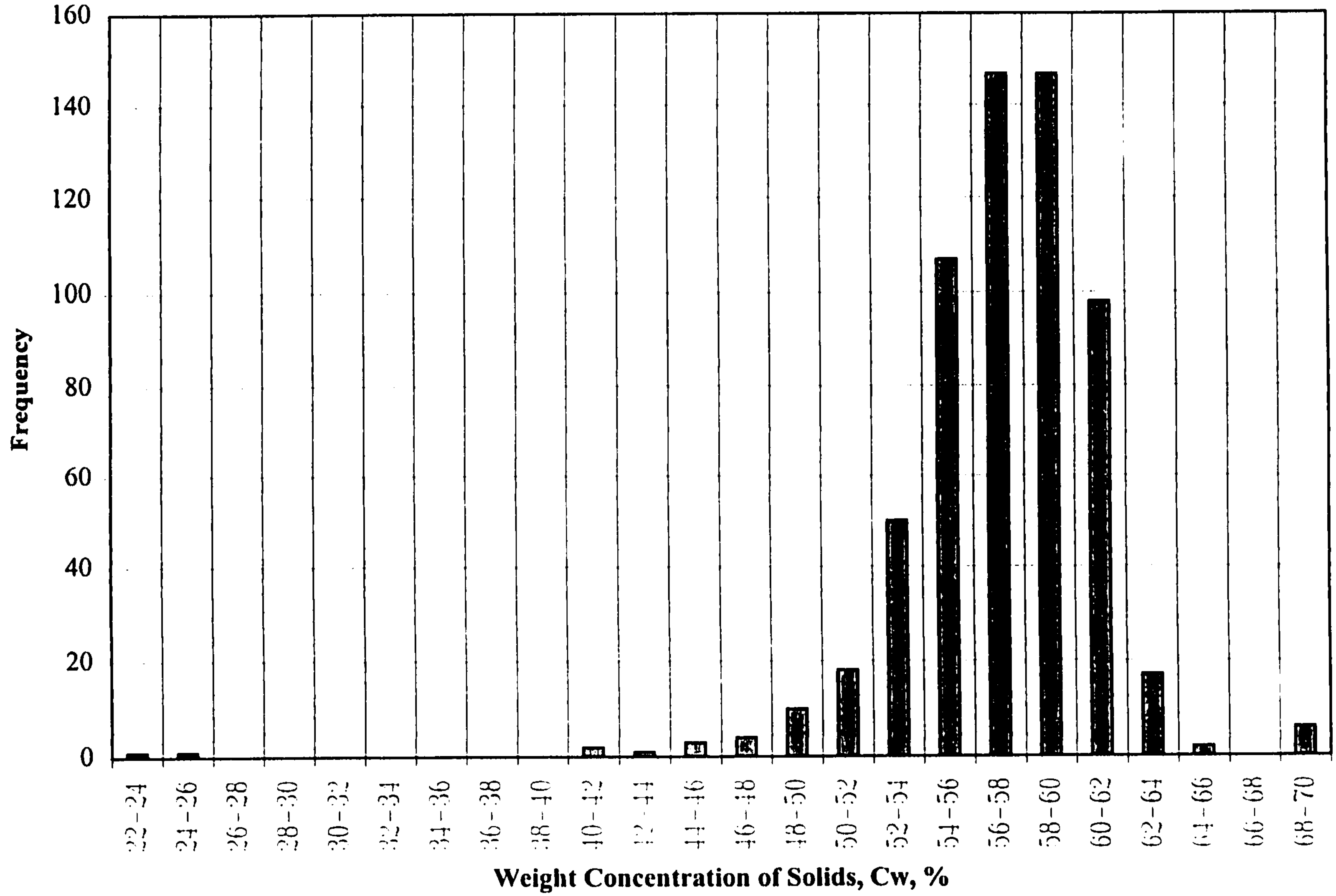

Figure 5.14: Frequency Distribution of Weight Concentration of Solids Observations

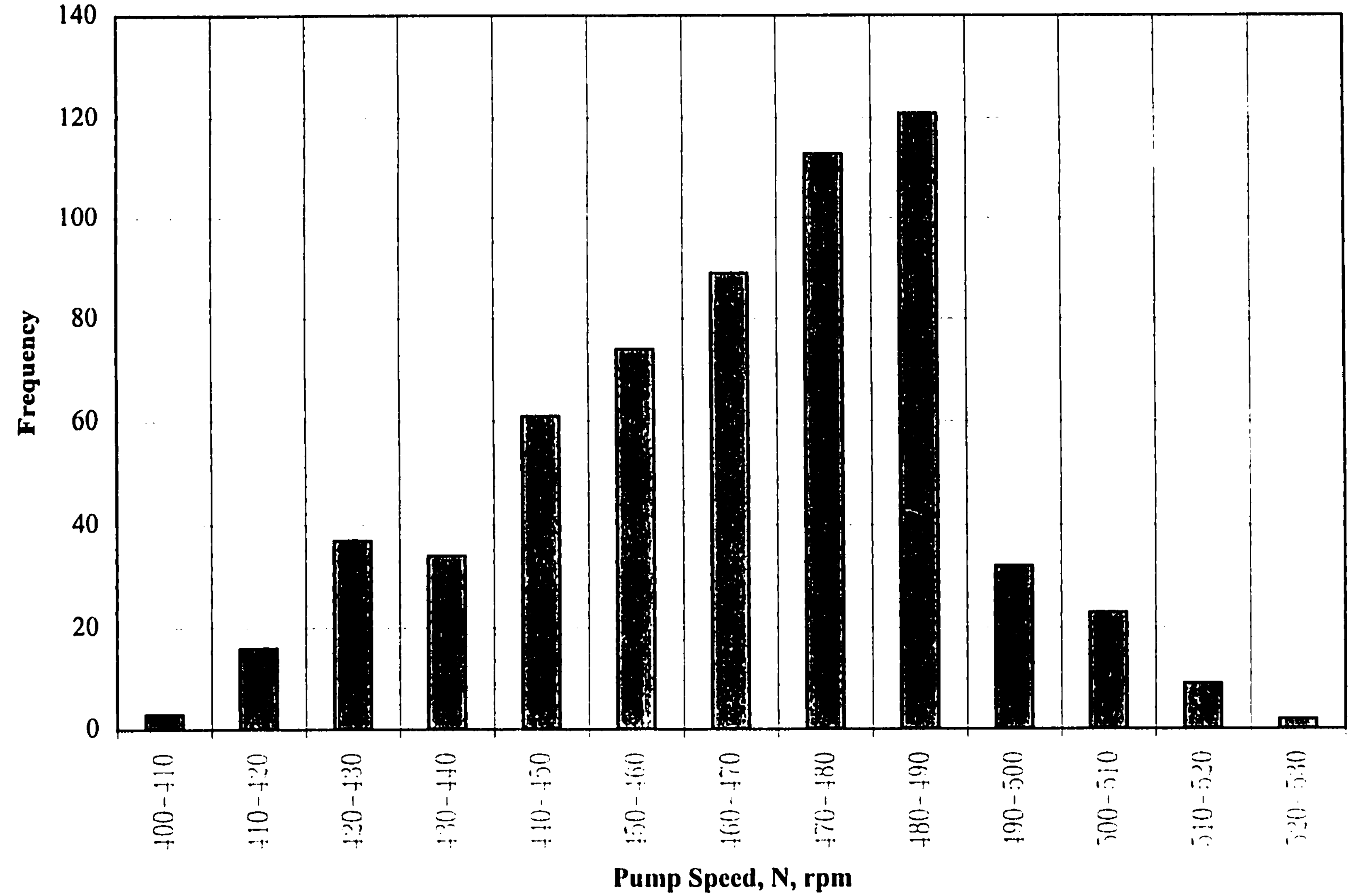

Figure 5.15: Frequency Distribution of Pump Speed Observations

The transformation functions are detailed thus:

Cumulative Throughput (ΣQ): to transform ΣQ of range [0, 10,424] kt to scaled variable x_1 of range [-1, 1] the following function was derived:

$$x_1 = \frac{\Sigma Q}{5212} - 1 \qquad \text{...(5.7)}$$
$$\Sigma Q = 5212(x_1 + 1)$$

Weight Concentration (C_w): to transform C_w of range [20.6, 67.3] % to scaled variable x_2 of range [-1, 1] the following function was derived:

$$x_2 = \frac{C_W}{23.35} - 1.882 \qquad \text{...(5.8)}$$
$$C_W = 23.35(x_2 + 1.882)$$

Pump Speed (N): to transform N of range [392, 512] rpm to scaled variable x_3 of range [-1, 1] the following was derived:

$$x_3 = \frac{N}{60.5} - 7.479 \qquad \text{...(5.9)}$$
$$N = 60.5(x_3 + 7.479)$$

5.3 Correlations

5.3.1 Independence of Variables

In creating an initial estimate of the form of the correlation, one must decide whether or not to include compounded terms such as x_1x_2 in the ccrrelation. If the variables are independent, then no compounding in necessary. If the variables are not truly independent, then compound terms will have to be considered. Figures 5.16 to 5.18 depict scatter plots of the three pairs of variables. At first sight there does not appear to be any obvious interdependence. The correlation coefficient for these three pairs of variable were calculated. They are as follows:

x_1-x_2 correlation coefficient: 0.0508

x_1-x_3 correlation coefficient: 0.1395

x_2-x_3 correlation coefficient: 0.08793

From this it can be stated that the three variables are statistically independent to the degree that it can be assumed that no compounded terms are required. The variables are assumed to be fully independent.

Initial estimates for the correlations of head and efficiency ratios were performed using all three input variables in both first and second-degree form, that is, correlations of the

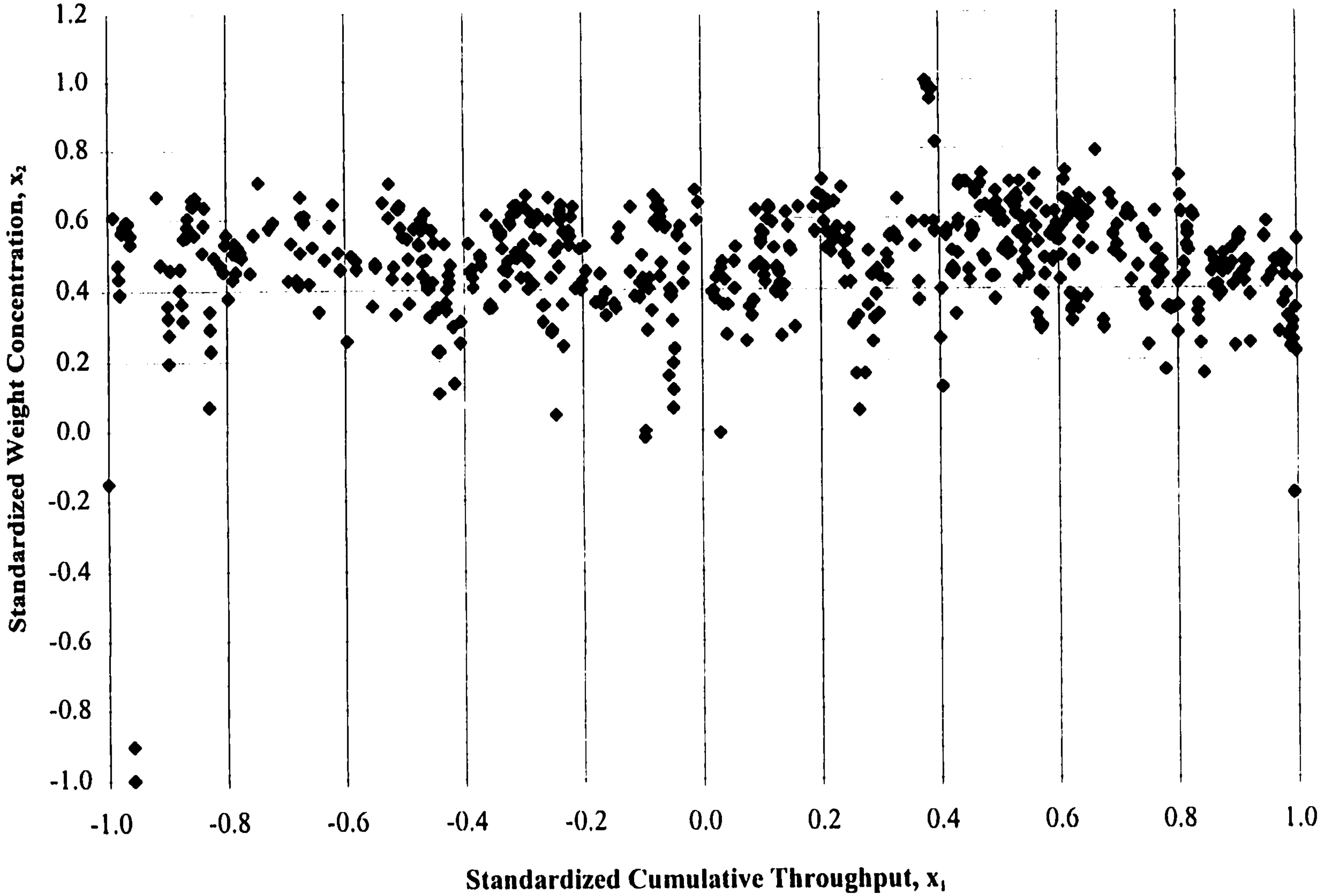

Figure 5.16: Standardized Weight Concentration vs. Standardized Cumulative Throughput

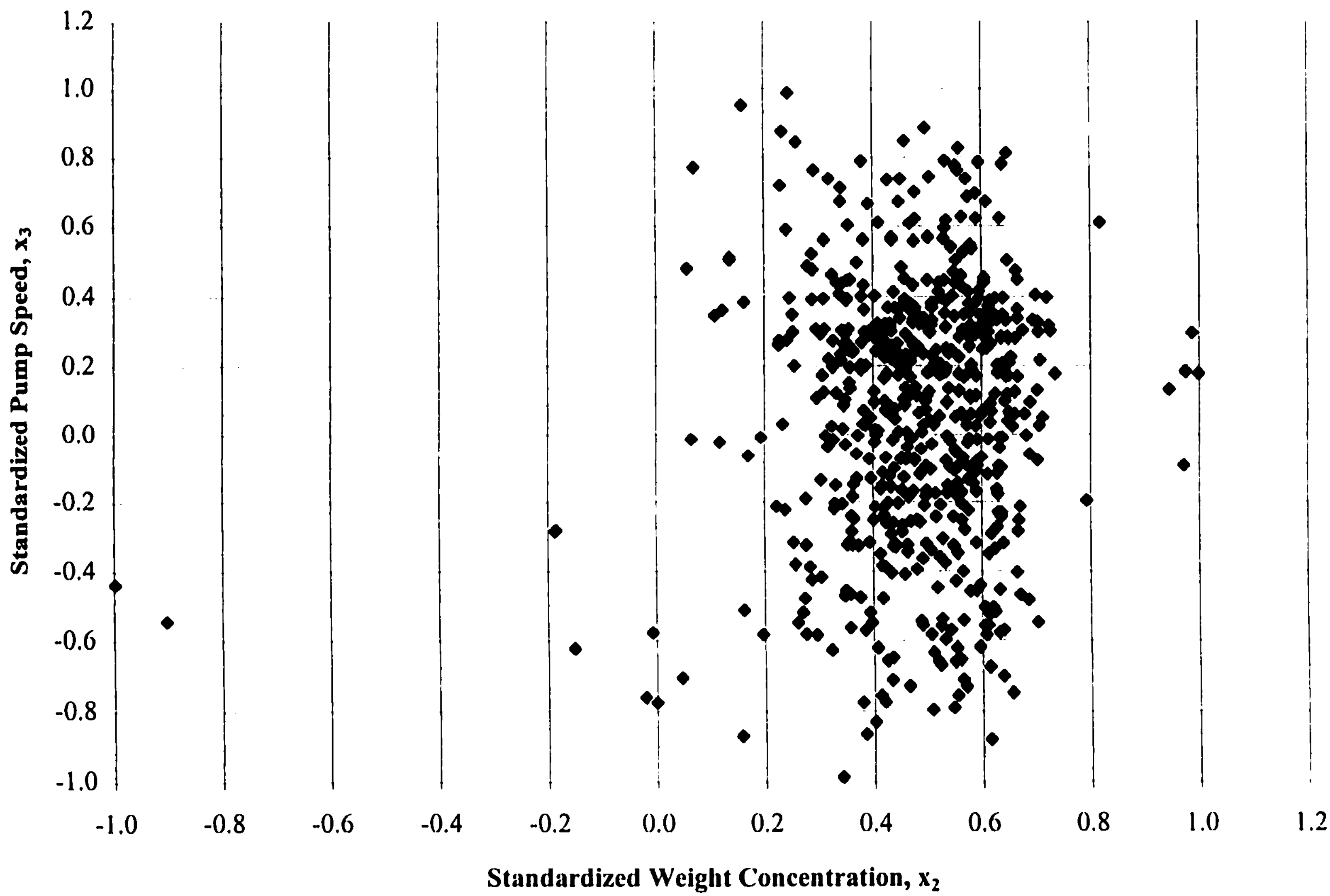

Figure 5.17: Standardized Pump Speed vs. Standardized Weight Concentration

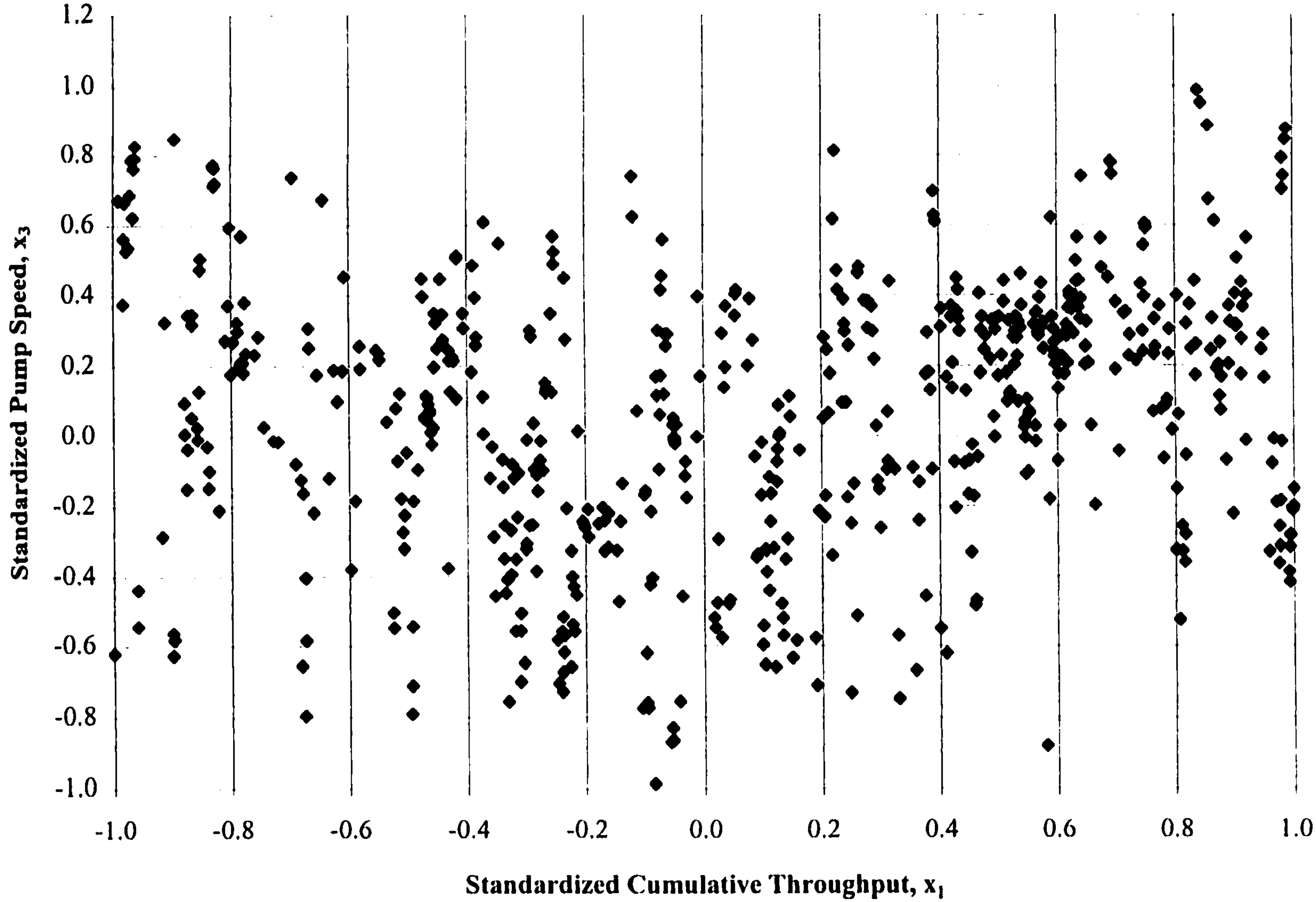

Figure 5.18: Standardized Pump Speed vs. Standardized Cumulative Throughput

form $y = \alpha + \beta_1 x_1 + \beta_2 x_2 + \beta_3 x_3 + \beta_{11} x_1^2 + \beta_{22} x_2^2 + \beta_{33} x_3^2$ were developed. The results are shown in Table 5.4.

Table 5.4: First Estimated Correlation Parameters.

Parameter	Pump 1, Head	Pump 1, Efficiency	Pump 2, Head	Pump 2, Efficiency	Pump 3, Head	Pump 3, Efficiency
α	0.9074	0.9672	0.9254	0.9836	0.8377	0.9031
β_1 (x_1 term)	0.0017	-0.0518	-0.0384	-0.0395	-0.0499	-0.0592
β_2 (x_2 term)	-0.0474	-0.0672	-0.0494	-0.0592	-0.0396	-0.0647
β_3 (x_3 term)	-0.0107	-0.0119	-0.0139	-0.0091	-0.0019	-0.0036
β_{11} (x_1^2 term)	-0.0464	-0.0249	-0.1201	-0.0414	-0.0907	-0.0383
β_{22} (x_2^2 term)	0.0035	-0.0088	-0.0289	0.0003	-0.0299	0.0131
β_{33} (x_3^2 term)	0.0036	-0.0189	-0.0006	-0.0102	-0.0023	-0.0070
R^2	0.680	0.591	0.914	0.849	0.903	0.951
Mean Error	1.18%	1.48%	1.44%	1.24%	1.40%	1.14%

After examining the correlations with the weakest terms eliminated, the following final values were accepted, as illustrated in Table 5.5. In all cases the removal of the weakest terms involved negligible effects on the regression correlation coefficient, R^2, or the mean error.

Table 5.5: Final Correlation Parameters

Parameter	Pump 1, Head	Pump 1, Efficiency	Pump 2, Head	Pump 2, Efficiency	Pump 3, Head	Pump 3, Efficiency
α	0.9074	0.9672	**0.9253**	**0.9855**	**0.8386**	0.9031
β_1	0	-0.0518	-0.0384	**-0.0400**	**-0.0501**	-0.0592
β_2	**-0.0477**	-0.0672	**-0.0493**	**-0.0617**	**-0.0409**	-0.0647
β_3	**-0.0106**	-0.0119	-0.0139	0	0	0
β_{11}	**-0.0485**	-0.0249	-0.1201	**-0.0451**	**-0.0913**	**-0.0374**
β_{22}	**0.0033**	-0.0088	-0.0289	0	**-0.0293**	**0.0089**
β_{33}	**0.0037**	-0.0189	0	**-0.0161**	0	0
R^2	0.680	0.591	0.914	**0.839**	**0.902**	**0.936**
Mean Error	1.18%	1.48%	1.44%	**1.28%**	1.40%	**1.16%**

These were calculated by ignoring the terms assumed to be zero, and recalculating the least-squares best fit correlation parameters. The parameters that changed to a visible degree are shown in boldface type in Table 5.5. Using the reverse transformation functions listed in Equations 5.7-5.9, the correlations, as described in terms of the original variables take the following form:

$$Ratio = a + b_1 \Sigma Q + b_2 C_W + b_3 N + b_{11} (\Sigma Q)^2 + b_{22} C_W^2 + b_{33} N^2$$

Details of the correlation calculations and the procedure for transformation from "α" and "β" coefficients to "a" and "b" coefficients is found in Appendix "B", Statistical Methods.

The values of the parameters for the transformed correlations are shown in Table 5.6. These are the final multivariate correlations developed to describe the performance of these pumps with respect to cumulative throughput, weight concentration of solids and pump speed. The values in Table 5.6 are much smaller than those in Table 5.5 because they are multiplying values of throughput up to 10,500 kt, speeds up to 512 rpm, and concentrations up to 67%. The values in Table 5.5 are only multiplying standardized variables with ranges of minus one to one. A plot of these correlations versus cumulative throughput, with weight concentration set at 57% and pump speed set at 450 rpm, is shown in Figure 5.19

Table 5.6: Parameters for Transformed Correlations

Parameter	Pump 1		Pump 2		Pump 3	
	Head	Efficiency	Head	Efficiency	Head	Efficiency
a	1.2245	0.1191	0.938	0.1935	0.7705	1.0778
b_1	0.00001863	-0.0000003715	0.00003872	0.000009612	0.00002543	0.000003
b_2	-0.001503	-0.001453	0.002538	-0.002643	0.002975	-0.004185
b_3	-0.001097	0.004485	-0.0002294	0.003992	0	0
b_{11}	-0.000000001787	-0.000000000919	-0.000000004422	-0.000000001658	-0.000000003362	-0.000000001378
b_{22}	-0.000006142	-0.00001621	-0.00005291	0	-0.00005378	0.00001607
b_{33}	0.000001019	-0.000005173	0	-0.000004411	0	0

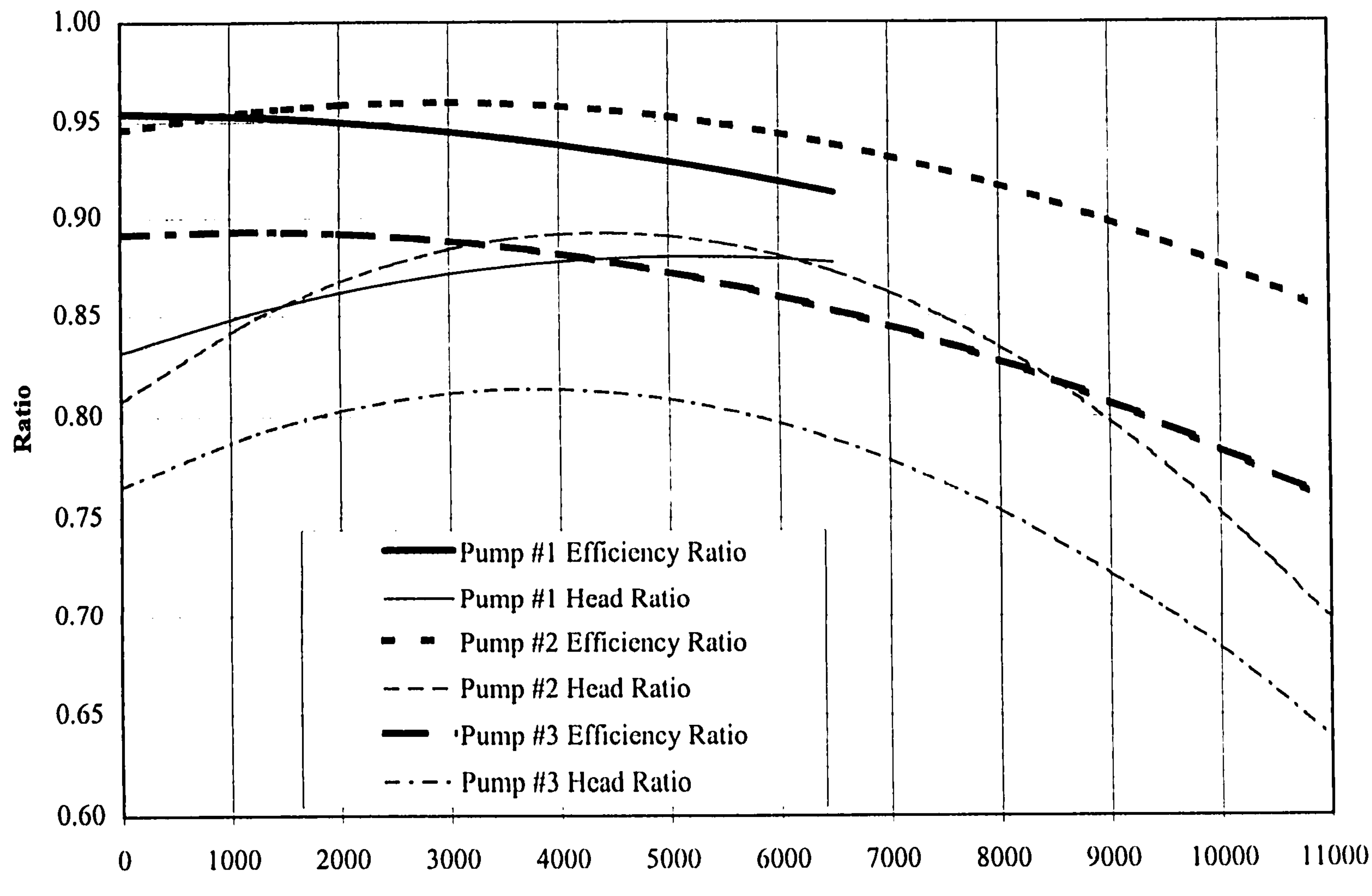

Figure 5.19: Plot of Multivariate Correlations

5.4 Water Performance

The head and efficiency ratios of the pumps while operating on water were calculated. Plots of head and efficiency ratio versus cumulative throughput and pump speed are displayed in Figures 5.20 to 5.25. The performance factors were calculated in the same way as the slurry performance factors, with specific gravity constant at 1.

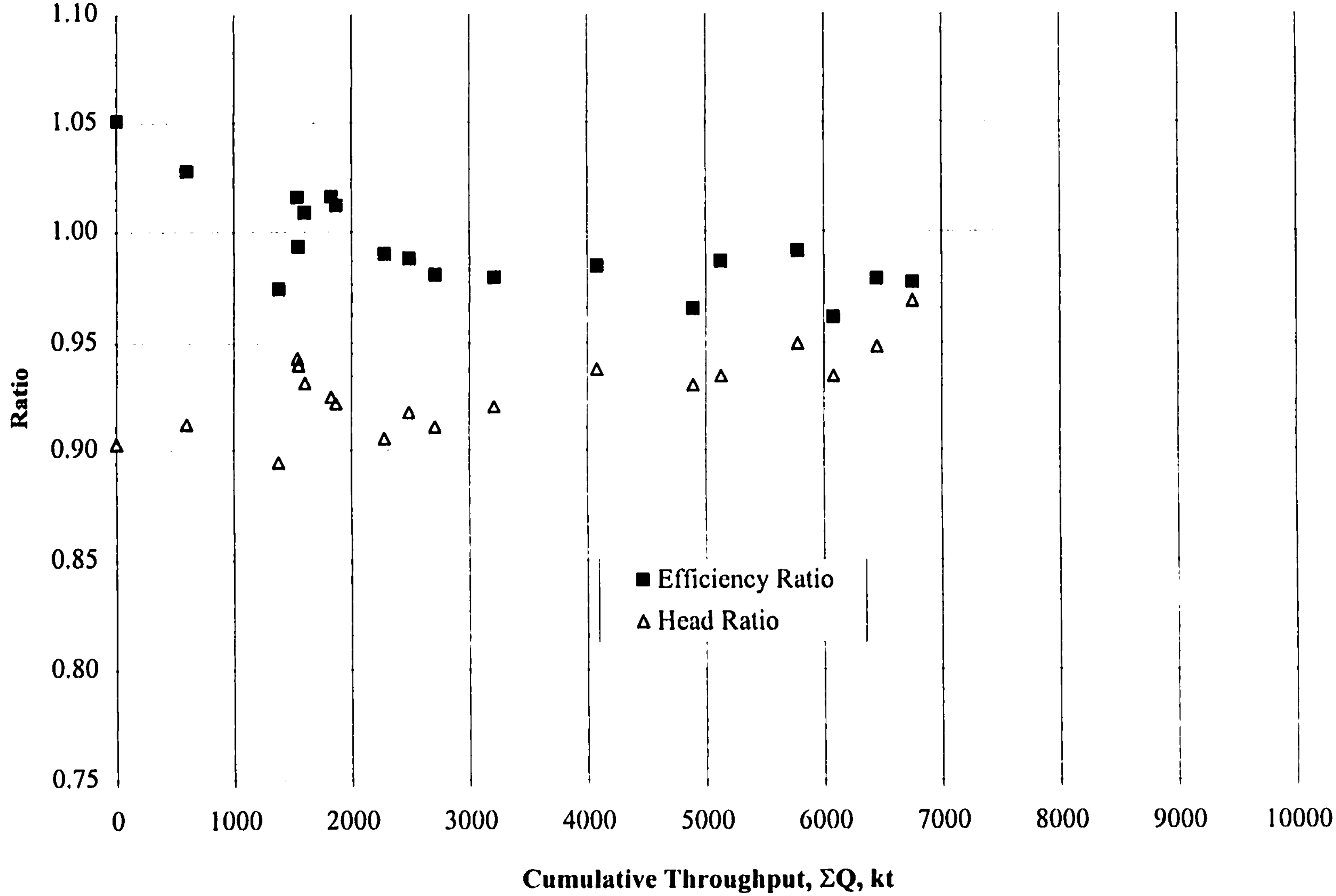

Figure 5.20: Water Performance vs. Cumulative Throughput, Pump #1

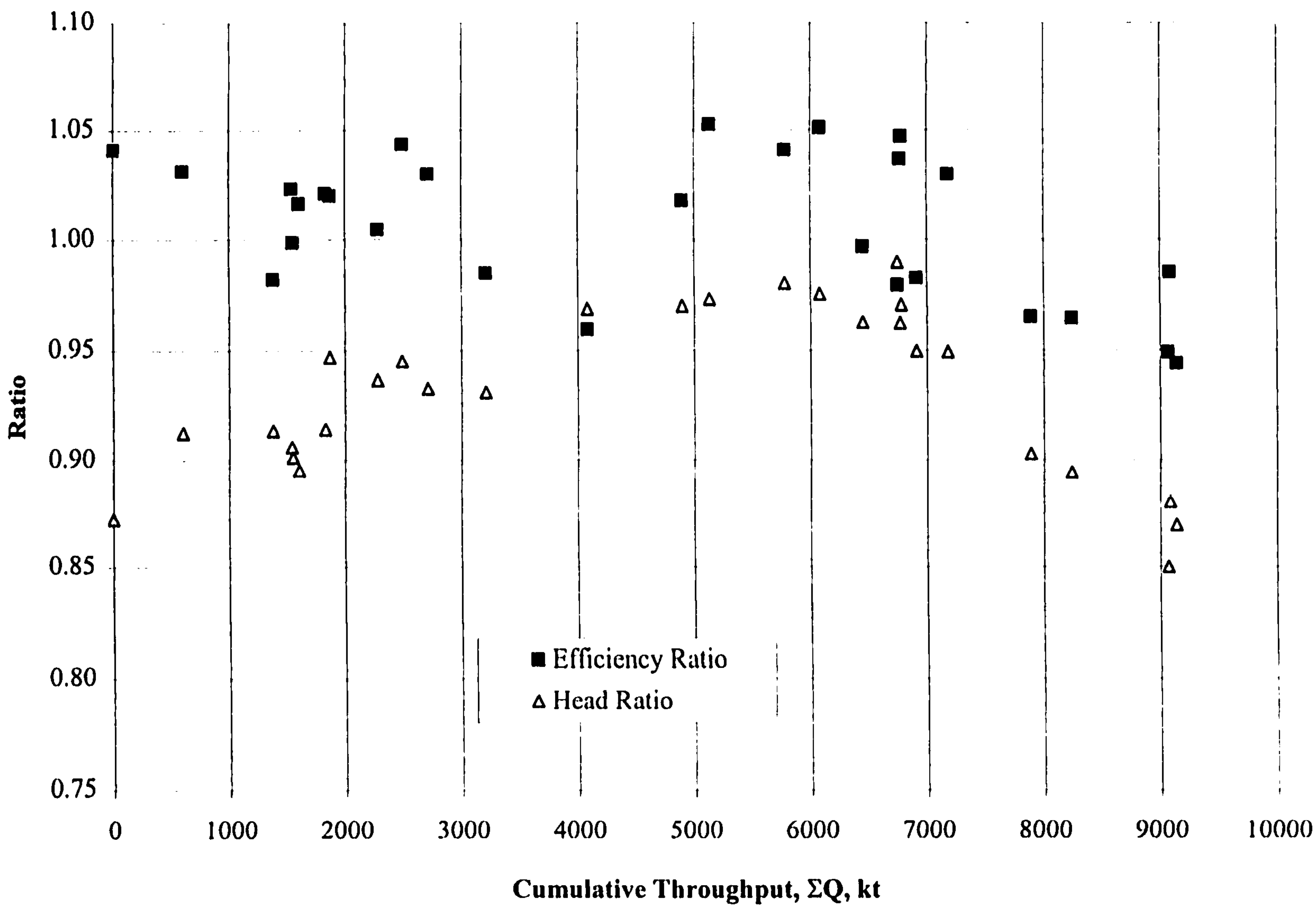

Figure 5.21: Water Performance vs. Cumulative Throughput, Pump #2

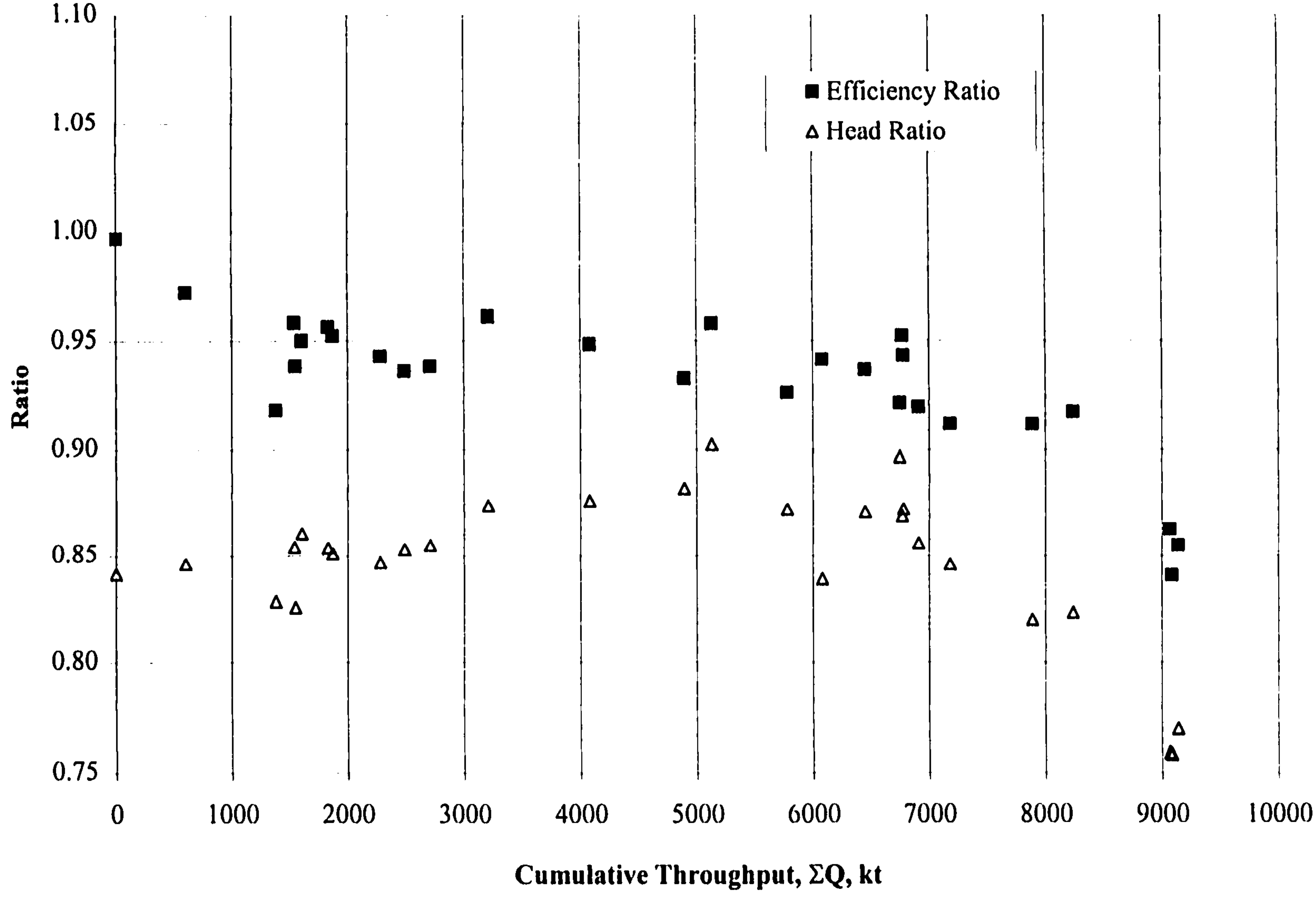

Figure 5.22: Water Performance vs. Cumulative Throughput, Pump #3

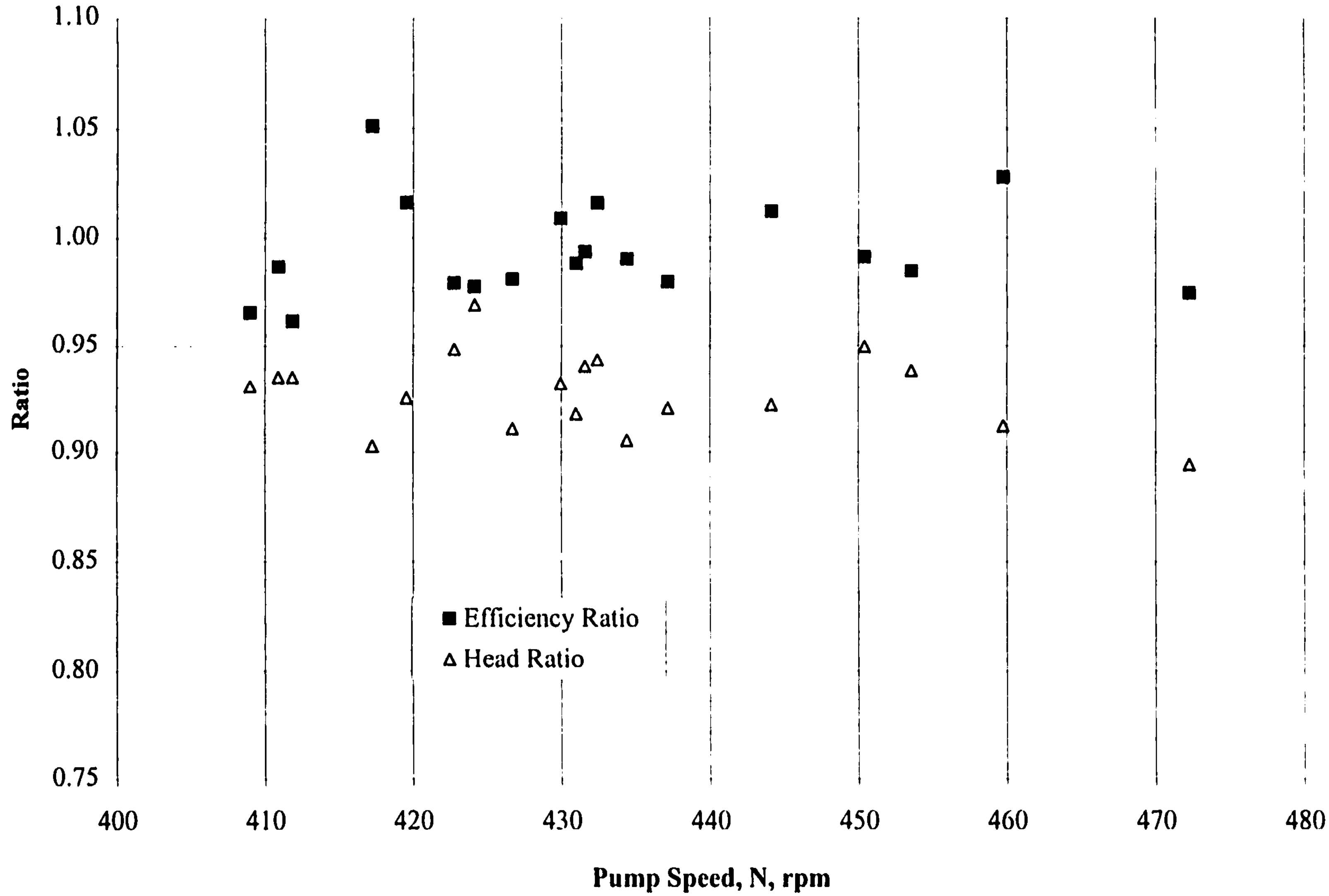

Figure 5.23: Water Performance vs. Pump Speed, Pump #1

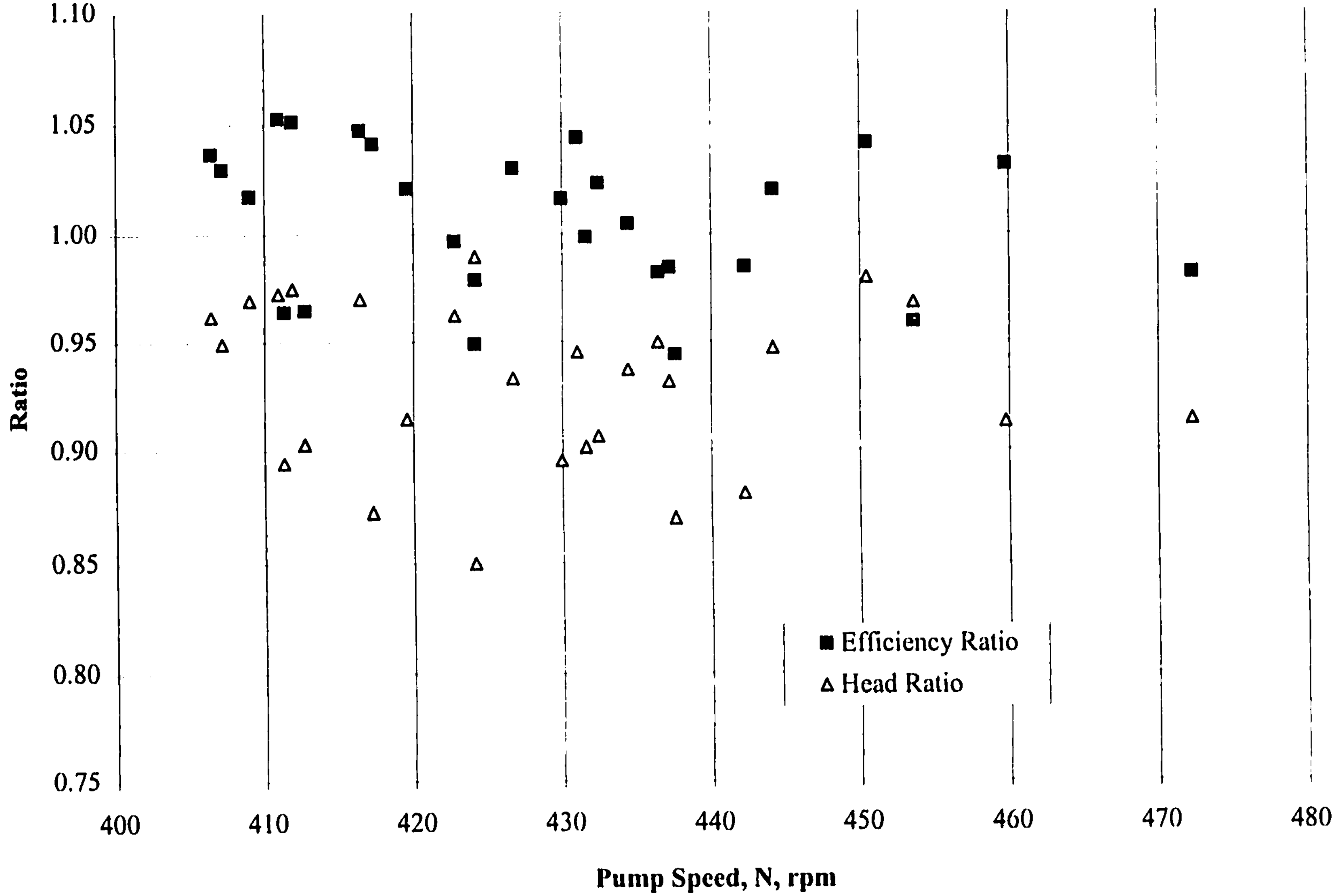

Figure 5.24: Water Performance vs. Pump Speed, Pump #2

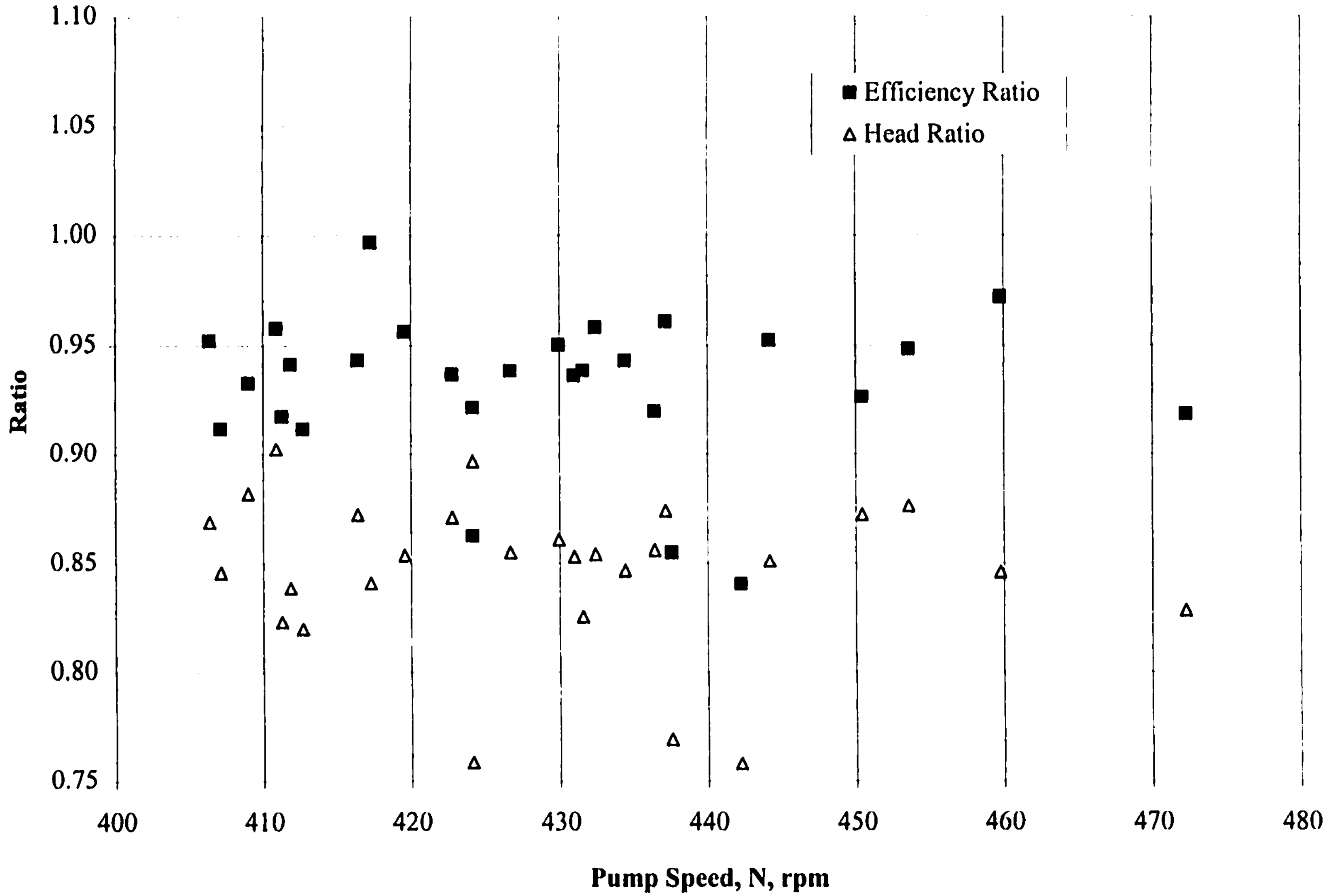

Figure 5.25: Water Performance vs. Pump Speed, Pump #3

6.0 Discussion

6.1 Use of Operating Facilities

This study made use of an actual operating industrial installation as experimental apparatus. In order to study the long term operation of industrial scale slurry pumps, this is necessary. It would be financially impossible to process 10,000 kilotonnes of sand through three pumps powered by 1650 HP motors over a six month period in a research facility. To study the performance it was necessary to use an operating system, with the knowledge that the priority of use lay with SCL Operations, and not with the persons performing this study. This was viewed as a compromise that was necessary, but unavoidable. While it was understood in advance that this may lead to difficulties in data collection, several points arose that caused problems.

It was desired to examine pump performance over two or more impeller cycles. Had the additional instrumentation been installed in 1996 then it would have been possible to use data for the period July 1996-May 1997. Instead, the extra pressure transmitters were not installed until June 1997, and thus a great deal of potentially useful data were not available for analysis.

Difficulties with the PI data acquisition system made it impossible to extend the analysis past October 1997. In November 1997 the sampling interval for many PI data points changed from a constant value of one minute to a highly variable number. It was not uncommon to see intervals of 20 minutes or more between data points. Worse, the intervals were seemingly random. Data would be collected on one-minute intervals for some period of time, followed by larger intervals. Such a situation obviously would cause any one-hour averages to be invalid, as they would not in fact be the average of 60 observations, but of two or three.

Almost all of the reviewed literature uses particle size or particle size distribution as a variable in examining pump performance. As there is no continuous, on-line particle size measurement, it was impossible to include this as a variable in this study. It can be stated that from observation of previous analyses, the particle size distribution and fines content remains reasonably stable at SCL. With oilsand currently being mined by seven separate machines there is some degree of blending performed so that unusually rich ore, which typically has larger sand grains, is not processed en bloc.

Attempts were made to perform test runs that would form the basis of an experimental factorial design. These runs involved holding pump speed at a fixed level for several minutes, while holding slurry density constant. One such experiment was performed before the end of the final time frame, but a sample was not obtained. Three other experiments were performed after the end of the time frame of this analysis, but a sample was only obtainable for one of these runs. As the bulk of these experiments were run after the impellers that form the basis of this study were changed out, the analysis of such experiments would not yield any results that would be useful in the context of this study.

6.2 Clear Water Performance

It was desired to model the performance of the pumps while operating on water in order to establish a moving baseline for comparison to slurry performance. Unfortunately, there were not enough observations to develop correlations that would have any reasonable degree of fit to the observed data. What can be seen from Figures 5.20 5.21 and 5.22 is that the head ratio at all times was considerably lower than the expected value of approximately 100%. The efficiency ratio for all three pumps was significantly higher, frequently around the 100% level, as expected. At cursory examination, the behavior of the pumps while pumping water over time seems to parallel that when pumping slurry. Pumps #2 and #3 show head ratios increasing to a maximum at 5000-6000 kt cumulative throughput, and decline after that point. The head ratio of Pump #1 appears to rise with respect to cumulative throughput. It is not immediately obvious why the head ratio of a new pump is significantly lower than 100%. While faulty instrumentation may be considered, the head ratios for operation on water are similar to those on slurry operation, and thus any correction to the water head ratio would increase the slurry head ratio to approximately 100%, which is counter to all theoretical considerations to date.

6.3 Effects of Specific Variables

6.3.1 Manufacturer's Specified Performance Factors

The pump manufacturer has specified a head reduction of 9.7% and an efficiency reduction of 6.8% due to the solids effect. These describe a head ratio of 90.3% and an efficiency ratio of 93.2%

6.3.2 Effect of Cumulative Throughput

Examination of Figures 5.4, 5.5 and 5.6, shows well defined functions of efficiency and head ratio versus cumulative sand throughput. When examining the importance of the correlation parameters in Table 5.5 it can be seen that the throughput and throughput squared terms are the second and third largest parameters in the efficiency ratio correlations. The throughput terms are secondary in importance to the weight concentration parameter. In all cases, the parameters are negative, meaning that as cumulative throughput increases the efficiency ratio decreases. This mirrors the behavior that is observed in Figures 5.4, 5.5 and 5.6. Pumps #1 and #2 exhibit similar efficiency behavior, commencing at approximately 95%, appearing to rise slightly to about 97% at about 3000 kt of throughput, and decline to about 93% at 6500 kt. The data for Pump #1 stops at this point due to an impeller changeout. For Pump #2 after 6500 kt the efficiency shows a sharper decline to about 88% at 10,400 kt. Pump #3 shows a similar profile, but commences at a lower value, 90%, and ends at a lower value, about 80% at 10,400 kt. In addition, there is also a local maximum at about 3000 kt.

When one examines the correlation parameters in Table 5.5, it can be seen that the β_{11} term, that for sand throughput squared, is the strongest term in the head ratio correlations. The β_1 term for head ratio is also quite prominent in Pumps #2 and #3, but neglected in Pump #1. Examining Figures 5.4, 5,5 and 5.6 it can be seen that for Pump #1 the head ratios starts at approximately 85% and increases to approximately 90% after 6000 kt have been processed. Pump #2 begins with a head ratio of approximately 83%, which rises to 90% at 5000 to 6000 kt of sand, and then sharply declines to about 78% at 10,400 kt. For Pump #3 the head ratio starts at slightly less than 80%, climbs to 83% at 5000-6000 kt, and than declines to about 68% at 10,400 kt.

Why do these pumps exhibit similar but slightly different behavior? In all cases a slight improvement in performance was exhibited over the first 6000 kt of pump operation, and then a decline to 10,400 kt in Pumps #2 and #3. Pump #1 had an impeller changeout at 6700 kt. Pump #1 had both a new impeller and casing at the beginning of this study, and thus was essentially a new pump. It had the best efficiency ratio performance, and the best head ratio at the beginning of the study, but the head ratio did not climb to as high a value as Pump #2 after 6000kt. Pump #2 had a new impeller, but had a casing which was described as being worn in the throat area. One would expect this to lead to increased vortex formation and extra shock losses, and thus lower efficiency ratios. This was not observed. Pump #3 exhibited similar trends to Pump #2, but at absolute levels about 5% lower. This was assumed to be due to the fact that Pump #3 had a reconditioned, and not new impeller at the inception of this study. It is not known if the shroud or vanes had been reconditioned.

One must consider why the head ratios exhibit the behavior of starting at a certain level, increasing to a maximum at a certain point in time, and then decreasing almost linearly with sand throughput. Both Vocadlo (5), and SCL have seen pump performance improve shortly after installation, mainly due to the polishing effect of the slurry on casting imperfections and abrasive areas in the pump. However, in this case the improvement continues until about 6000 kt of sand throughput, or a period of over three months. A non-rigorous hypothesis for the reason behind this behavior is described below.

It has long been known that the phenomenon referred to as "slip" is one of the sources of efficiency drop and head loss in a pump. When examining a flow triangle for the exit of an impeller, the meridional velocity component is assumed to be travelling at the same angle as the pump vane, known as β_2. (Please refer to Figure 2.2) In reality, the meridional component rapidly assumes a more acute angle. This is what is referred to as slip. The net result is that the resultant composite velocity is smaller than that that would be seen if the meridional velocity at the impeller exit followed the vane angle, B_2.

The vane has a finite thickness throughout its length, in this case over one inch. It has been shown by Hergt, *et al.* (13) that when the fluid adjacent to the vane exits the impeller it encounters a region of low velocity that extends out from the impeller at the region bounded by the end of the vane. This leads to a pressure imbalance, and the resulting low-pressure area is filled by fluid exiting at the vane face. This has the result of reducing the average velocity at the pump outlet, and thus reducing the velocity head generated by the impeller.

As the pump ages, the vane is eroded. Being the region of maximum kinetic energy, the vane tip is eroded fastest, in such a manner that the vane becomes thinner as the tip is approached. Eventually, the front and back surfaces of the vane will meet, and there is no effective vane thickness at the tip.

At this point in time the region of low velocity adjacent to the vane tip will no longer exist, as the vane has no apparent thickness and thus there is no region blocked by the vane. It is theorized that this is the point at which maximum head ratio is observed. The diameter of the impeller at this point is assumed to be the same as originally installed, as all of the erosion has taken place on the front face of the vane, reducing the thickness but not the length of the vane.

At any point in time after this the vane will continue to erode, and reduce in diameter. It is this reduction in diameter that explains the reduction in head ratio after approximately 6000 kt of sand transported. The pump affinity laws state that head decreases with the square of diameter, e.g., a 10% reduction in diameter will lead to a 19% reduction in head generated (0.9 x 0.9 = 0.81). It is theorized that Pump #1 would have exhibited similar behavior had the impeller not been changed out after 7000 kt of sand transported. The change in vane tip profile is shown in Figure 6.1.

This condition is analogous to the practice referred to as "tip filing". In the chemical processing industries it is not uncommon for the tips of centrifugal pump impellers to be filed down to a sharp point in order to gain a small amount of head for the same diameter impeller, operating at the same pump speed. This procedure is only practised on pumps in low-erosive applications. If the front face of the vane is filed this is referred to as "over-filing". It is more common to file the back of the vane as this does not effect the vane angle. This is referred to as "under-filing". This practice is detailed in Karassik (14).

6.3.3 Effect of Weight Concentration of Solids

When examining Figures 5.7, 5.8 and 5.9 it is difficult to observe any discernible trends, mainly due to the masking of the effects of cumulative throughput. Only when one examines the parameters in the correlations does the significance of weight

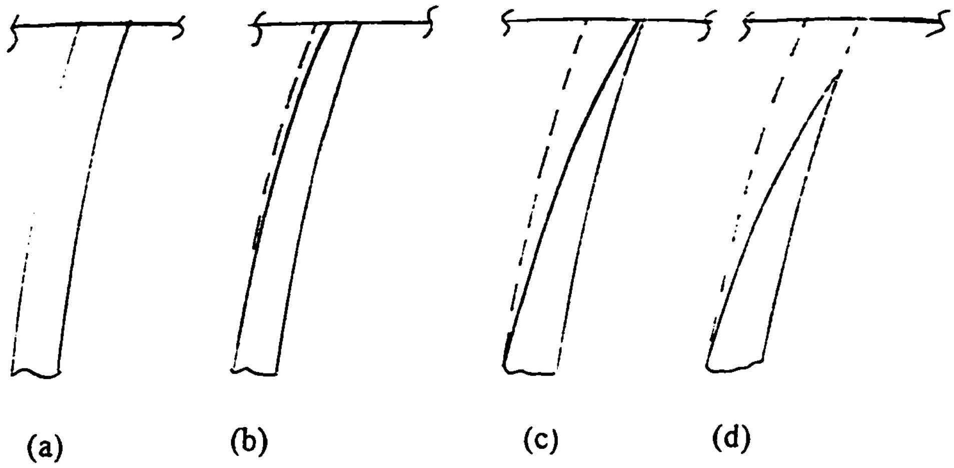

(a) Original Impeller Vane Profile

(b) Reduction in Vane Tip Thickness

(c) Vane Tip Reduced to Minimun Thickness

(d) Reduction in Vane Length

Figure 6.1: Vane Tip Erosion Stages

concentration, and hence slurry density, come into effect. In the existing literature it is strongly suggested that head ratios decrease linearly with increased weight concentration. When examining the β_2 terms in Table 5.5 it can be seen that for all efficiencies, and for the head ratio of Pump #1, this effect is linear and negative, i.e., the linear term is much stronger than the second degree term, β_{22}. However, for the head ratios of Pumps #2 and #3 the squared term is about 60-70% the significance of the linear term. It must thus be stated that for these two pumps, the head ratio decreases quadratically with an increase in weight concentration. The difference between Pump #1 and Pumps #2 and #3 is likely largely due to the fact that Pump #1 was only studied over the first half of the erosion cycle, and did not perform during the "diameter reduction" phase. This leads one to the conclusion that the concentration squared term is necessary to fit a single curve to the head ratio curve that is, in effect, a composite of two near linear curves that both describe fundamentally different modes of operation.

6.3.4 Effect of Pump Speed

The authors reviewed who mentioned pump speed as a variable were unanimous in the statement that pump speed was not a discernible variable in slurry pump performance. The correlations developed in this study do show a small dependence for Pump #1 and an even smaller one for Pump #2. However, pump speed can be neglected completely for Pump #3 with no effect on the fit of the correlation. While the input variables were considered by the author to be independent, there is a slight possibility that pump speed could be related to cumulative throughput, in that as the pump ages and the impeller decreases in diameter, the pump must be run faster to obtain the same head output. However, while this may be intuitively true, when calculated a correlation coefficient of only 0.14 was found for these two variables. Thus, an extremely weak positive correlation exists between these two variables.

6.3.5 Discussion of Other Effects

In addition to the previously mentioned particle size, there are several other potential variables that were not examined in this study. These are: fines content, lump content, bitumen content and air content. A few brief points about each will be mentioned here.

Fines content:

The majority of sand particles are large enough that they will, in a brief amount of time, settle out. A slurry consisting of only particles such as this is referred to as a heterogeneous, or settling slurry. Below a particle size of about 50μm the sand grains, known at this size as fines, do not settle out except over a very long time. A slurry of such particles is referred to as a homogeneous slurry, as the particles are relatively evenly distributed throughout the fluid medium, even at rest. Non-settling slurries exhibit very different rheological properties to settling slurries.

Lump Content:

Particles that are too large to be captured by a sampler are referred to as lumps. These can only be observed at the exit of a pipeline. Lumps can cause problems with plugging of impeller passages. Lumps of up to two inches in diameter can enter this system due to the North Mine screening system.

Air Content:

Potentially the most important variable not examined. As the system being examined is fed by several settling and processing vessels, and has collection tanks along the line that are open to the atmosphere, it is quite unlikely that significant volumes of air or entrained organic gases infiltrate into the slurry. This variable is much more important when studying oilsand transport systems, which are fed by cyclofeeders and contain a large percentage of organic material.

Bitumen Content:

The stream in question always contains a small amount of bitumen, typically 0.3 to 1.0% by weight. It is beyond the scope of this paper to examine the effects of this small amount of bitumen on pump performance. It is known that bitumen tends to accumulate in spots of low fluid velocity. Whether bitumen deposited inside pumps on impellers and volutes acts as a lubricant or a retardant is unknown to the author.

Suction Conditions:

The three pumps in question operate at very different suction pressures, typically 100, 650 and 1200 kPa respectively. In addition, Pump #1 is fed from a feed hopper, with flow that is approximately proportional to the tank level, whereas the second and third pumps are fed by the previous pumps. Due to the slow speed and small number of vanes of these pumps the delivery pressure will not be smooth, but will exhibit a vane-induced periodicity, with a frequency of about 35-40 Hz for most operating speeds. The effects of this periodicity on the efficiency of the following pump are unknown, and beyond the scope of this study.

6.4 Instrumentation Error and Effects

One of the drawbacks of using an operating facility was the difficulty in controlling the accuracy of instruments, at least to the same degree of control one would have in a laboratory.

The largest possible source of error is the venturi meter. SCL uses a coefficient of discharge (Cv) of 0.984. However, Shook & Masliyah (15) have observed Cv's for a horizontal venturi meter measuring a settling slurry with a value of ≈1.01. If this is in fact the case, then the actual flow rates would be ≈2.5% higher than observed. Examining the pump curve (Figure 3.1), it can be seen that an increase of flow of 2.5% results in a drop in head generated by 0.7-1.0%. This would have the effect of increasing head ratios by 0.7-1.0%. This amount is well within the bounds of normal experimental error.

The discharge pressure measurement is suspect in that it is not known whether fully developed flow is encountered at the locations of the discharge pressure transmitters. It is recommended engineering practice to locate pressure transmitters at least 20 pipe diameters downstream from any flow disturbance, but in this case the transmitters are 3-5 pipe diameters downstream of the pumps.

All instruments were examined for zero behavior. All tags were found to zero correctly during downtime except for the power reading from the VFD. A steady value of 9 kW was observed during shutdown periods. This was assumed to be the power required to maintain VFD control and instrumentation during downtime. The venturi flow meter observed strange zero behavior. Under zero flow, high-pressure situations the flow meter read zero. Under zero flow, low-pressure conditions a value for flow of 200-300 L/s was often observed. This was assumed to be caused by residual bitumen in the impulse lines. The bitumen maintained an apparent pressure on the diaphragms of the pressure transmitters. Under low-pressure situations the apparent pressure were different, thus yielding a pressure differential and an apparent flow. When the line flowing into the venturi was drained, such as when the pumps were being disassembled, the apparent flow gradually decreased to zero as the bitumen slowly drained out of the impulse lines. Shutdown pressure readings were consistent with the head in the pump feed hopper, and when the line was reduced to atmospheric pressure, such as when the pumps were disassembled the pressures zeroed to within 2-3 kPa.

6.5 Conclusion

When one takes into consideration all of the variables that were not examined, the fact that data averaging using an arbitrary definition of "steady state" was used, and the possible error sources from instrumentation, one can only conclude that the data displayed in Figures 5.4, 5.5 and 5.6 and the subsequent correlations should only be used as the broadest of guidelines in studying slurry pump behavior, and not applied rigorously. While detailed calculations of error propagation were not performed, it can be seen that if one assumes the normal error range of ±5% for pressure instruments and venturi meters, and then takes into account the fact that the input data are normally distributed averages with a 95% confidence interval of ±4%, then the potential error would be much greater than the narrow range of head and efficiency ratios observed . This is not meant to discount the validity of all the work performed here. While there is considerable error in the absolute values, trends are observed that correspond to and are explainable by physical phenomena.

7.0 Recommendations

7.1 Recommendations With Respect to Pump Design

7.1.1 Impeller Design

The applicability of a pump for a certain application can be judged by comparing the range of operation with the best efficiency point of the pump. If the design is good, a great deal of the steady state operation should be close to the best efficiency point. As this is a variable speed pump, there is not in fact a best efficiency point, but a locus of best efficiency points for each pump speed. For the pumps in question this line can be approximated by the following quadratic curve:

$$\text{Head (feet)} = (9 \times 10^{-8} \times \text{GPM}^2) + (0.0098 \times \text{GPM}) - 74.3 \qquad ...(7.1)$$

Figure 7.1 shows the distribution of the actual head output of the pumps divided by the best operating line head. As can be seen, the majority of the actual heads are 5-10% below the best efficiency line. In all cases the drop is almost identical to head ratio. It thus appears that the best efficiency line of these pumps matches exactly the system operating curve, and as such they are well designed.

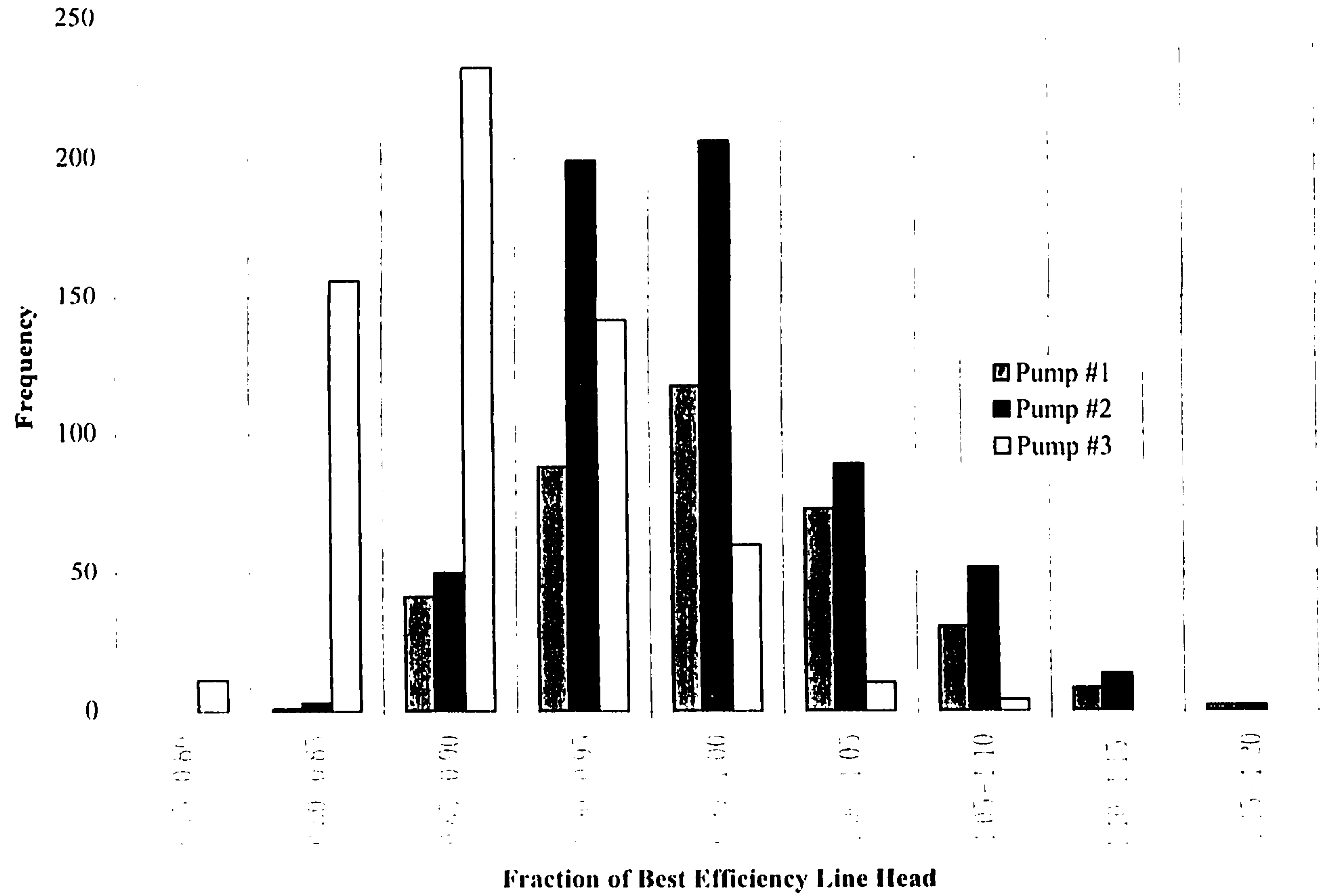

Figure 7.1: Distribution of Operating Head as a Fraction of Best Operating Line Head

Referring to the discussion of the change in efficiency and head ratios with erosion of the impellers in Section 6.3.2, the question of vane design must be addressed. What is the optimum vane thickness? An increase in vane thickness would decrease the cross sectional area of the impeller channels, and would likely increase friction losses, but then the impeller would have a longer life before reaching the point where the vane thickness is zero at the tip, and would increase impeller life between changeouts. Previously impellers have been designed with a single best static performance in mind, but there has not been consideration of the change in performance with respect to time. A study of the hydrodynamic performance of impellers coupled with an analysis of the changes with respect to throughput could lead to impeller designs that would be more economical.

Recommendation One:

> Further study of the effect of impeller tip design should be undertaken. A comprehensive analysis examining the change in impeller performance over time, as a result of wear, is needed. This could lead to the design of an impeller with optimal lifetime economic performance.

7.1.2 Motor Design

Another factor to be considered is motor size. While the author is not familiar with normal practices with respect to sizing of motors for specific applications, and normal overcapacity factors, it appears that the motors in this application are largely oversized.

The costs of oversizing the motors are twofold. The larger motor incurs larger capital cost, both in motor cost and motor mounting and anchoring cost. As can be seen in Figure 5.2, these motors operate at optimum efficiency at 75-90% load. Consistently operating the motors at 50-70% load results in a loss of efficiency.

Figure 7.2 shows the frequency distribution of motor load factor, as defined in Section 5.1.4. As can be seen, for the vast majority of observations the motor was operating at less than 70% of load. The maximum observed load factor was 86%, and only 5 of 614 observations, or 0.8%, were above 80%. As the motors are capable of operating at up to 125% of their rated capacity, it would appear that these motors are overdesigned by a factor of at least 1.33. A motor of nominal output 1250 HP would operate such that the average load factor would be 81%, and load factors above 100% would be observed only 5% of the time. A normal reason for oversizing motors is the fact that startup torque requirements are frequently much greater than operating torques, but in this case the VFD is used to provide low torque "soft" starts, at low speeds, and motor speed is ramped up at 45 rpm per second. This compares with a

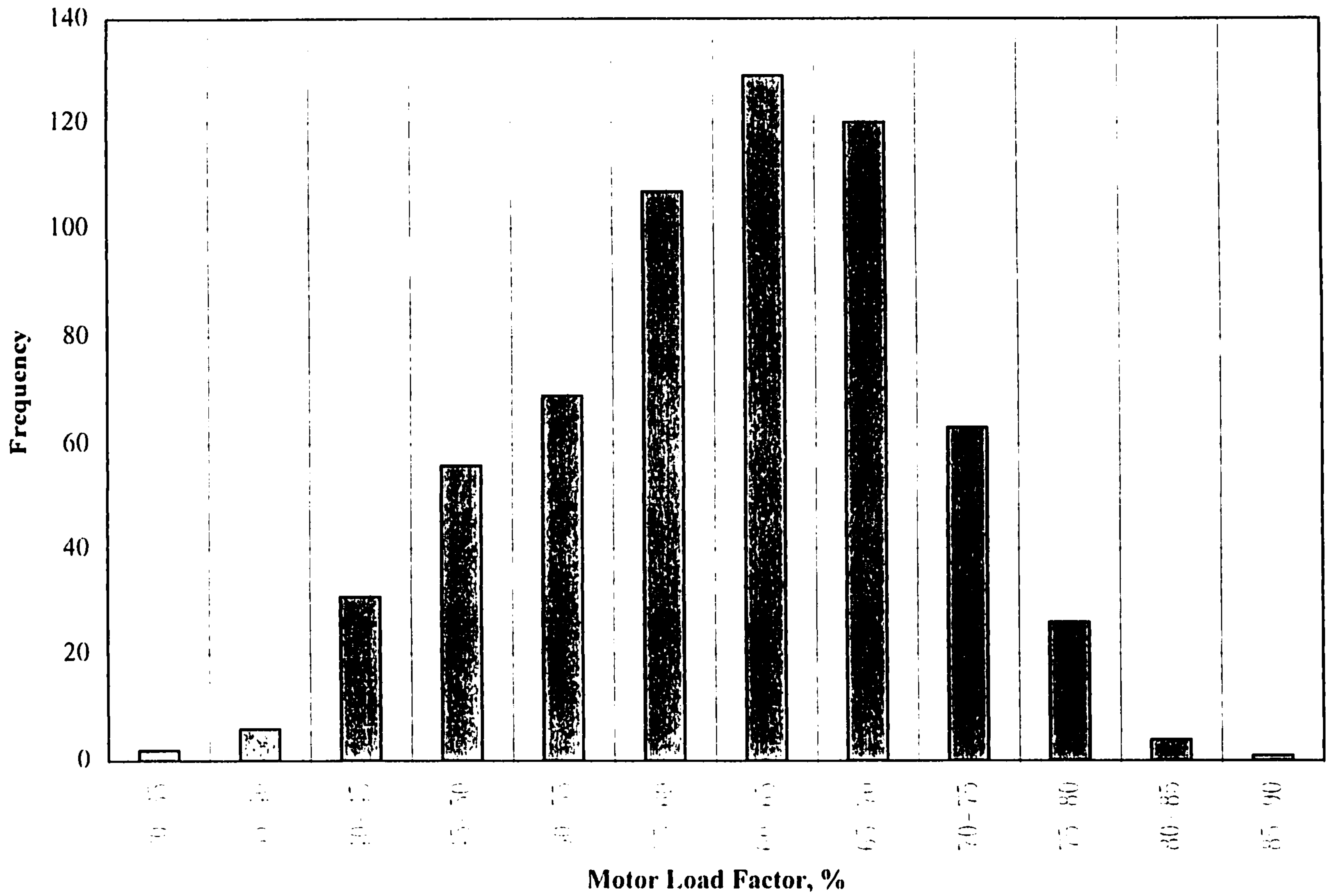

Figure 7.2: Frequency Distribution of Motor Load Factor

normal motor, which reaches speeds of 1800 rpm typically within 15 seconds of starting, or an average acceleration of 120 rpm/second. The startup torque requirement is further reduced by the fact that the system is always started up with water as the working fluid. Water requires only 66% the torque of a 1.5 SG slurry.

Recommendation Two:

> The motor size for any similar pump applications purchased in the future should be closely evaluated to find out whether the 1650 HP motors are oversized for this specific application. It is proposed that 1250 HP motors may be better suited to this application.

7.2 Recommendations With Respect to Pump Operation

It was observed earlier in this study that less than 20% of the operating hours of these pumps are considered as "steady state" under the definitions contained herewithin. Figure 7.3 displays the pump speed versus time for a randomly selected 42-hour period. As can be seen, the pump speed frequently sawtooths between 390 and 510 rpm. According to the affinity laws, reducing pump speed from 510 to 390 rpm would lead to reductions of 42% in head and 24% in flow. The speed of the pumps, when under automatic control, is controlled by the level in the pump feed hopper. These

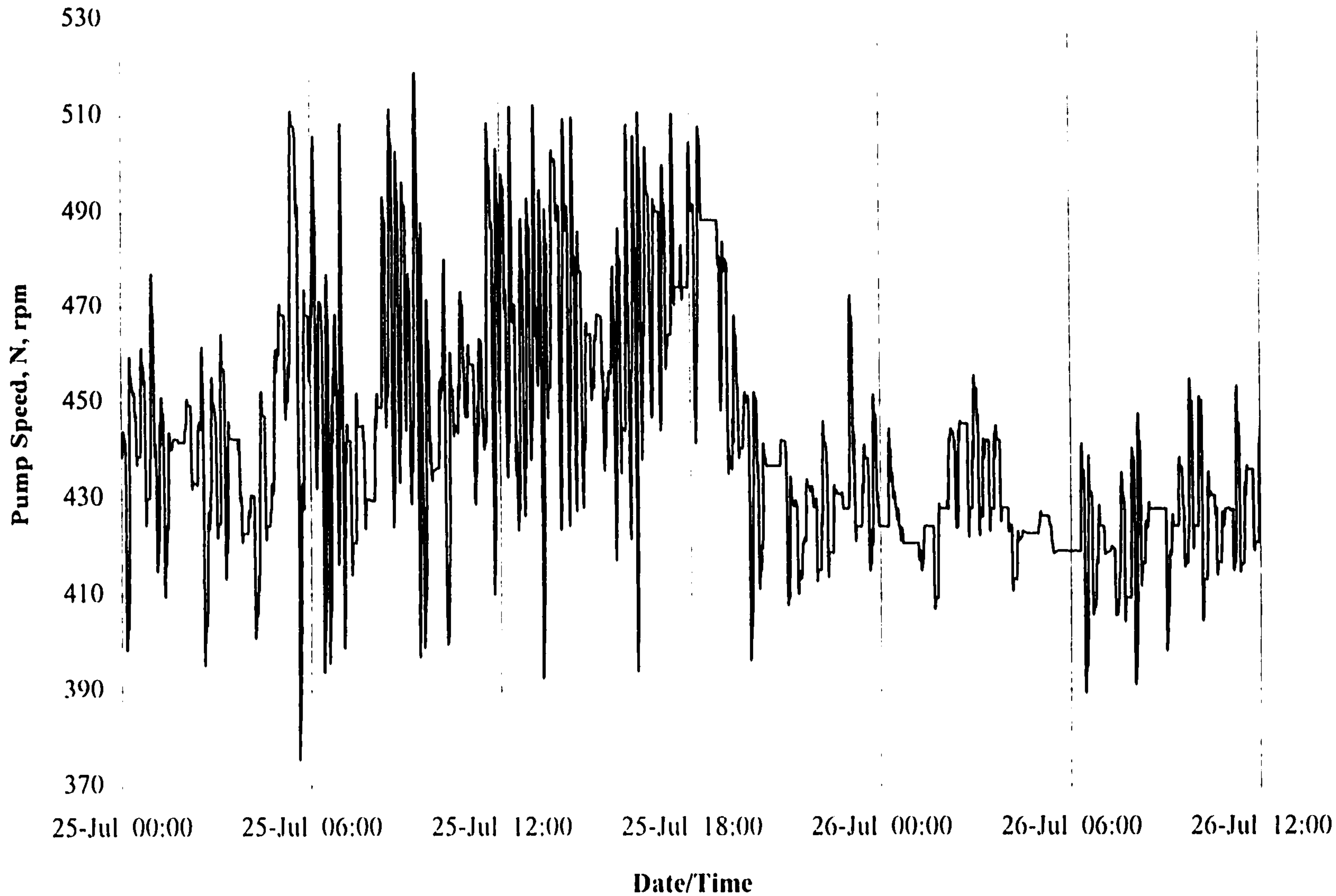

Figure 7.3: Pump Speed vs. Time, Typical Period of Operatin

pumps have a maximum net positive suction head (NPSH) requirement of 15 feet of head at 500 rpm. (The NPSH is the static pressure at the suction of a pump minus the inlet line friction losses and the vapour pressure of the fluid). The feed hopper has a capacity of approximately 30,000 US Gallons between the normal level of 33 feet, and an NPSH safe low level of 20 feet. At the design flow rate of 16,400 USGPM, this equates to a time of almost 100 seconds for the level to decrease from 32 feet to 20 feet. However, the level controller is tuned very aggressively to maintain a level between 30 and 34 feet. This is the cause of the rapid shuttling of pump speed. The controller is tuned so aggressively as to act as a quasi-on/off controller. A PID controller with the correct tuning, and a wider band of operation would lead to much smoother operation of the pumps, and a large reduction in the standard deviation of pump speed. Such operation would have the benefits of reducing transient accelerations of the impeller, thus reducing localized fluid accelerations in the pump and reducing wear, as well as allowing the pump to operate closer to the best efficiency point. It is also theorized that less transient operation may lead to improvements in the service life of pump mechanical seals, but that question is beyond the scope of this study.

Recommendation Three:

> The level control system currently in operation should be modified such that the level in the pump feed boxes be allowed to vary with broader limits. This would stabilize pump speed, allowing more

operation closer than the best efficiency point of the pumps, reduce power consumption due to frequent acceleration of the pumps, and may have a beneficial effect on mechanical seal lifespan.

7.3 Recommendations With Respect to Pump Maintenance

It is necessary to define a criterion for the replacement of impellers. As previously noted in this study, the impeller in Pump #1 was replaced after 6740 kt was transported. The impeller was described by SCL Maintenance staff as 'badly worn". However, when examining Figure 5.4 it can be seen that the head and efficiency ratios had only just entered the period of decline observed in Figures 5.5 and 5.6. While the author did not have an opportunity to observe the impeller, it seems quite obvious from Figure 5.4 that the process of diameter reduction had only just began. It is likely that any wear observed was in the impeller shrouds. Upon removal, other impellers have had holes as large as 4" in diameter in the rear shrouds.

A method of scheduled, preventative maintenance is currently used. It is common practice to disassemble and examine the pumps after approximately 2000 and 4000 calendar hours, or about 6000 kt and 12,000 kt cumulative throughput. The impeller is usually replaced after 4000 hours. If it is desired to move towards a program of predictive maintenance it will be necessary to define more rigid criteria for impeller replacement, coupled with a pump performance monitoring process. As the impeller diameter decreases, and as the head and efficiency ratios decline a critical point will be reached where it is no longer economical to continue operation without an impeller changeout. This is a classic optimization problem, with variables being the cost of electricity, the cost of lifespan reduction of the pumps and motors, and the cost of replacing impellers. Such a function needs to be developed, and pump performance be continuously monitored to identify the optimal time for pump maintenance, based on the condition of the pumps and trends of head and efficiency ratio.

Recommendation Four:

> A programme of equipment monitoring be instituted, in conjunction with the development of specific power consumption criteria for the replacement of pump impellers, leading to optimal impeller changeout intervals.

8.0 References

(1) Wilson, K.C., Addie, G.R., & Clift, R. "Slurry Transport Using Centrifugal Pumps". 167-177, Elsevier, London, 1992

(2) Shook. C.A., & Roco, M.C., "Slurry Flow: Principles and Practice", Butterworth- Heinemann, Boston, 1991

(3) Stepanoff, A.J., "Pumps and Blowers: Two Phase Flow", 161-187, John Wiley and Sons, New York, 1965.

(4) Wiedenroth, W., "The Influence of Sand and Gravel on the Characteristics of Centrifugal Pumps", *Proc. Hydrotransport 1*, Paper E1, BHRA Fluid Engineering, Cranfield, UK, 1976

(5) Hunt, W.A., & Faddick, R.R., "The Effects of Solids on Centrifugal Pump Characteristics", from "Advances in Solid-Liquid Flow in Pipes and its Application", Zandi, I., Ed., Pergamon Press, Amsterdam, 1971

(6) Vocadlo, J.J, Koo, J.K., & Prang, A.J., "Performance of Centrifugal Pumps in Slurry Service", *Proc. Hydrotransport 3*, Paper J2, BHRA Fluid Engineering, Cranfield, UK, 1974

(7) Burgess, K.E. & Reizes, J.A., "The Effect of Sizing, Specify Gravity and Concentration on the Performance of Centrifugal Slurry Pumps", *Proc. Instn. Mech. Engrs.*, 190, 391-399, 1976

(8) Cave, I., "Effects of Suspended Solids on the Performance of Centrifugal Pumps", *Proc. Hydrotransport 4*, Paper H3, BHRA Fluid Engineering. Cranfield, UK, 1976

(9) Sellgren, A., "Performance of a Centrifugal Pump When Pumping Ores and Industrial Minerals", *Proc. Hydrotransport 6*, Paper G1, BHRA Fluid Engineering, Cranfield, UK, 1979

(10) Mez, W, "The Influence of Solids Concentration, Solids Density and Grain Size Distribution on the Working Behavior of Centrifugal Pumps", *Proc. Hydrotransport 9*, Paper H1, BHRA Fluid Engineering, Cranfield, UK, 1984

(11) Roco, M.C., Marsh, M., Addie, G.R., & Maffett, J.R., "Dredge Pump Performance Prediction", *Journal of Pipelines*, 5, 171-190, 1986

(12) Gahlot, V.K., Seshadri, V., & Malhotra, R.C., "Effect of Density, Size Distribution and Concentration of Solid on the Characteristics of Centrifugal Pumps", *Trans. ASME*, 114, 386-389, 1992

(13) Hergt, P., Brodersen, K.V., Brodersen, S., & Visintainer, R.J., "A Study of the Outlet Velocity Characteristics of Slurry Pump Impellers", *ASME Liquid - Solid Flows*, 189, 197-205, 1994

(14) Karassik, I.J., "Centrifugal Pump Clinic" 2nd Edition, 21-22, Marcel Dekker, Inc., New York, 1989

(15) Shook, C.A. & Masliyah, J.H., "Flow of Slurry Through a Venturi Meter", *Can. Journal Chem. Eng.*, 52, 228-233, 1974

9.0 Appendix A: Data and Sample calculations

Section: **Page**

Sample Calculations:

The basis for the sample calculations shall be the observation of 09:50, May 8, 1997. The PI inputs for this time, as seen in Table A1, are as follows:

Tag	Value	Units
23pi1725	95.3	kPa
233p2500	497.8	kPa
233p2501	904.6	kPa
23pi1726	1276.4	kPa
23fi1729	1020.9	Litres/second
5di351	1.34	SG units
23ji1747	1484.6	kW
23si1748	414.9	rpm
23ii1742	119.5	Amps
23ii1743	116.8	Amps
23ii1744	116.7	Amps

Calculation of Inputs:

The inputs, as seen in Table A2, are calculated thus:

Pump Head:

$$\Delta H_{1,obs} = \left[\frac{(p_2 - p_1)}{(9.81m/s^2)S_1} + (z_2 - z_1)\right] \times 3.2808 ft/m$$

or: $$\Delta H_{1,obs} = \left[\frac{(497.8kPa - 95.3kPa)}{(9.81m/s^2)1.34} + (0.708m)\right] \times 3.2808 ft/m = 103.0 ft$$

0.708m is the difference between the suction and discharge levels. For Pumps #1 and #3 the discharge is higher. For Pump #2 the discharge is lower.

Motor Power:

The motor power is defined thus:

$$HP = \frac{I_1}{(I_1 + I_2 + I_3)} P_1 \eta_{VFD} \left(\frac{1.34HP}{kW}\right)$$

or $$SHP_{1,obs} = \frac{119.5A}{353.0A}(1484kW)x0.985 \times \left(\frac{1.34HP}{kW}\right) = 659.9HP$$

Flow:

To convert from L/s to USGPM, multiply by 15.702, there fore

1020.9 L/s x 15.702 = 16,182 USGPM.

Head Ratio:

The expected head at the observed flow and speed must be extracted from Table 4.2 by linear interpolation.

For the case in hand, the pump speed, along the x-axis of the table, is 414.9 rpm, and the flow, along the y-axis, is 16,182 USGPM.

We must now lookup the head at the four points bounding the intersection of the actual speed and flow.

The heads at the bounds are as follows:

	410 rpm	415 rpm
16,000 GPM	109.54 ft	112.70 ft
16,500 GPM	108.26 ft	111.43 ft

By interpolating, it is found that the head at 414.9 rpm and 16,182 GPM = 112.2 ft.

The head ratio is obtained by dividing the actual head by the expected head, thus:

103.0 / 112.2 = 0.919 = 91.9%

Efficiency Ratio:

Firstly, the expected power must be extracted from Table 4.3. This is performed in the same manner as the calculation for expected head from Table 4.2, as above, except that the x-axis is the observed flow, and the y-axis is the expected head. In the case at hand, the bounds are as follows:

	16,000 GPM	16,500 GPM
110 feet	503.6 HP	519.5 HP
115 feet	527.6 HP	544.0 HP

By interpolating it is found that the expected shaft power at 16,182 GPM and 112.2 feet = 519.9 HP.

This is the water horsepower. To obtain the expected slurry HP, we must multiply by SG.

Slurry Power = 519.9 HP x 1.34 = 694.7 HP.

To find the actual shaft power, it is necessary to multiply the motor power by the motor efficiency and the drive efficiency. The motor efficiency is a function of the load factor, where load factor = actual motor power/1650 HP.

In this case, Load Factor = 660/1650 = 0.4

Efficiency = $0.089\ LF^3 - 0.266\ LF^2 + 0.245\ LF + 0.891$

or $= 0.089\ (0.4)^3 - 0.266\ (0.4)^2 + 0.245\ (0.4) + 0.891 = 0.952$

The drive efficiency was assumed to be 0.985.

Therefore, actual shaft power = 660 HP x 0.952 x 0.985 = 618.8 HP

The efficiency ratio = head ratio x (expected shaft power / actual shaft power)

Efficiency Ratio = 0.919 x (694.7 HP/618.8 HP) = 1.031 = 103.1%

Tables of Input Data and Sample Calculations:

The following four tables, numbered Table A1 to A4, are examples of the calculation results. Table A4 list the unmanipulated PI input data. Table A2 details the calculated input data obtained from manipulation of the data in Table A1. Table A3 illustrates the calculation steps and results for head ratio calculations, and Table A4 does the same for efficiency ratio calculations.

Obviously, there are many more data points (time observations) than illustrated in these four tables, and the head and performance calculations are only displayed for Pump #1. These tables are intended to give an illustration of the data and calculations only. Anybody requiring complete copies of the data may obtain them by contacting the author.

Table A1: PI Input Data

Time	23pi1725	233p2500	233p2501	23pi1726	23fi1729	5di351	23ji1747	23si1748	23ii1742	23ii1743	23ii1744
	(kPa)	(kPa)	(kPa)	(kPa)	(kPa)	(SG)	(kW)	(rpm)	(Amps)	(Amps)	(Amps)
08-May-97 09:50	95	498	905	1276	1021	1.34	1485	415	120	117	117
09-May-97 11:03	99	707	1320	1886	1215	1.57	2861	493	180	176	177
09-May-97 22:02	102	670	1241	1769	1132	1.52	2489	475	165	160	162
09-May-97 23:38	100	690	1286	1835	1162	1.51	2679	487	172	167	169
10-May-97 02:19	95	694	1294	1849	1190	1.49	2756	493	175	169	171
10-May-97 07:23	104	698	1300	1855	1172	1.55	2710	484	174	170	172
10-May-97 12:11	103	705	1313	1873	1166	1.56	2727	485	175	171	172
10-May-97 15:53	101	717	1342	1916	1210	1.56	2872	494	180	176	178
10-May-97 19:26	101	745	1396	1994	1196	1.56	3000	500	186	181	183
10-May-97 22:56	101	712	1330	1903	1184	1.56	2820	490	178	174	177
11-May-97 01:15	102	730	1370	1957	1201	1.55	2944	499	182	179	180
11-May-97 03:19	95	725	1365	1953	1206	1.54	2938	500	182	178	179
11-May-97 04:20	99	745	1397	2000	1183	1.55	2968	503	183	178	180
11-May-97 10:07	78	439	809	1135	990	1.17	1262	420	103	102	98
11-May-97 11:24	73	440	815	1142	1005	1.15	1312	426	105	104	99
14-May-97 03:32	118	625	1133	1599	958	1.59	1918	435	143	138	139
14-May-97 11:23	102	646	1207	1718	1141	1.52	2430	472	160	159	159
15-May-97 06:22	111	548	987	1384	948	1.48	1626	418	129	125	124
15-May-97 07:31	108	528	959	1344	949	1.47	1565	415	125	123	122
15-May-97 10:03	102	511	934	1319	971	1.43	1559	417	122	122	122
15-May-97 11:07	106	523	950	1338	972	1.46	1572	417	124	123	122
15-May-97 14:32	96	708	1346	1924	1223	1.52	2962	504	180	180	180
16-May-97 23:53	103	628	1165	1654	1076	1.50	2135	458	148	146	146
17-May-97 00:37	105	620	1149	1628	1073	1.52	2090	453	147	145	145
17-May-97 05:31	104	582	1074	1521	1069	1.48	1962	443	141	140	140
17-May-97 08:09	101	589	1094	1547	1081	1.47	2012	450	142	142	140
17-May-97 10:46	106	674	1255	1786	1103	1.55	2466	473	163	160	161
17-May-97 18:39	110	641	1186	1682	1059	1.55	2175	456	151	149	149

Table A2: Calculated Inputs

Time	Σ Sand	Speed CoV	Dens CoV	#1 Head	#2 Head	#3 Head	Discharge	#1 Motor	#2 Motor	#3 Motor
	(kt)	-		(feet)	(feet)	(feet)	(USGPM)	(HP)	(HP)	(HP)
08-May-97 09:50	1	1.2%	1.1%	103	99	95	16182	660	644	644
09-May-97 11:03	48	1.6%	0.2%	132	129	123	19254	1273	1240	1252
09-May-97 22:02	87	1.4%	0.2%	127	123	118	17943	1109	1076	1089
09-May-97 23:38	93	0.5%	0.3%	133	130	124	18425	1192	1162	1171
10-May-97 02:19	101	1.7%	0.5%	136	132	127	18868	1231	1191	1206
10-May-97 07:23	118	1.5%	0.6%	130	127	122	18583	1203	1175	1188
10-May-97 12:11	136	1.5%	0.3%	131	128	122	18485	1213	1183	1193
10-May-97 15:53	150	0.8%	0.7%	135	132	126	19182	1275	1248	1257
10-May-97 19:26	164	1.2%	0.6%	140	137	130	18964	1334	1303	1312
10-May-97 22:56	177	1.8%	0.4%	133	130	125	18762	1250	1221	1240
11-May-97 01:15	186	0.9%	0.4%	138	136	129	19029	1304	1281	1290
11-May-97 03:19	194	0.4%	0.3%	139	137	130	19117	1304	1277	1286
11-May-97 04:20	197	1.0%	0.1%	142	138	132	18754	1319	1286	1302
11-May-97 10:07	214	1.2%	1.1%	106	104	96	15690	562	556	537
11-May-97 11:24	215	1.1%	0.5%	109	107	98	15932	588	580	553
14-May-97 03:32	433	0.9%	0.6%	109	105	100	15184	857	828	835
14-May-97 11:23	460	1.6%	0.4%	122	121	115	18090	1070	1062	1064
15-May-97 06:22	523	1.1%	0.8%	101	97	92	15027	728	706	701
15-May-97 07:31	526	0.8%	0.3%	98	96	90	15043	694	686	675
15-May-97 10:03	533	0.7%	0.7%	98	96	92	15388	684	681	682
15-May-97 11:07	535	0.7%	0.3%	98	96	91	15414	694	686	684
15-May-97 14:32	545	1.4%	0.2%	137	138	130	19391	1299	1302	1299
16-May-97 23:53	629	1.2%	0.2%	119	118	111	17050	944	931	933
17-May-97 00:37	631	1.4%	0.8%	116	114	108	17005	924	913	911
17-May-97 05:31	647	1.1%	0.2%	110	109	103	16940	865	857	857
17-May-97 08:09	655	1.2%	0.6%	113	113	105	17130	888	884	874
17-May-97 10:46	663	1.6%	0.3%	125	123	117	17479	1090	1074	1080
17-May-97 18:39	690	2.0%	0.4%	117	115	109	16778	961	948	950

Table A3: Pump #1 Head Ratio Calculations

Time	Speed (x)	Speed (1)	Speed (2)	Disch (y)	Disch (1)	Disch (2)	Head (1,1)	Head (2,1)	Head (1,2)	Head (2,2)	Head (x,1)	Head (x,2)	Head (x,y)	Obs. Head	Head Ratio
	(rpm)	(rpm)	(rpm)	(USGPM)	(USGPM)	(USGPM)	(feet)	(feet)	(feet)	(feet)	(feet)	(feet)	(feet)	(feet)	
08-May-97 09:5(	414.9	410	415	16182	16000	16500	109.54	112.70	108.26	111.43	112.62	111.35	112.2	103.0	91.9%
09-May-97 11:03	493.2	490	495	19254	19000	19500	156.55	160.33	155.02	158.80	158.95	157.42	158.2	131.9	83.4%
09-May-97 22:02	475.2	475	480	17943	17500	18000	149.79	153.46	148.38	152.05	149.95	148.55	148.7	127.3	85.6%
09-May-97 23:38	486.5	485	490	18425	18000	18500	155.75	159.50	154.30	158.04	156.89	155.43	155.7	133.2	85.6%
10-May-97 02:19	492.8	490	495	18868	18500	19000	158.04	161.82	156.55	160.33	160.15	158.67	159.1	136.4	85.8%
10-May-97 07:23	484.4	480	485	18583	18500	19000	150.59	154.30	149.12	152.82	153.87	152.39	153.6	130.3	84.8%
10-May-97 12:11	485.1	485	490	18485	18000	18500	155.75	159.50	154.30	158.04	155.80	154.34	154.4	131.5	85.2%
10-May-97 15:53	494.0	490	495	19182	19000	19500	156.55	160.33	155.02	158.80	159.59	158.06	159.0	134.7	84.7%
10-May-97 19:2(	500.1	500	505	18964	18500	19000	165.64	169.49	164.15	168.00	165.71	164.22	164.3	140.0	85.2%
10-May-97 22:5(	490.2	490	495	18762	18500	19000	158.04	161.82	156.55	160.33	158.17	156.69	157.4	133.1	84.6%
11-May-97 01:15	498.7	495	500	19029	19000	19500	160.33	164.15	158.80	162.61	163.13	161.59	163.0	137.9	84.6%
11-May-97 03:19	500.3	500	505	19117	19000	19500	164.15	168.00	162.61	166.46	164.41	162.87	164.0	139.1	84.8%
11-May-97 04:20	502.6	500	505	18754	18500	19000	165.64	169.49	164.15	168.00	167.61	166.11	166.8	141.6	84.9%
11-May-97 10:07	419.6	415	420	15690	15500	16000	113.94	117.15	112.70	115.91	116.87	115.64	116.4	106.0	91.1%
11-May-97 11:24	426.0	425	430	15932	15500	16000	120.39	123.68	119.16	122.45	121.04	119.81	120.0	109.4	91.2%
14-May-97 03:32	435.2	435	440	15184	15000	15500	128.20	131.57	127.01	130.37	128.36	127.16	127.9	108.9	85.1%
14-May-97 11:23	472.1	470	475	18090	18000	18500	144.75	148.38	143.30	146.93	146.31	144.85	146.0	122.0	83.5%
15-May-97 06:22	418.4	415	420	15027	15000	15500	115.13	118.34	113.94	117.15	117.29	116.09	117.2	100.8	86.0%
15-May-97 07:31	414.5	410	415	15043	15000	15500	111.96	115.13	110.77	113.94	114.84	113.64	114.7	97.7	85.1%
15-May-97 10:03	417.2	415	420	15388	15000	15500	115.13	118.34	113.94	117.15	116.55	115.35	115.6	97.7	84.5%
15-May-97 11:07	417.3	415	420	15414	15000	15500	115.13	118.34	113.94	117.15	116.59	115.40	115.6	97.9	84.7%
15-May-97 14:32	503.8	500	505	19391	19000	19500	164.15	168.00	162.61	166.46	167.10	165.56	165.9	137.4	82.8%
16-May-97 23:53	458.3	455	460	17050	17000	17500	136.86	140.37	135.50	139.01	139.16	137.80	139.0	119.4	85.9%
17-May-97 00:37	452.9	450	455	17005	17000	17500	133.38	136.86	132.02	135.50	135.41	134.06	135.4	115.9	85.6%
17-May-97 05:31	443.4	440	445	16940	16500	17000	127.86	131.26	126.54	129.94	130.20	128.88	129.0	110.0	85.2%
17-May-97 08:09	450.3	450	455	17130	17000	17500	133.38	136.86	132.02	135.50	133.58	132.22	133.2	113.4	85.1%
17-May-97 10:4(	473.3	470	475	17479	17000	17500	147.52	151.15	146.16	149.79	149.91	148.54	148.6	125.0	84.1%
17-May-97 18:39	455.7	455	460	16778	16500	17000	138.18	141.69	136.86	140.37	138.67	137.35	137.9	117.2	84.9%
17-May-97 20:2(	471.7	470	475	17449	17000	17500	147.52	151.15	146.16	149.79	148.77	147.41	147.5	124.7	84.5%
17-May-97 21:2(	473.4	470	475	17513	17500	18000	146.16	149.79	144.75	148.38	148.62	147.21	148.6	124.1	83.5%
18-May-97 09:02	454.0	450	455	16482	16000	16500	135.98	139.46	134.70	138.18	138.74	137.46	137.5	115.3	83.8%
18-May-97 10:02	452.0	450	455	16367	16000	16500	135.98	139.46	134.70	138.18	137.36	136.08	136.4	114.5	84.0%
18-May-97 14:11	460.2	460	465	16942	16500	17000	141.69	145.25	140.37	143.93	141.84	140.52	140.7	118.1	83.9%
18-May-97 17:31	481.2	480	485	17893	17500	18000	153.46	157.16	152.05	155.75	154.34	152.93	153.2	128.0	83.5%
18-May-97 18:43	483.0	480	485	17949	17500	18000	153.46	157.16	152.05	155.75	155.70	154.30	154.4	129.0	83.5%
19-May-97 09:34	450.8	450	455	16606	16500	17000	134.70	138.18	133.38	136.86	135.23	133.92	135.0	113.8	84.3%

Table A4: Pump #1 Efficiency Ratio Calculations

Time	SG	Motor HP	Head Ratio	Disch (x) (USGPM)	Disch (1) (USGPM)	Disch (2) (USGPM)	Head (y) (Feet)	Head (1) (Feet)	Head (2) (Feet)	Power (1,1) (HP)	Power (2,1) (HP)	Power (1,2) (HP)
08-May-97 09:50	1.34	660	91.9%	16182	16000	16500	112.2	110	115	503.61	519.51	527.64
09-May-97 11:03	1.57	1273	83.4%	19254	19000	19500	158.2	155	160	844.42	864.79	870.57
09-May-97 22:02	1.52	1109	85.6%	17943	17500	18000	148.7	145	150	732.06	751.90	757.79
09-May-97 23:38	1.51	1192	85.6%	18425	18000	18500	155.7	155	160	803.55	823.79	829.27
10-May-97 02:19	1.49	1231	85.8%	18868	18500	19000	159.1	155	160	823.79	844.42	849.68
10-May-97 07:23	1.55	1203	84.8%	18583	18500	19000	153.6	150	155	797.84	818.22	823.79
10-May-97 12:11	1.56	1213	85.2%	18485	18000	18500	154.4	150	155	777.76	797.84	803.55
10-May-97 15:53	1.56	1275	84.7%	19182	19000	19500	159.0	155	160	844.42	864.79	870.57
10-May-97 19:26	1.56	1334	85.2%	18964	18500	19000	164.3	160	165	849.68	870.57	875.52
10-May-97 22:56	1.56	1250	84.6%	18762	18500	19000	157.4	155	160	823.79	844.42	849.68
11-May-97 01:15	1.55	1304	84.6%	19029	19000	19500	163.0	160	165	870.57	891.03	896.69
11-May-97 03:19	1.54	1304	84.8%	19117	19000	19500	164.0	160	165	870.57	891.03	896.69
11-May-97 04:20	1.55	1319	84.9%	18754	18500	19000	166.8	165	170	875.52	896.69	901.36
11-May-97 10:07	1.17	562	91.1%	15690	15500	16000	116.4	115	120	511.41	527.64	535.16
11-May-97 11:24	1.15	588	91.2%	15932	15500	16000	120.0	115	120	511.41	527.64	535.16
14-May-97 03:32	1.59	857	85.1%	15184	15000	15500	127.9	125	130	542.60	559.09	566.27
14-May-97 11:23	1.52	1070	83.5%	18090	18000	18500	146.0	145	150	751.90	771.81	777.76
15-May-97 06:22	1.48	728	86.0%	15027	15000	15500	117.2	115	120	495.82	511.41	519.10
15-May-97 07:31	1.47	694	85.1%	15043	15000	15500	114.7	110	115	472.76	487.87	495.82
15-May-97 10:03	1.43	684	84.5%	15388	15000	15500	115.6	115	120	495.82	511.41	519.10
15-May-97 11:07	1.46	694	84.7%	15414	15000	15500	115.6	115	120	495.82	511.41	519.10
15-May-97 14:32	1.52	1299	82.8%	19391	19000	19500	165.9	165	170	896.69	917.32	922.82
16-May-97 23:53	1.50	944	85.9%	17050	17000	17500	139.0	135	140	661.92	680.57	687.33
17-May-97 00:37	1.52	924	85.6%	17005	17000	17500	135.4	135	140	661.92	680.57	687.33
17-May-97 05:31	1.48	865	85.2%	16940	16500	17000	129.0	125	130	593.48	611.24	618.39
17-May-97 08:09	1.47	888	85.1%	17130	17000	17500	133.2	130	135	636.55	654.83	661.92
17-May-97 10:46	1.55	1090	84.1%	17479	17000	17500	148.6	145	150	712.74	732.06	738.16
17-May-97 18:39	1.55	961	84.9%	16778	16500	17000	137.9	135	140	643.39	661.92	668.46
17-May-97 20:26	1.56	1077	84.5%	17449	17000	17500	147.5	145	150	712.74	732.06	738.16

Table A4 (Continued)

Time	Power (2,2) (HP)	Power (x,1) (HP)	Power (x,2) (HP)	Power (x,y) (HP)	Power x SG (HP)	Load Factor	Motor Eff.	Obs SHP (HP)	Efficiency Ratio
08-May-97 09:50	544.02	509.40	533.60	519.9	694.7	0.40	0.95	618.8	103.1%
09-May-97 11:03	891.03	854.75	880.95	871.4	1366.1	0.77	0.96	1206.6	94.4%
09-May-97 22:02	777.76	749.62	775.47	768.8	1168.9	0.67	0.96	1051.2	95.2%
09-May-97 23:38	849.68	820.75	846.61	824.1	1242.8	0.72	0.96	1130.1	94.1%
10-May-97 02:19	870.57	838.99	865.07	860.2	1284.8	0.75	0.96	1167.0	94.4%
10-May-97 07:23	844.42	801.21	827.20	820.1	1273.3	0.73	0.96	1140.9	94.7%
10-May-97 12:11	823.79	797.25	823.20	820.0	1277.5	0.73	0.96	1149.9	94.6%
10-May-97 15:53	891.03	851.84	878.02	873.0	1358.1	0.77	0.96	1209.1	95.1%
10-May-97 19:26	896.69	869.07	895.17	891.6	1393.6	0.81	0.96	1264.8	93.8%
10-May-97 22:56	870.57	834.61	860.63	847.1	1322.4	0.76	0.96	1185.5	94.3%
11-May-97 01:15	917.32	871.76	897.89	887.6	1375.3	0.79	0.96	1236.3	94.1%
11-May-97 03:19	917.32	875.38	901.54	896.5	1381.8	0.79	0.96	1236.3	94.8%
11-May-97 04:20	922.82	886.27	912.26	895.9	1388.7	0.80	0.96	1250.4	94.2%
11-May-97 10:07	551.84	517.58	541.50	524.3	611.4	0.34	0.95	524.0	106.2%
11-May-97 11:24	551.84	525.43	549.57	549.5	630.5	0.36	0.95	549.0	104.7%
14-May-97 03:32	583.20	548.66	572.50	562.6	893.8	0.52	0.96	809.7	94.0%
14-May-97 11:23	797.84	755.49	781.38	760.9	1157.4	0.65	0.96	1014.2	95.3%
15-May-97 06:22	535.16	496.67	519.98	507.0	751.8	0.44	0.95	684.6	94.4%
15-May-97 07:31	511.41	474.07	497.17	495.9	729.9	0.42	0.95	651.6	95.4%
15-May-97 10:03	535.16	507.90	531.55	510.8	732.1	0.41	0.95	641.8	96.4%
15-May-97 11:07	535.16	508.72	532.39	511.6	745.5	0.42	0.95	651.6	96.9%
15-May-97 14:32	943.74	912.83	939.19	917.5	1391.0	0.79	0.96	1231.1	93.6%
16-May-97 23:53	706.31	663.77	689.21	684.2	1024.6	0.57	0.96	893.5	98.5%
17-May-97 00:37	706.31	662.12	687.53	664.1	1007.6	0.56	0.96	874.2	98.6%
17-May-97 05:31	636.55	609.12	634.39	629.5	934.8	0.52	0.96	817.3	97.5%
17-May-97 08:09	680.57	641.30	666.77	657.8	966.8	0.54	0.96	839.0	98.1%
17-May-97 10:46	757.79	731.25	756.97	749.8	1160.0	0.66	0.96	1033.7	94.4%
17-May-97 18:39	687.33	653.71	678.97	668.5	1034.7	0.58	0.96	910.0	96.6%
17-May-97 20:26	757.79	730.10	755.79	743.2	1157.5	0.65	0.96	1021.1	95.8%

10.0 Appendix B: Statistical Methods

References:

Box, G.E.P, Hunter, W.G., & Hunter, J.S., "Statistics For Experimenters", John Wiley & Sons, New York, 1978

Barnes. J.W, "Statistical Analysis for Engineers", Prentice-Hall, Englewood Cliffs, NJ, 1988

Nomenclature & Methodology:

y_i = Observed value of ratio at observation i.
$\hat{y}_i$ = Best fit correlation value at observation i.
$\bar{y}$ = Mean value of observed ratio

SSE = Sum of Squares of Error, $\sum_{i=1}^{n}(y_i - \hat{y}_i)^2$

SSR = Sum of Squares of Regression, $\sum_{i=1}^{n}(\bar{y} - \hat{y}_i)^2$

SST = Sum of Squares of Terms, $\sum_{i=1}^{n}(\bar{y} - y_i)^2$

Mean Error = $\sqrt{\dfrac{SSE}{n}}$

Correlation Coefficient, $R^2 = \dfrac{SSR}{SST}$

The multivariable regression parameters were found by using the Solver function in Microsoft Excel. A table was set up displaying the actual values of the ratio in question, the value described by the least-squares best fit correlation and the square of the difference between these two values.

The best fit correlation was the one that gave the smallest sum of the squares of the errors.

The values of the best correlation parameters, the sums of squares , the mean error and correlation coefficients are displayed in Table B2. The actual values for each observation for the three pumps are shown in Tables B2, B3 and B4.

Transformation of Correlation Parameters

The correlations are calculated using standardized variables in order to properly test the relative importance of variables. However, for everyday use is necessary to have the correlations in terms of the actual variables. In other words, we wish to go from this:

$$y = \alpha + \beta_1 x_1 + \beta_2 x_2 + \beta_3 x_3 + \beta_{11} x_1^2 + \beta_{22} x_2^2 + \beta_{33} x_3^2 \qquad \text{...(B1)}$$

To this:

$$y = a + b_1 \Sigma Q + b_2 C_W + b_3 N + b_{11} (\Sigma Q)^2 + b_{22} C_W^2 + b_{33} N^2 \qquad \text{...(B2)}$$

This is performed by substituting the transformation functions into equation (B1) and rearranging the terms.

The transformation functions can be written as follows:

$$x_1 = \frac{\Sigma Q}{k_{11}} + k_{12} \qquad \ldots(B3)$$

$$x_2 = \frac{C_W}{k_{21}} + k_{22} \qquad \ldots(B4)$$

$$x_3 = \frac{N}{k_{31}} + k_{32} \qquad \ldots(B5)$$

Substituting (B3), (B4) and (B5) into (B1) we get

$$y = \alpha + \beta_1 \left(\frac{\Sigma Q}{k_{11}} + k_{12} \right) + \beta_2 \left(\frac{C_W}{k_{21}} + k_{22} \right) + \beta_3 \left(\frac{N}{k_{31}} + k_{32} \right)$$

$$+ \beta_{11} \left(\frac{\Sigma Q}{k_{11}} + k_{12} \right) + \beta_{22} \left(\frac{C_W}{k_{21}} + k_{22} \right)^2 + \beta_{33} \left(\frac{N}{k_{31}} + k_{32} \right)^2$$

Expanding and collecting terms, we get:

$$y = a + b_1\Sigma Q + b_2 C_W + b_3 N + b_{11}(\Sigma Q)^2 + b_{22} C_W^2 + b_{33} N^2$$

Where:

$$a = \alpha + \beta_1 k_{12} + \beta_2 k_{22} + \beta_3 k_{32} + \beta_{11} k_{12}^2 + \beta_{22} k_{22}^2 + \beta_{33} k_{32}^2$$

$$b_1 = \frac{\beta_1}{k_{11}} + \frac{2k_{12}}{k_{11}}$$

$$b_2 = \frac{\beta_2}{k_{21}} + \frac{2k_{22}}{k_{21}}$$

$$b_3 = \frac{\beta_3}{k_{31}} + \frac{2k_{32}}{k_{31}}$$

$$b_{11} = \frac{\beta_{11}}{k_{11}^2}$$

$$b_{22} = \frac{\beta_{22}}{k_{21}^2}$$

$$b_{33} = \frac{\beta_{33}}{k_{31}^2}$$

Results:

The calculated results are shown in Table B1. Table B2 displays a sample of the input data and correlation calculations. Table B2 is designed for illustrative purposes only. Anybody requiring a full listing of the correlation data may receive it by contacting the author.

Table B1: Summary of Correlation Calculations

	Pump #1		Pump #2		Pump #3	
	Head	**Efficiency**	**Head**	**Efficiency**	**Head**	**Efficiency**
α	0.9074	0.9672	0.9253	0.9855	0.8386	0.9031
β_1	0	-0.05184	-0.0384	-0.04000	-0.0501	-0.05922
β_2	-0.04769	-0.06718	-0.04932	-0.06171	-0.04089	-0.06474
β_3	-0.01058	-0.01189	-0.01388	0	0	0
β_{11}	-0.04854	-0.02495	-0.12011	-0.04505	-0.09133	-0.03743
β_{22}	-0.00335	-0.00884	-0.02885	0	-0.02932	0.00876
β_{33}	0.00373	-0.01893	0	-0.01615	0	0
Sum of Squares of Errors	0.050	0.079	0.126	0.101	0.120	0.083
Mean Error	1.18%	1.48%	1.44%	1.28%	1.40%	1.16%
Sum of SST	0.155	0.193	1.470	0.629	1.229	0.945
Sum of SSR	0.106	0.114	1.343	0.528	1.109	0.885
Correlation Coefficient	0.680	0.591	0.914	0.839	0.902	0.936
Average of Ratio	0.875	0.941	0.851	0.935	0.778	0.857

Table B2: Pump #1 Correlation Calculations

			Head Ratio Correlations					Efficiency Ratio Correlations				
x_1	x_2	x_3	Head Ratio	Best Fit	Error	SST	SSR	Eff. Ratio	Best Fit	Error	SST	SSR
-1.000	-0.151	-0.622	0.919	0.874	0.00200	0.00194	0.00000	1.031	1.004	0.00075	0.00809	0.00392
-0.991	0.609	0.673	0.834	0.824	0.00010	0.00166	0.00257	0.944	0.933	0.00012	0.00001	0.00007
-0.983	0.472	0.376	0.856	0.834	0.00049	0.00035	0.00168	0.952	0.953	0.00000	0.00011	0.00014
-0.982	0.435	0.563	0.856	0.834	0.00045	0.00036	0.00162	0.941	0.950	0.00009	0.00000	0.00008
-0.981	0.391	0.666	0.858	0.836	0.00046	0.00029	0.00149	0.944	0.950	0.00003	0.00001	0.00007
-0.977	0.566	0.528	0.848	0.828	0.00040	0.00070	0.00214	0.947	0.942	0.00003	0.00003	0.00000
-0.974	0.581	0.539	0.852	0.828	0.00056	0.00054	0.00219	0.946	0.940	0.00004	0.00002	0.00000
-0.971	0.575	0.687	0.847	0.828	0.00037	0.00077	0.00222	0.951	0.935	0.00025	0.00010	0.00004
-0.969	0.595	0.787	0.852	0.826	0.00065	0.00053	0.00235	0.938	0.930	0.00008	0.00001	0.00014
-0.966	0.590	0.623	0.846	0.828	0.00032	0.00085	0.00222	0.943	0.937	0.00005	0.00000	0.00002
-0.964	0.557	0.763	0.846	0.829	0.00029	0.00083	0.00211	0.941	0.934	0.00005	0.00000	0.00006
-0.963	0.533	0.791	0.848	0.830	0.00032	0.00072	0.00200	0.948	0.934	0.00018	0.00004	0.00005
-0.962	0.559	0.828	0.849	0.829	0.00040	0.00068	0.00213	0.942	0.931	0.00013	0.00000	0.00011
-0.959	-0.903	-0.544	0.911	0.910	0.00000	0.00128	0.00124	1.062	1.048	0.00020	0.01461	0.01140
-0.959	-0.998	-0.438	0.912	0.912	0.00000	0.00135	0.00142	1.047	1.054	0.00005	0.01109	0.01261
-0.917	0.667	-0.285	0.851	0.837	0.00022	0.00054	0.00145	0.940	0.947	0.00005	0.00000	0.00003
-0.912	0.474	0.325	0.835	0.841	0.00003	0.00156	0.00116	0.953	0.954	0.00000	0.00013	0.00016
-0.900	0.357	-0.564	0.860	0.858	0.00000	0.00022	0.00029	0.944	0.969	0.00062	0.00001	0.00077
-0.899	0.323	-0.627	0.851	0.861	0.00008	0.00054	0.00020	0.954	0.971	0.00030	0.00015	0.00087
-0.898	0.196	-0.583	0.845	0.866	0.00045	0.00088	0.00007	0.964	0.981	0.00028	0.00050	0.00153
-0.897	0.276	-0.582	0.847	0.862	0.00025	0.00079	0.00015	0.969	0.975	0.00004	0.00074	0.00112
-0.895	0.459	0.849	0.828	0.840	0.00013	0.00218	0.00123	0.936	0.937	0.00000	0.00003	0.00002
-0.879	0.403	0.096	0.859	0.849	0.00009	0.00025	0.00066	0.985	0.964	0.00045	0.00189	0.00049
-0.879	0.463	0.007	0.856	0.847	0.00008	0.00036	0.00077	0.986	0.960	0.00068	0.00202	0.00036
-0.876	0.364	-0.149	0.852	0.854	0.00000	0.00051	0.00043	0.975	0.969	0.00003	0.00111	0.00077
-0.874	0.317	-0.036	0.851	0.855	0.00002	0.00056	0.00038	0.981	0.972	0.00008	0.00155	0.00091
-0.873	0.550	0.344	0.841	0.840	0.00000	0.00111	0.00121	0.944	0.947	0.00001	0.00001	0.00004
-0.868	0.552	0.053	0.849	0.843	0.00004	0.00064	0.00101	0.966	0.953	0.00016	0.00059	0.00013
-0.866	0.580	0.318	0.845	0.839	0.00003	0.00089	0.00126	0.958	0.946	0.00015	0.00027	0.00002

IMAGE EVALUATION TEST TARGET (QA-3)

150mm

6"